COM-02-041-2
Revision 0
May 1983
64.305.1101

DRESDEN NUCLEAR
POWER STATION
UNITS 2 AND 3
PLANT UNIQUE ANALYSIS REPORT
VOLUME 2
SUPPRESSION CHAMBER ANALYSIS

Prepared for:
Commonwealth Edison Company

Prepared by:
NUTECH Engineers, Inc.
San Jose, California

Approved by:

G. L. Howard, P.E.
Project Engineer

I. D. McInnes, P.E.
Engineering Manager

R. H. Adams, P.E.
Engineering Director

Issued by:

A. G. Brnilovich
Project Manager

R. H. Buchholz
Project Director

nutech ENGINEERS

REVISION CONTROL SHEET

SUBJECT: Dresden Station, Units 2 and 3 Plant Unique Analysis Report Volume 2

REPORT NUMBER: COM-02-041-2 Revision 0

V. N. Anderson/Senior Engineer	VNA Initials
C. W. Fong/Specialist	CWF Initials
M. J. Girard/Consultant I	IDM for MJG Initials
G. L. Howard/Senior Engineer	GLH Initials
M. C. Hsieh/Specialist	MCH Initials
S. S. Lee/Engineer	SSL Initials
I. D. McInnes/Engineering Manager	IDM Initials
C. F. Parker/Technician II	CFP Initials
C. T. Shyy/Senior Engineer	CTS Initials
D. C. Talbott/Consultant I	DCT Initials
R. E. Wise/Consultant I	REW Initials

TITLE: Dresden Station, Units 2 and 3 Plant Unique Analysis Report Volume 2

REPORT NUMBER: COM-02-041-2 Revision 0

EFFECTIVE PAGE(S)	REV	PREPARED	ACCURACY CHECK	CRITERIA CHECK
2-I through 2-XV	0	GLH	CKP	CTS
2-1.1 through 2-1.7		GLH	CTS	
2-2.1 through 2-2.22		IDM & MJG	DCT	
2-2.23 through 2-2.49		GLH	REW	
2-2.50		MCH	GLH	
2-2.51		GLH	MCH	
2-2.52 through 2-2.53		MCH	SSL	
2-2.54 through 2-2.55		GLH	MCH	
2-2.56		VMA	CWF	
2-2.57 through 2-2.58		GLH	MCH	
2-2.59 through 2-2.60		VMA	CWF	
2-2.61 through 2-2.66		GLH	MCH	
2-2.67		SSL	MCH	
2-2.68		MCH	SSL	
2-2.69		GLH	MCH	
2-2.70	0	MCH	GLH	CTS
2-2.71	0	GLH	MCH	CTS
2-2.72		MCH	SSL	
2-2.73 through 2-2.77		MCH	GLH	
2-2.78		MCH	SSL	
2-2.79 through 2-2.95		GLH	MCH	
2-2.96 through 2-2.99		GLH	CTS	
2-2.100 through 2-2.101		GLH	MCH	
2-2.102 through 2-2.118		GLH	CTS	
2-2.119 through 2-2.121		MCH	GLH	
2-2.122 through 2-2.124		VMA	CWF	
2-2.125		GLH	MCH	
2-2.126 through 2-2.128		MCH	GLH	
2-2.129 through 2-2.134		GLH	MCH	
2-2.135		MCH	GLH	
2-2.136		SSL	MCH	
2-2.137	0	MCH	GLH	CTS

nutech ENGINEERS

REVISION CONTROL SHEET
(Concluded)

TITLE: Dresden Station, Units 2 and 3 Plant Unique Analysis Report Volume 2

REPORT NUMBER: COM-02-041-2 Revision 0

EFFECTIVE PAGE(S)	REV	PREPARED	ACCURACY CHECK	CRITERIA CHECK	EFFECTIVE PAGE(S)	REV	PREPARED	ACCURACY CHECK	CRITERIA CHECK
2-2.138 through 2-2.141	0	GLH	CTS	CTS					
2-2.142 through 2-2.144		GLH	MCH						
2-2.145 through 2-2.147		MCH	GLH						
2-2.148		GLH	MCH						
2-2.149 through 2-2.151		MCH	GLH						
2-2.152		GLH	MCH						
2-2.153 through 2-2.156		MCH	GLH						
2-2.157 through 2-2.161		GLH	CTS						
2-3.1	0	GLH	CKP	CTS					

QEP-001.4-00

nutech ENGINEERS

ABSTRACT

The primary containments for the Dresden Nuclear Power Station Units 2 and 3 were designed, erected, pressure-tested, and N-stamped in accordance with the ASME Boiler and Pressure Vessel Code, Section III, 1965 Edition with addenda up to and including Winter 1965 for the Commonwealth Edison Company (CECo) by the Chicago Bridge and Iron Company. Since then, new requirements have been established. These requirements affect the design and operation of the primary containment system and are defined in the Nuclear Regulatory Commission's (NRC) Safety Evaluation Report, NUREG-0661. This report provides an assessment of containment design loads postulated to occur during a loss-of-coolant accident or a safety relief valve discharge event. In addition, it provides an assessment of the effects that these postulated events have on containment systems operation.

This plant unique analysis report (PUAR) documents the efforts undertaken to address and resolve each of the applicable NUREG-0661 requirements. It demonstrates that the design of the primary containment system is adequate and that original design safety margins have been restored in accordance with NUREG-0661 acceptance criteria. The Dresden Units 2 and 3 PUAR is composed of the following seven volumes:

- Volume 1 - GENERAL CRITERIA AND LOADS METHODOLOGY
- Volume 2 - SUPPRESSION CHAMBER ANALYSIS
- Volume 3 - VENT SYSTEM ANALYSIS
- Volume 4 - INTERNAL STRUCTURES ANALYSIS
- Volume 5 - SAFETY RELIEF VALVE DISCHARGE LINE PIPING ANALYSIS
- Volume 6 - TORUS ATTACHED PIPING AND SUPPRESSION CHAMBER PENETRATION ANALYSES (DRESDEN UNIT 2)

- Volume 7 - TORUS ATTACHED PIPING AND SUPPRESSION CHAMBER PENETRATION ANALYSES (DRESDEN UNIT 3)

This volume documents the evaluation of the suppression chamber. Volumes 1 through 4 and 6 and 7 have been prepared by NUTECH Engineers, Incorporated (NUTECH), acting as an agent to the Commonwealth Edison Company. Volume 5 has been prepared by Sargent and Lundy (also acting as an agent to Commonwealth Edison), who performed the safety relief valve discharge line (SRVDL) piping analysis. Volume 5 describes the methods of analysis and procedures used in the SRVDL piping analysis.

TABLE OF CONTENTS

LIST OF ACRONYMS

ACI	American Concrete Institute
ADS	Automatic Depressurization System
ASME	American Society of Mechanical Engineers
CB&I	Chicago Bridge and Iron Company
CECo	Commonwealth Edison Company
CO	Condensation Oscillation
DBA	Design Basis Accident
DBE	Design Basis Earthquake
DC	Downcomer
DLF	Dynamic Load Factor
ECCS	Emergency Core Cooling System
FSI	Fluid-Structure Interaction
IBA	Intermediate Break Accident
ID	Inside Diameter
IR	Inside Radius
LDR	Load Definition Report
LOCA	Loss-of-Coolant Accident
MC	Midcylinder
MJ	Miter Joint
NOC	Normal Operating Conditions
NRC	Nuclear Regulatory Commission
NVB	Non-Vent Line Bay
OBE	Operating Basis Earthquake
OD	Outside Diameter

LIST OF ACRONYMS
(Concluded)

PUAAG	Plant Unique Analysis Application Guide
PUAR	Plant Unique Analysis Report
PULD	Plant Unique Load Definitions
QSTF	Quarter-Scale Test Facility
RPV	Reactor Pressure Vessel
SAR	Safety Analysis Report
SBA	Small Break Accident
SPTMS	Suppression Pool Temperature Monitoring System
SRSS	Square Root of the Sum of Squares
SRV	Safety Relief Valve
SRVDL	Safety Relief Valve Discharge Line
SSE	Safe Shutdown Earthquake
TAP	Torus Attached Piping
VB	Vent Line Bay
VH	Vent Header
VL	Vent Line

LIST OF TABLES

LIST OF TABLES
(Concluded)

LIST OF FIGURES

LIST OF FIGURES
(Continued)

LIST OF FIGURES
(Continued)

LIST OF FIGURES
(Concluded)

2-1.0 INTRODUCTION

In conjunction with Volume 1 of the PUAR, this volume documents the efforts undertaken to address the NUREG-0661 requirements which affect the Dresden Units 2 and 3 suppression chambers. Since the components and loads for the two units are identical, only one analysis was performed. The suppression chamber PUAR is organized as follows:

- o INTRODUCTION
  - Scope of Analysis
  - Summary and Conclusions
- o SUPPRESSION CHAMBER ANALYSIS
  - Component Description
  - Loads and Load Combinations
  - Acceptance Criteria
  - Methods of Analysis
  - Analysis Results

The INTRODUCTION section contains an overview of the scope of the suppression chamber evaluation, as well as a summary of the conclusions derived from the comprehensive evaluation of the suppression chamber. The SUPPRESSION CHAMBER ANALYSIS section contains a

comprehensive discussion of the suppression chamber loads and load combinations and a description of the suppression chamber components affected by these loads. The section also contains a discussion of the methodology used to evaluate the effects of these loads, the evaluation results, and the acceptance limits to which the results are compared.

2-1.1 Scope of Analysis

The criteria presented in Volume 1 are used as the basis for the Dresden Units 2 and 3 suppression chamber evaluation. The suppression chamber is evaluated for the effects of loss-of-coolant accident (LOCA)-related and safety relief valve (SRV) discharge-related loads defined by the Nuclear Regulatory Commission (NRC) Safety Evaluation Report NUREG-0661 (Reference 1) and by the "Mark I Containment Program Load Definition Report" (LDR) (Reference 2), as well as for loads considered in the original design of the suppression chamber.

The LOCA and SRV discharge loads used in this evaluation are formulated using the methodology discussed in Volume 1 of this report. The loads are developed using the plant unique operating parameters and test results contained in the "Mark I Containment Program Plant Unique Load Definition" (PULD) report (Reference 3). The effects of increased suppression pool temperatures which occur during SRV discharge events are also evaluated. These temperatures are taken from the "Dresden 2 and 3 Nuclear Generating Plants Suppression Pool Temperature Response" (Reference 4). The normal

operating condition (NOC) pressure loads are taken from the plant unique "Containment Data" specifications (References 5 and 6) and the seismic loads are taken from the plants' design specification (Reference 7).

The evaluation includes a structural analysis of the suppression chamber for the effects of LOCA-related and SRV discharge-related loads to confirm that the design of the modified suppression chamber is adequate. Rigorous analytical techniques are used in this evaluation, including the use of detailed analytical models for computing the dynamic response of the suppression chamber. Effects such as fluid-structure interaction (FSI) are also considered in the analysis.

The results of the structural evaluation of the suppression chamber for each load are used to evaluate load combinations and fatigue effects in accordance with the "Mark I Containment Program Structural Acceptance Criteria Plant Unique Analysis Applications Guide" (PUAAG) (Reference 8). The analysis results are compared with the acceptance limits specified by the PUAAG and the applicable sections of the American Society of Mechanical Engineers (ASME) Code (Reference 9).

2-1.2 Summary and Conclusions

The evaluation documented in this volume is based on the modified Dresden Units 2 and 3 suppression chambers described in Section 1-2.1. The overall load-carrying capacity of the suppression chamber and its supports is substantially greater than the original design.

The loads considered in the original design of the suppression chamber and its supports include dead weight, earthquake, and pressure and temperature loads associated with NOC and a postulated LOCA event. The additional loadings which affect the design of the suppression chamber and supports are defined generically in NUREG-0661. These loads are postulated to occur during small break accident (SBA), intermediate break accident (IBA), or design basis accident (DBA) LOCA events and during SRV discharge events. Each of these events results in hydrodynamic pressure loadings on the suppression chamber shell, hydrodynamic drag loadings on the submerged suppression chamber components, and interaction loadings caused by loads acting on structures attached to the suppression chamber.

The methodology used to develop plant unique loadings for the suppression chamber evaluation is discussed in Section 1-4.0. Applying this methodology results in conservative values for each of the significant NUREG-0661 loadings which envelop those postulated to occur during an actual LOCA or SRV discharge event.

The LOCA-related and SRV discharge-related loads are grouped into event combinations using the NUREG-0661 criteria discussed in Section 1-3.2. The event sequencing and event combinations specified and evaluated envelop the actual events expected to occur throughout the life of the plant.

The loads contained in the postulated event combinations which are major contributors to the total response of the suppression chamber include LOCA internal pressure loads, DBA pool swell torus shell loads, DBA condensation oscillation (CO) torus shell loads, and SRV discharge torus shell loads. Although considered in the evaluation, other loadings such as temperature loads, seismic loads, chugging torus shell loads, submerged structure loads, and containment structure reaction loads have a lesser effect on the total response of the suppression chamber.

The suppression chamber evaluation is based on the NUREG-0661 acceptance criteria discussed in Section 1-3.2. These acceptance limits are based on Section III of the ASME Code. Use of these criteria assures that the original suppression chamber design margins have been restored.

The controlling event combinations for the suppression chamber include loadings found to be major contributors to the response of the suppression chamber. The results for these controlling event combinations show that all of the suppression chamber stresses and support reactions are within Code limits.

As a result, the suppression chambers described in Section 1-2.1 have been shown to fulfill the margins of safety inherent in the original design documented in the plant's safety analysis report (SAR) (Reference 10). The NUREG-0661 requirements are therefore considered to be met.

2-2.0 SUPPRESSION CHAMBER ANALYSIS

Evaluations of each NUREG-0661 requirement which affects the design adequacy of the Dresden Units 2 and 3 suppression chambers are presented in the following sections. The criteria used in this evaluation are presented in Volume 1 of this report.

The suppression chamber components evaluated are described in Section 2-2.1. The loads and load combinations for which the suppression chamber is evaluated are presented in Section 2-2.2. The acceptance limits to which the analysis results are compared are described in Section 2-2.3. The methodology used to evaluate the effects of these loads and load combinations on the suppression chamber is discussed in Section 2-2.4. The analysis results and the corresponding suppression chamber design margins are presented in Section 2-2.5.

2-2.1 Component Description

The Dresden Units 2 and 3 suppression chambers are constructed from 16 mitered cylindrical shell segments joined together in the shape of a torus. Figure 2-2.1-1 illustrates the configuration of each suppression chamber. Figures 2-2.1-1 through 2-2.1-7 show the proximity of the suppression chamber to other components of the containment.

The suppression chamber is connected to the drywell by eight vent lines (VL) which, in turn, are connected to a common vent header (VH) within the suppression chamber. Attached to the vent header are downcomers (DC) which terminate below the surface of the suppression pool. The vent system is supported vertically at each miter joint (MJ) by two support columns which transfer reaction loads to the suppression chamber (Figure 2-2.1-4). A bellows assembly is provided at the penetration of the vent line to the suppression chamber to allow differential movement of the suppression chamber and vent system to occur (Figure 2-2.1-3).

Figure 2-2.1-1 shows that the major radius of the suppression chamber is 54'6", measured at midbay of each mitered cylinder. The inside diameter (ID) of the

mitered cylinders which make up the suppression chamber is 30'0". The suppression chamber shell thickness is typically 0.585" above the horizontal centerline and 0.653" below the horizontal centerline, except at penetrations, where it is locally thicker (Figure 2-2.1-3).

The suppression chamber shell is reinforced at each miter joint location by a T-shaped ring girder (Figures 2-2.1-4, 2-2.1-7 and 2-2.1-9). A typical ring girder is located in a plane 4" from the miter joint and on the non-vent line bay (NVB) side of each miter joint. As such, the intersection of a ring girder web and the suppression chamber shell is an ellipse. The inner flange of a ring girder is rolled to a constant inside radius (IR) of 12'10-3/4". Thus, the ring girder web depth varies from 24" to 27-1/2" and has a constant thickness of 1". The ring girder flange is attached to the ring girder web with 5/16" fillet welds. The ring girder web is attached to the suppression chamber shell with 3/8" fillet welds (Figures 2-2.1-8, 2-2.1-9, and 2-2.1-10).

The ring girders are laterally reinforced at the base of the vent header support columns by 1" thick plate assemblies (Figures 2-2.1-4, 2-2.1-7, and 2-2.1-9).

There are five such assemblies in the bays with SRV discharge lines in both units. In the non-SRV discharge line bays, there are no such assemblies in Unit 2, and two assemblies in Unit 3. In addition to these lateral stiffeners, the ring-girder-web-plate-to-torus-shell fillet weld was increased from 3/8" to 5/8" over a 12'0" long arc near the outside torus support column (Figure 2-2.1-7).

The suppression chamber is supported vertically at each miter joint by inside and outside columns and by a saddle support (Figures 2-2.1-4, 2-2.1-7 and 2-2.1-8). The connection web plate is parallel to the mitered joint. During construction, the support columns were jacked radially outward before being bolted to the basemat, thus imposing a 3/16" preset in the inside column and 11/16" in the outside column. The saddle supports are located parallel to the associated miter joint and in the plane of the ring girder web. At each miter joint, the ring girder, the columns, the column connections, and the saddle support form an integral support system, which takes vertical loads acting on the suppression chamber shell and tranfers them to the reactor building basemat. The support system provides full vertical support for the suppression chamber, at the same time allowing radial movement and thermal expansion to occur.

The modified vertical support system shown in Figure 2-2.1-4 provides a load transfer mechanism which acts to reduce local suppression chamber shell stresses and to more evenly distribute reaction loads to the basemat. It also acts to raise the suppression chamber natural frequencies beyond the critical frequencies of most hydrodynamic loads, thereby reducing dynamic amplification effects.

The inside and outside column supports are pipe members. The inside column is an 8" diameter pipe reinforced by two, 160° segments of 10" diameter pipe. The outside column is a 10-3/4" outside diameter (OD) pipe with a 2-1/4" wall thickness. The column base plate assemblies consist of base plates, a pin, and anchor bolts (Figures 2-2.1-8 and 2-2.1-12).

The connection of the column supports to the suppression chamber shell is a column stub assembly consisting of a 1-1/2" thick column web plate, 1" thick stiffener plates, and either a 1-1/2" thick wing plate at the outside column or a 1-1/4" thick flange plate at the inside column (Figure 2-2.1-7).

The column connection web plates and saddle support web plates are connected with fillet welds and partial penetration welds.

Each saddle support consists of a 1-1/4" thick web plate, a 1-1/4" thick lower flange plate and saddle base plate assemblies (Figures 2-2.1-7 and 2-2.1-8). The saddle base plate assemblies consist of a 2-7/8" thick base plate, a 1/2" thick lubrite plate, and a 1" thick bearing plate. This assembly allows for radial growth due to thermal loads. The saddle is reinforced with 3/4" thick stiffener plates to ensure that buckling does not occur during peak loading conditions.

The anchorage of the suppression chamber saddle to the basemat consists of eight, 1-3/4" diameter, epoxy-grouted anchor bolts provided at each saddle base plate location. Four, 1-1/2", epoxy-grouted anchor bolts and two embedded in the original basemat pour are provided at each outside column base plate location, and two, epoxy-grouted anchor bolts and two embedded in the original basemat pour are provided at each inside column location. The saddle anchor bolts are anchored through a 3-13/16" long slotted hole in the base plate to allow for thermal growth. A total of 26 anchor bolts at each miter joint provides the principal mechanism for transfer of uplift loads on the suppression chamber to the basemat.

A sway rod assembly at the outside columns provides lateral support for the suppression chamber (Figure 2-2.1-11). This seismic sway rod consists of 3-1/2" diameter sway rods and 3-3/4" diameter turnbuckles to provide restraint for movement along the torus centerline resulting from lateral loads acting on the suppression chamber. The sway rods are joined to the 1-1/2" thick wing plate at the top of the column by 4" diameter pins. The lower ends of the sway rods are joined to a 2" thick seismic tie plate at the column base (Figure 2-2.1-12).

The suppression pool temperature monitoring system (SPTMS) used in Dresden Units 2 and 3 is described in Section 1-5.2. Each unit has 16 temperature monitoring devices, each of which is threaded into a thermowell. The thermowells are inserted through 0.75" diameter holes in the suppression chamber and are welded to it (Figures 2-2.1-3 and 2-2.1-5).

The T-quencher used in Dresden Units 2 and 3 is described in Section 1-4.2. Each unit has five T-quenchers located near midbay in the vent bays, with the associated quencher arms oriented down the centerline of the vent bay (Figure 2-2.1-13).

The quencher arms are supported by a horizontal pipe beam which spans the miter joint ring girders (Figure 2-2.1-14). Volume 5 of the PUAR provides a description of the SRVDL and the T-quencher support systems.

The suppression chamber provides support for many other containment-related structures, such as the vent system and the catwalk. Loads acting on the suppression chamber cause motions at the points where these structures attach to the suppression chamber. Loads acting on these structures also cause reaction loads on the suppression chamber. These containment interaction effects are evaluated in the analysis of the suppression chamber.

The overall load-carrying capacities of the suppression chamber components described in the preceding paragraphs provide additional design margins for those components of the original suppression chamber design, described in the plant's safety analysis report.

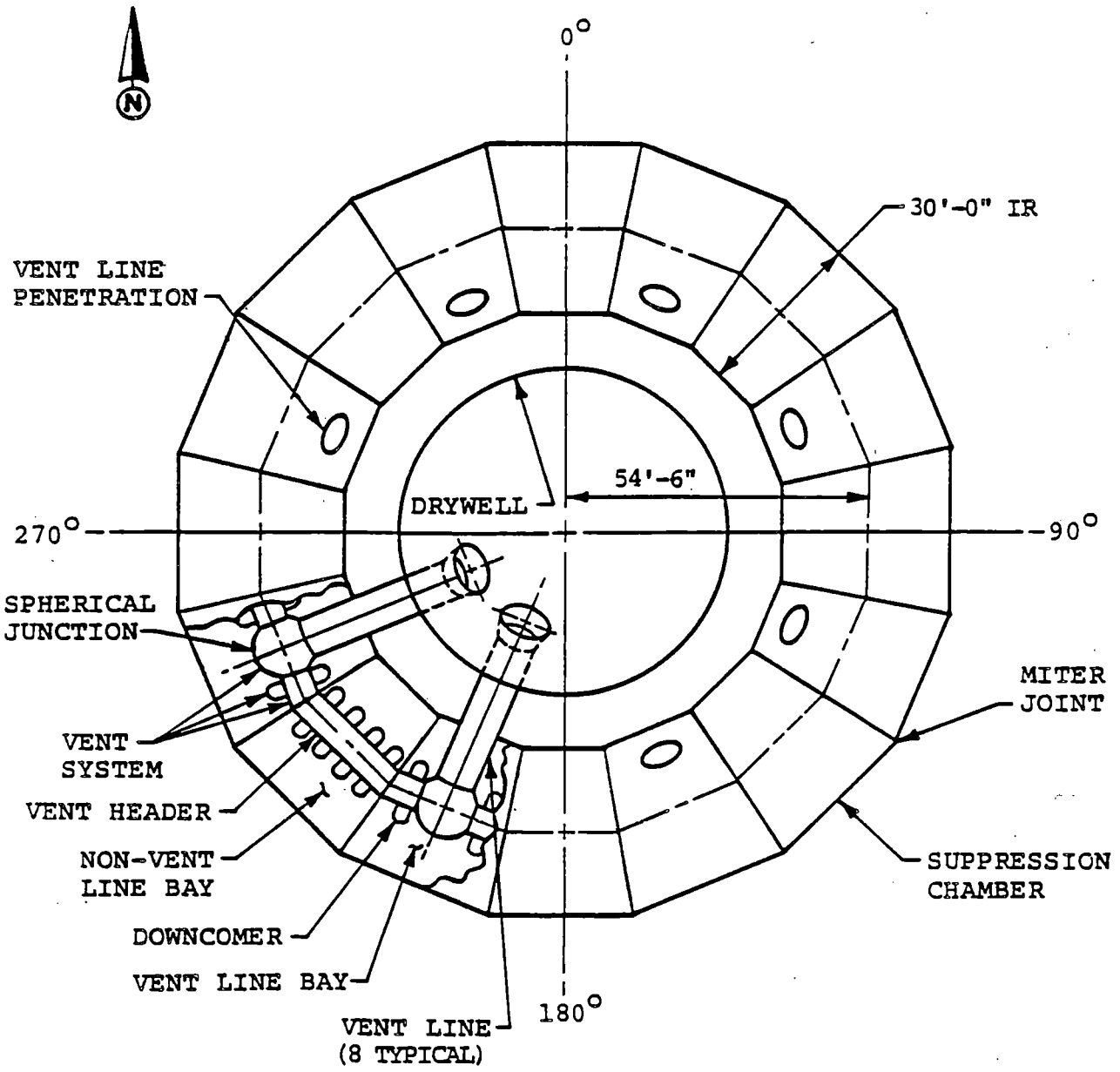

Figure 2-2.1-1

PLAN VIEW OF CONTAINMENT

nutech ENGINEERS

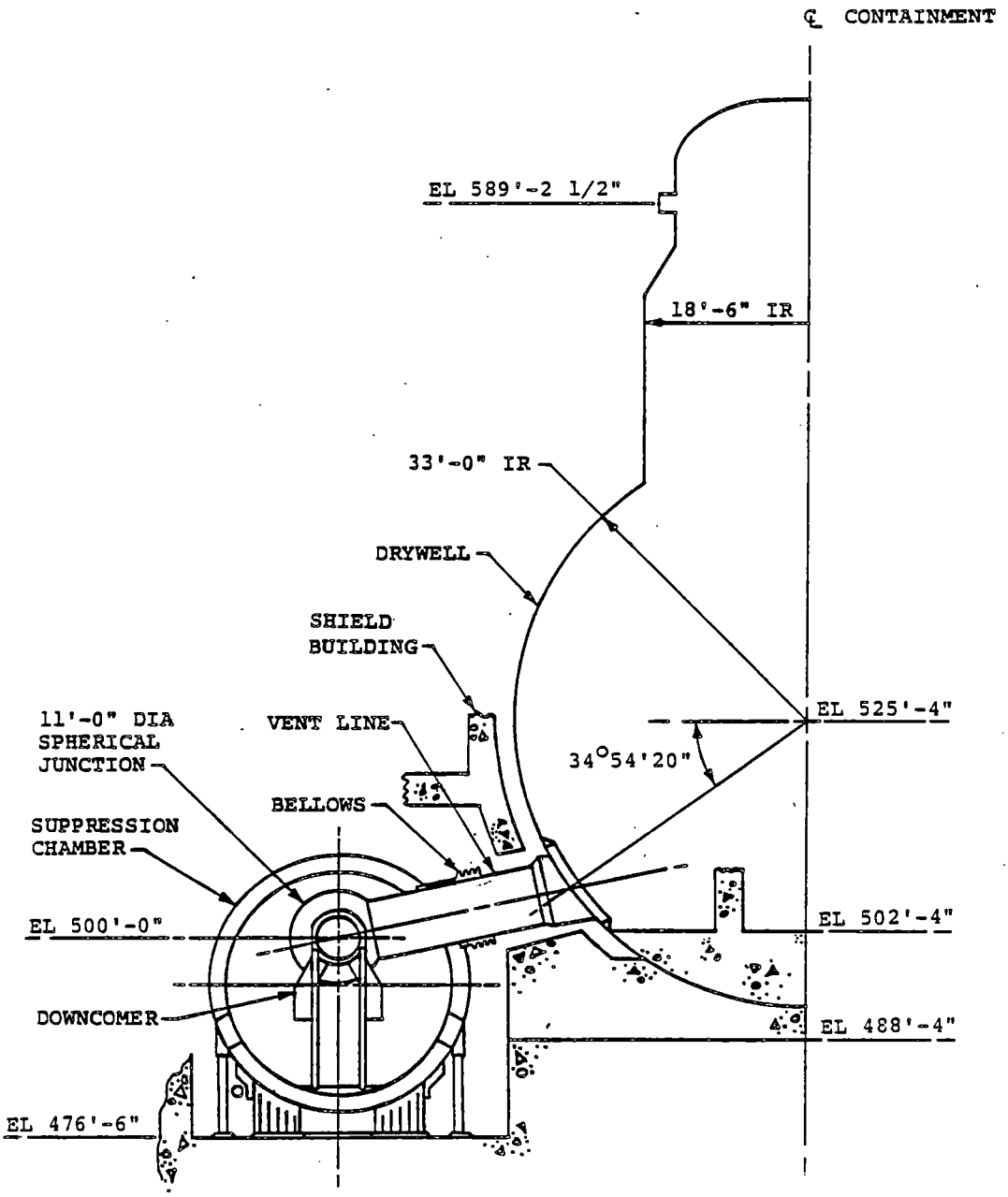

Figure 2-2.1-2

ELEVATION VIEW OF CONTAINMENT

nutech ENGINEERS

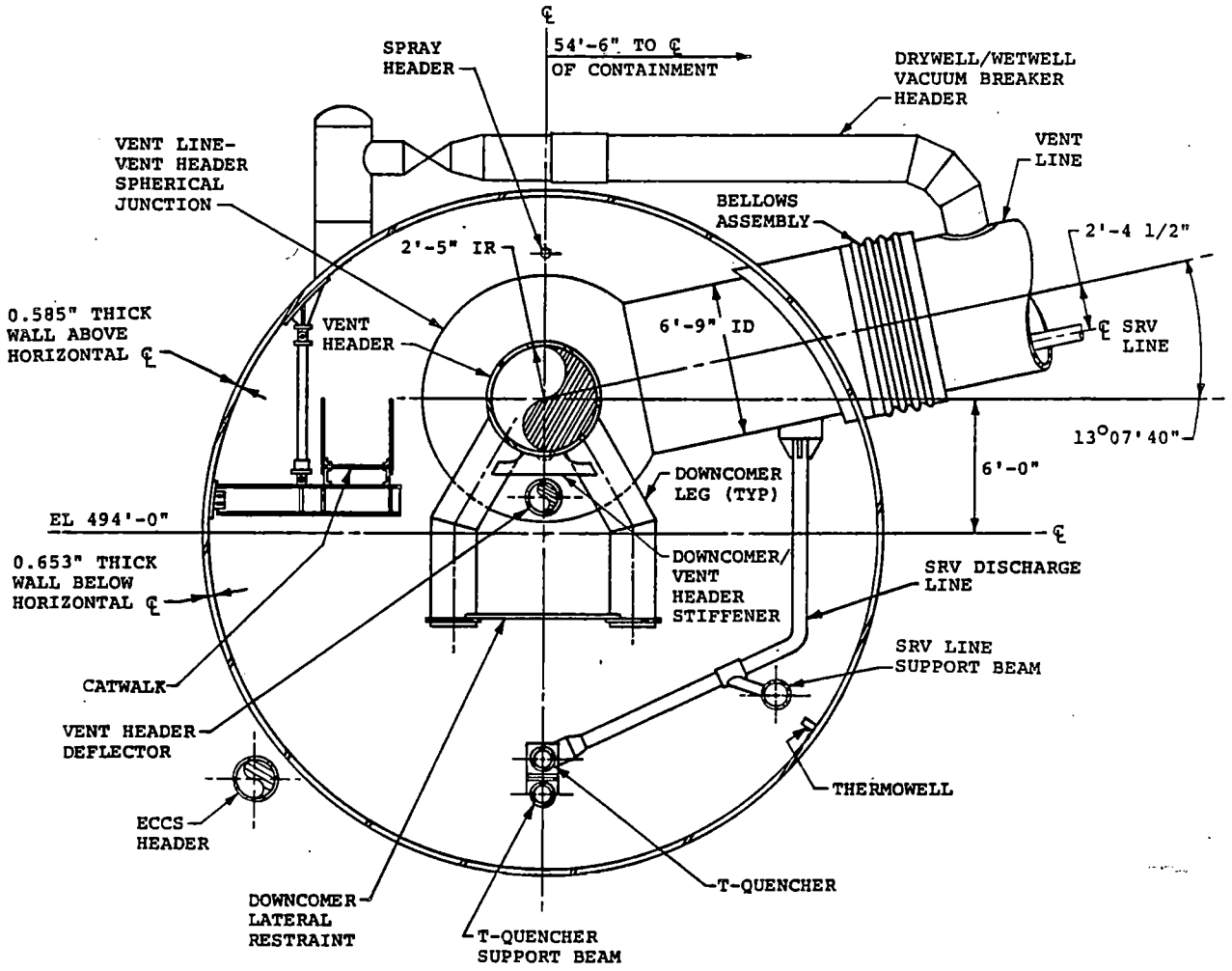

Figure 2-2.1-3

SUPPRESSION CHAMBER SECTION - MIDBAY

VENT LINE BAY

nutech ENGINEERS

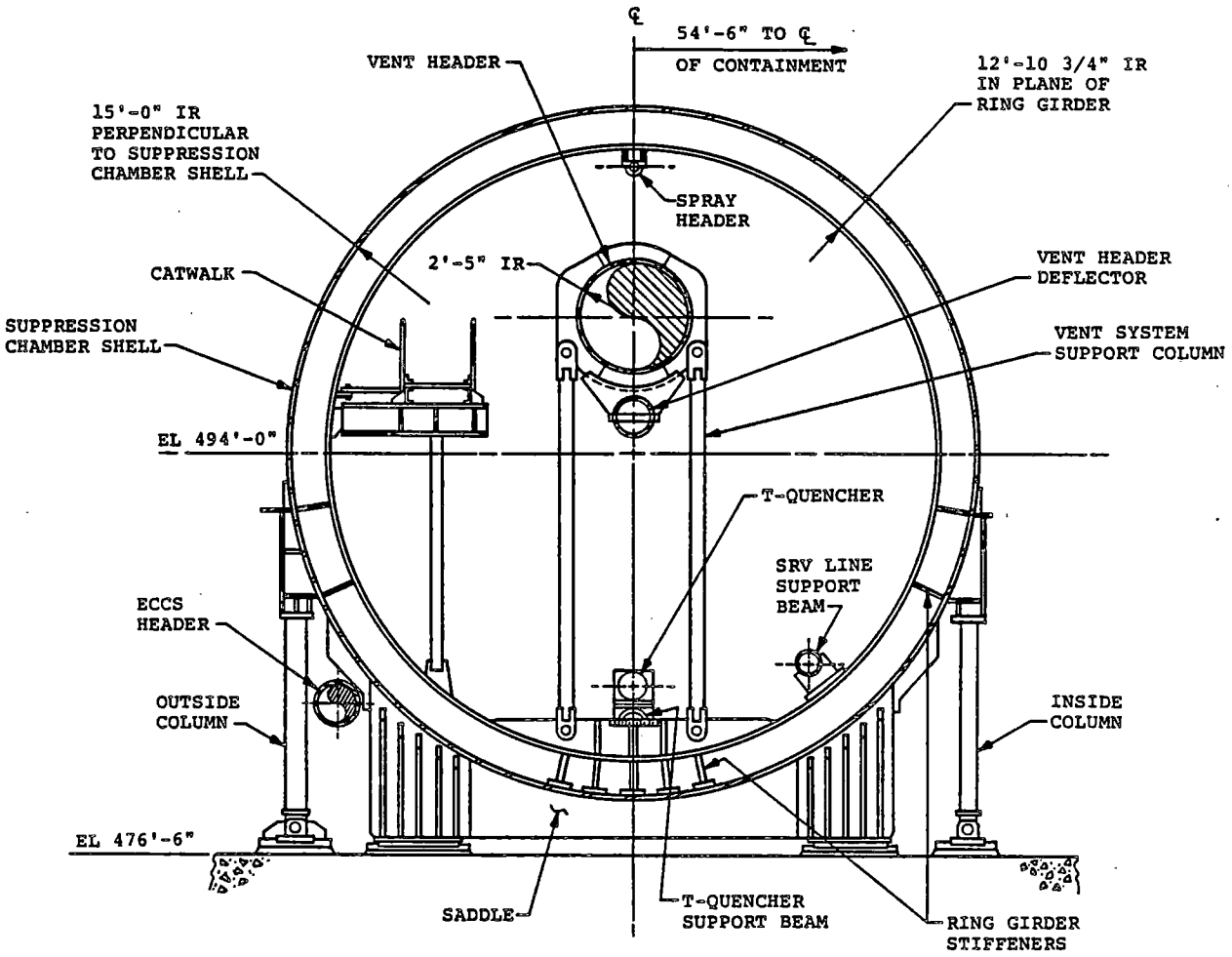

Figure 2-2.1-4

SUPPRESSION CHAMBER SECTION -
MITER JOINT

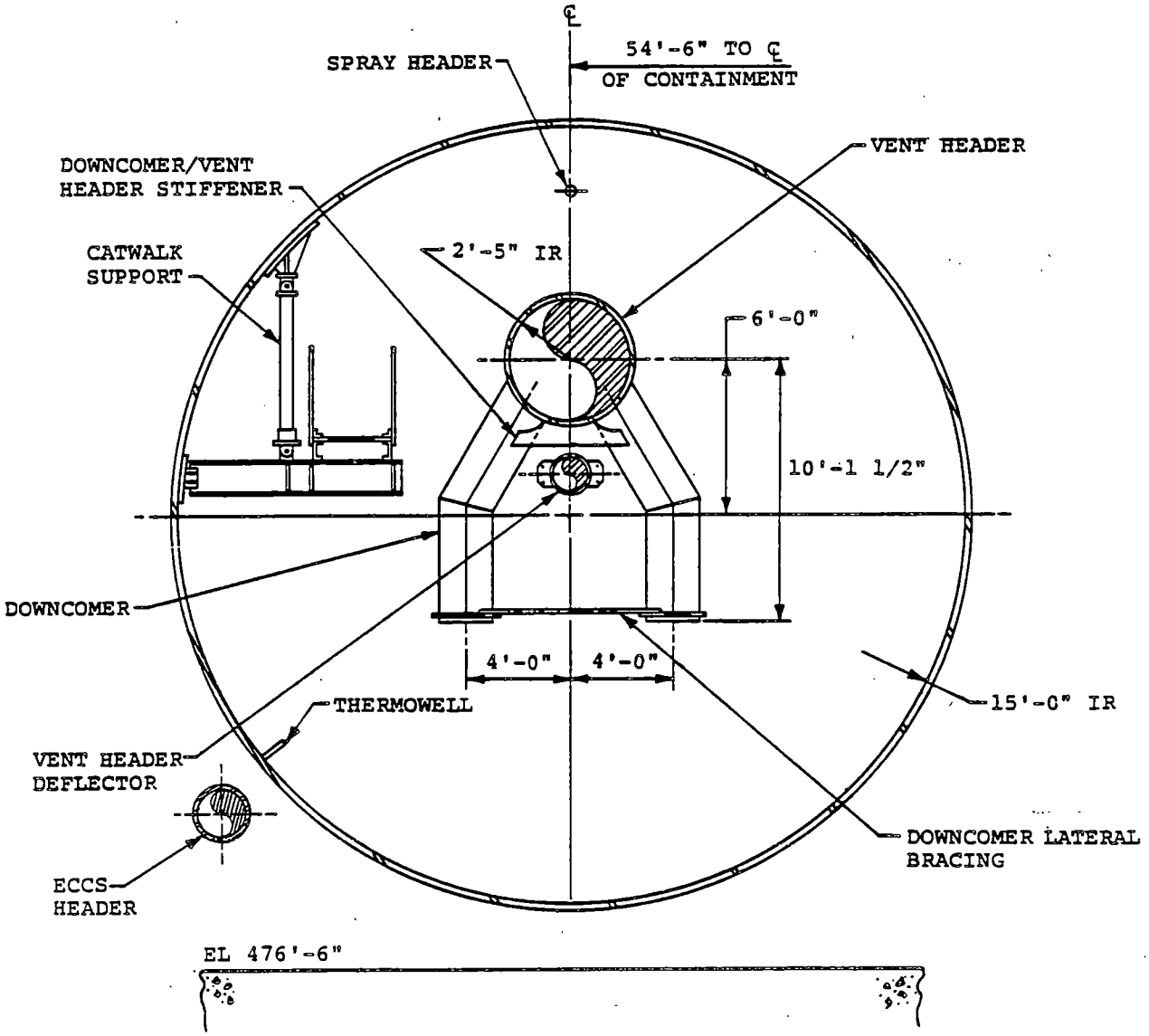

Figure 2-2.1-5

SUPPRESSION CHAMBER SECTION - MIDBAY

NON-VENT LINE BAY

nutech ENGINEERS

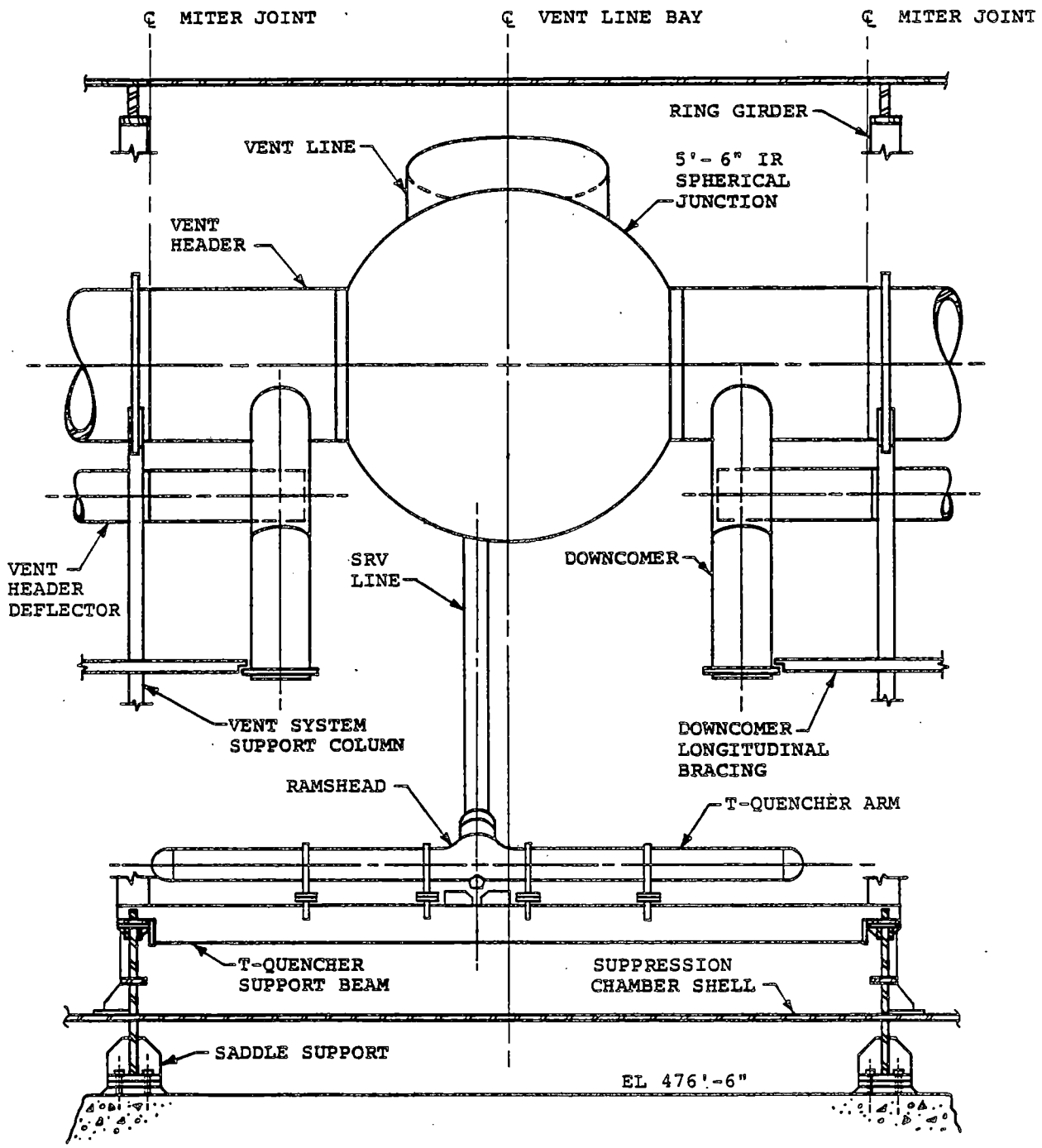

Figure 2-2.1-6

DEVELOPED VIEW OF SUPPRESSION CHAMBER SEGMENT

nutech ENGINEERS

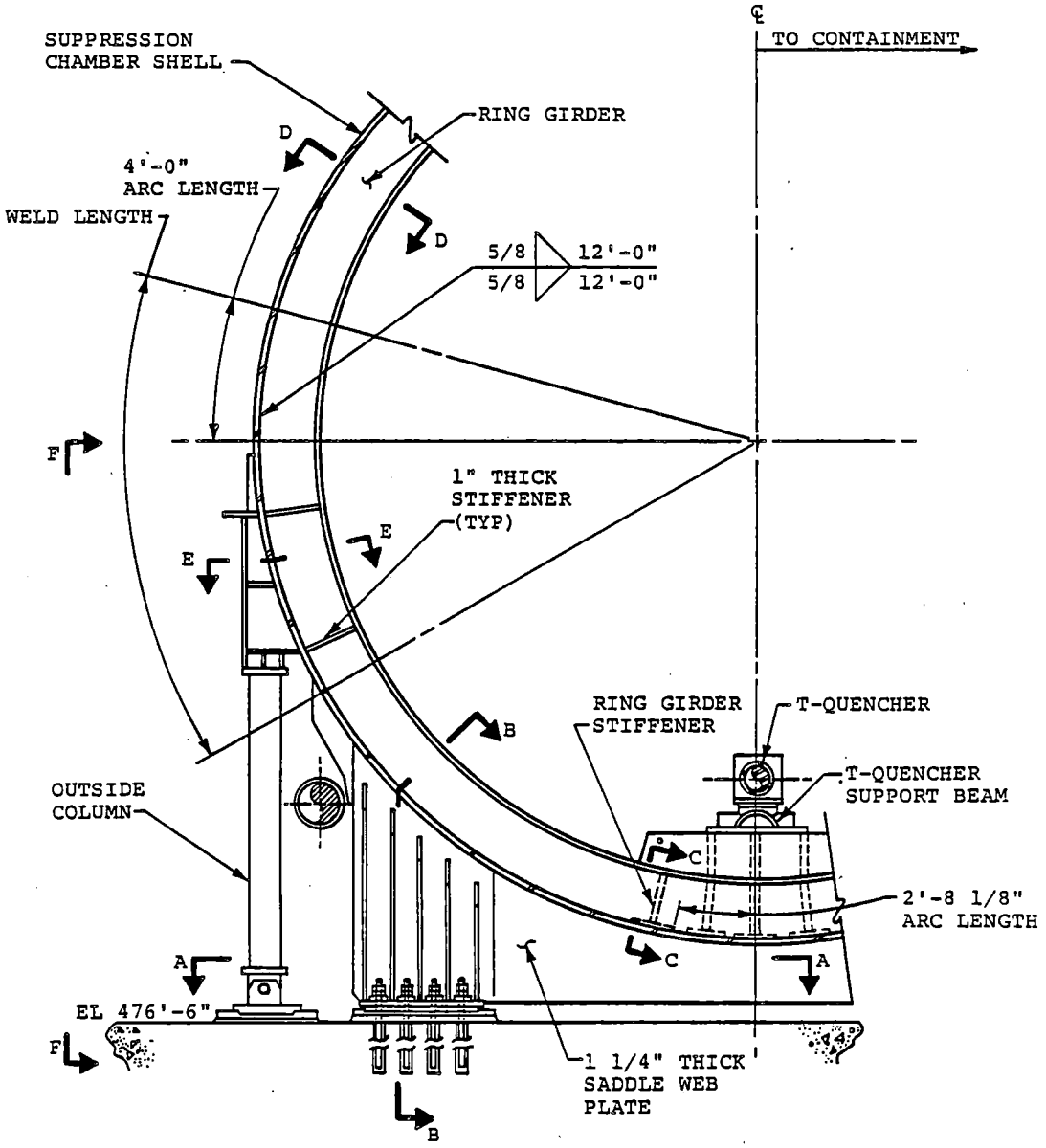

1. SEE FIGURES 2-2.1-8 THROUGH 2-2.1-11 FOR SECTIONS AND VIEWS, RESPECTIVELY.

Figure 2-2.1-7

SUPPRESSION CHAMBER RING GIRDER AND VERTICAL SUPPORTS - PARTIAL ELEVATION VIEW

nutech ENGINEERS

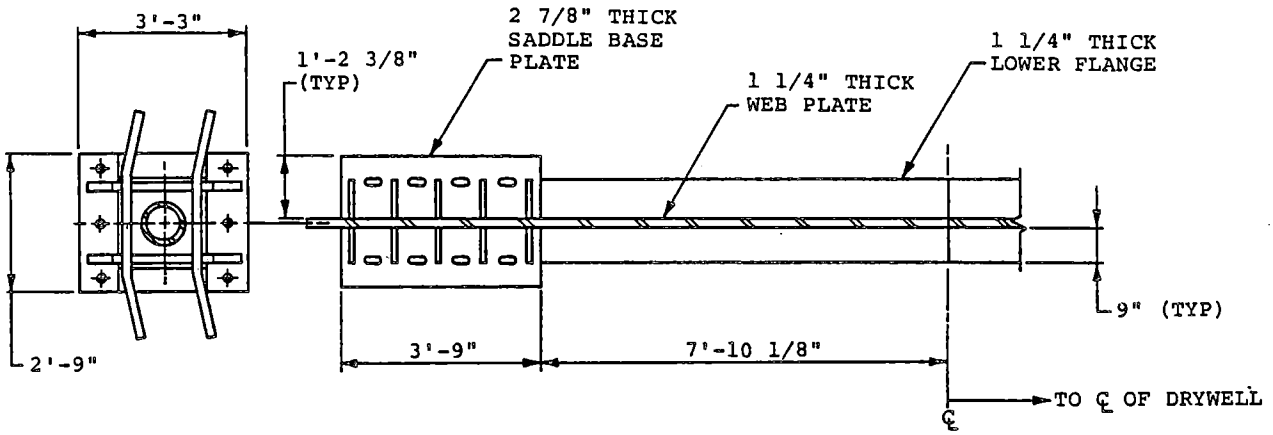

SECTION A-A

(FROM FIGURE 2-2.1-7)

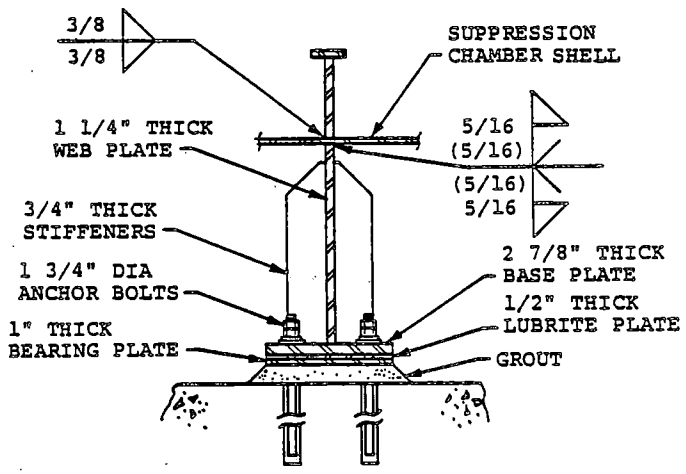

SECTION B-B

(FROM FIGURE 2-2.1-7)

Figure 2-2.1-8

SUPPRESSION CHAMBER VERTICAL SUPPORT BASE PLATES -
PARTIAL PLAN VIEW AND DETAILS

nutech ENGINEERS

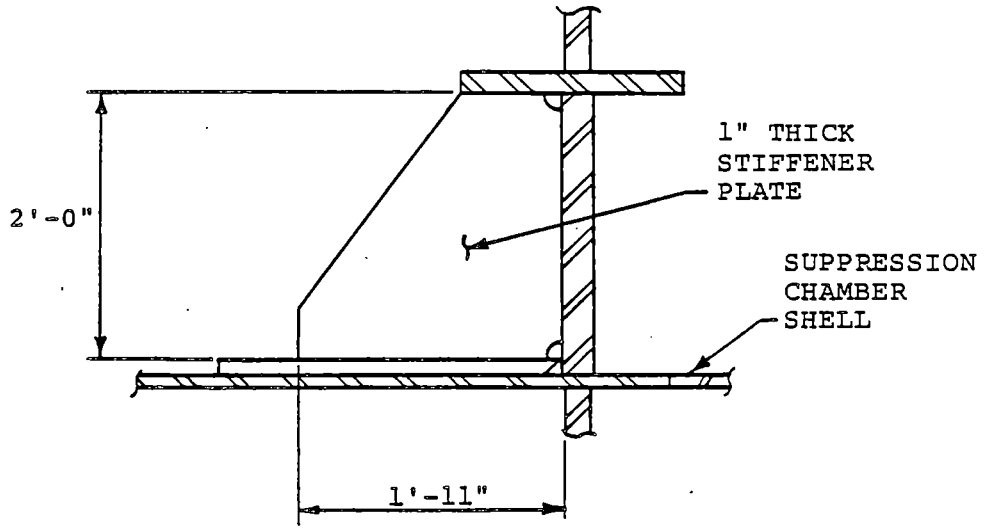

SECTION C-C
(FROM FIGURE 2-2.1-7)

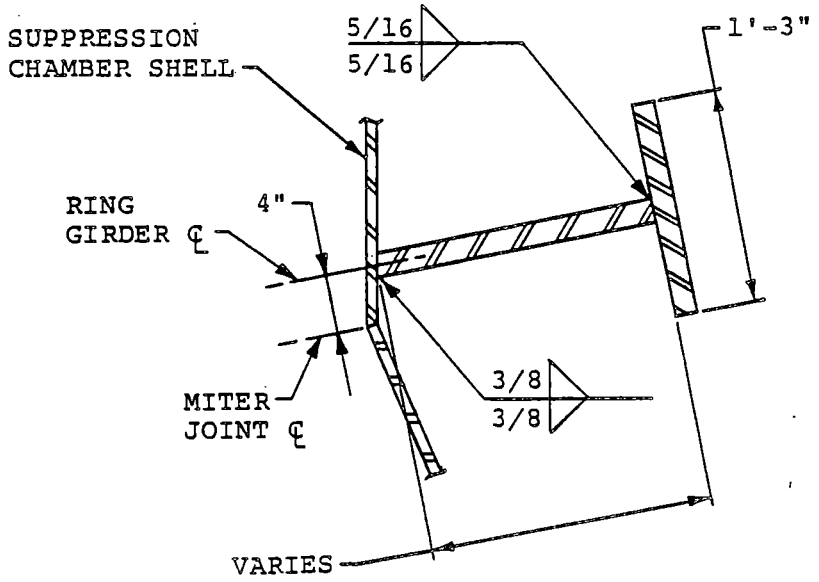

SECTION D-D
(FROM FIGURE 2-2.1-7)

Figure 2-2.1-9

SUPPRESSION CHAMBER RING GIRDER DETAILS

nutech ENGINEERS

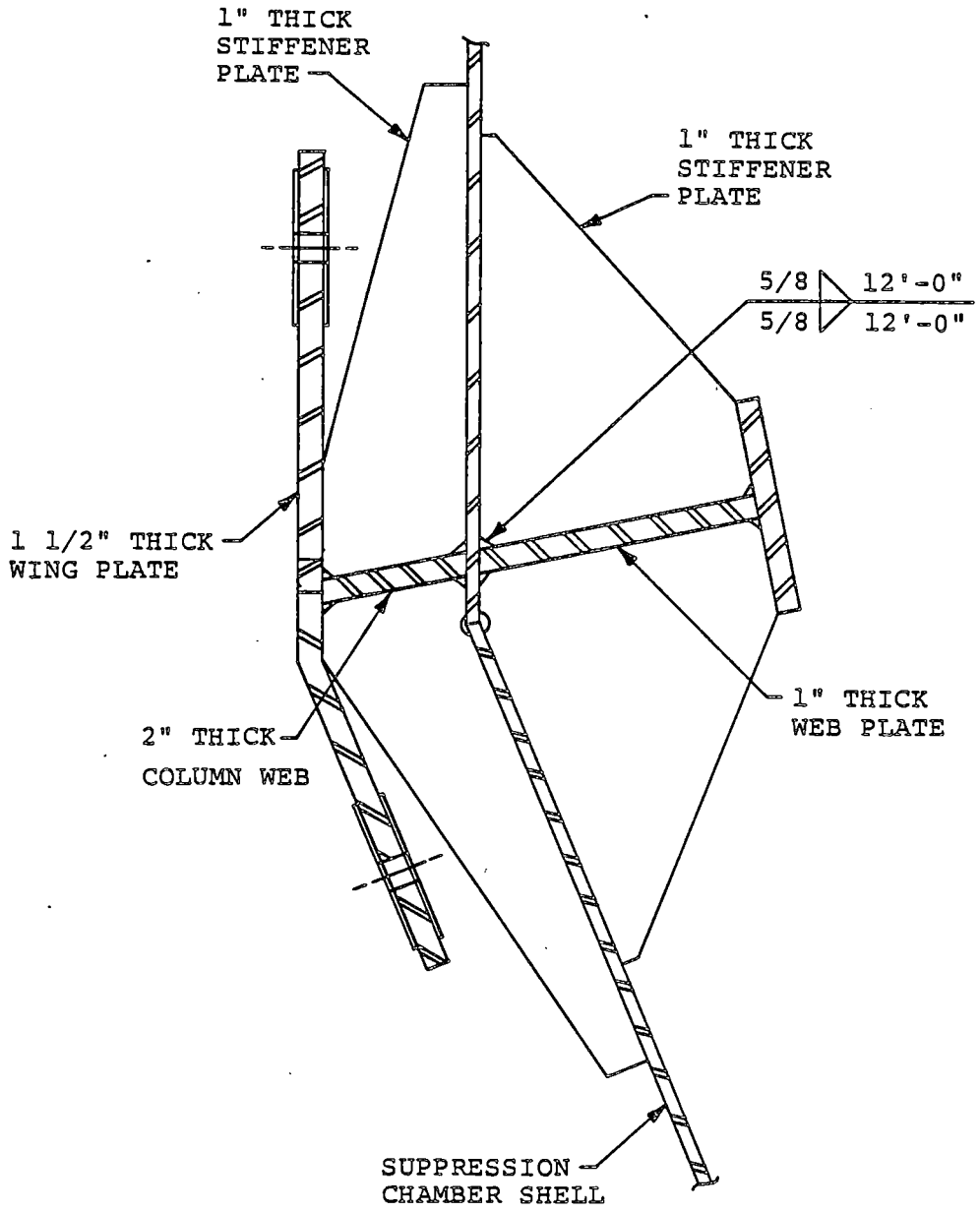

SECTION E-E
(FROM FIGURE 2-2.1-7)

Figure 2-2.1-10

SUPPRESSION CHAMBER RING GIRDER AND
COLUMN CONNECTION DETAILS

nutech ENGINEERS

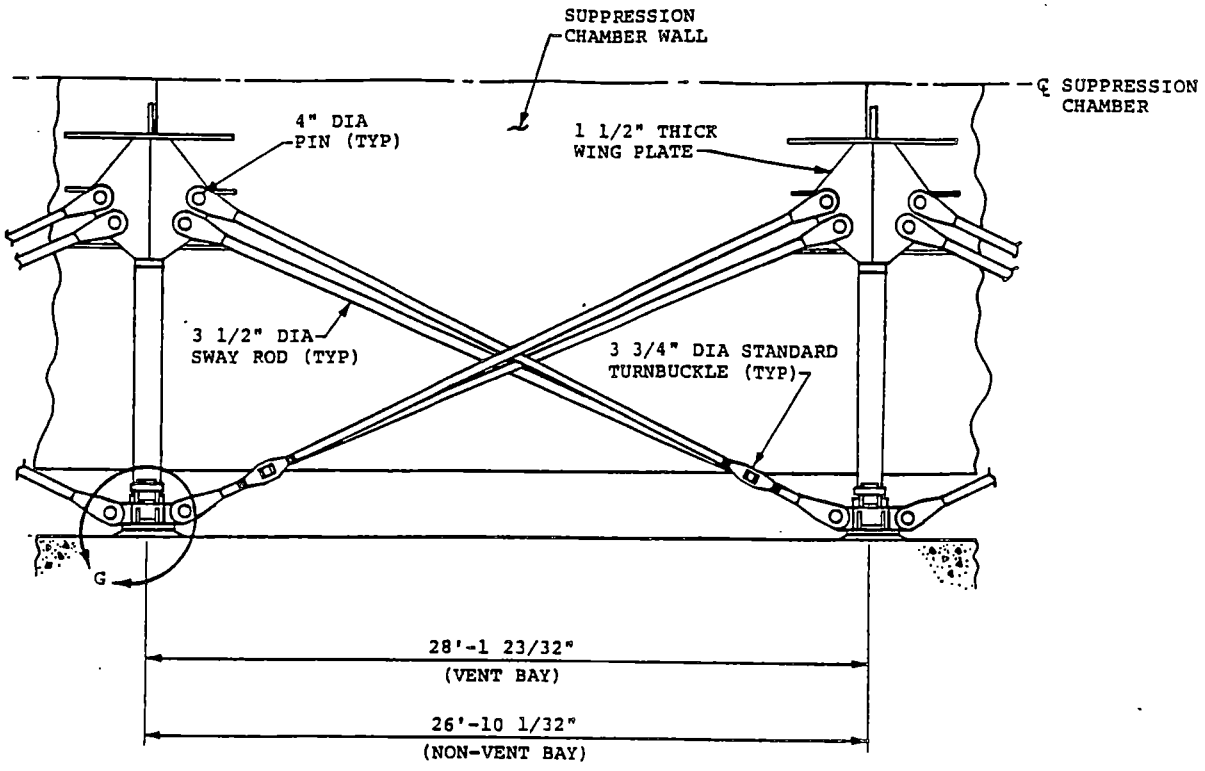

VIEW F-F
(FROM FIGURE 2-2.1-7)

1. SEE FIGURE 2-2.1-12 FOR DETAIL G.

Figure 2-2.1-11

SUPPRESSION CHAMBER SEISMIC RESTRAINT

nutech ENGINEERS

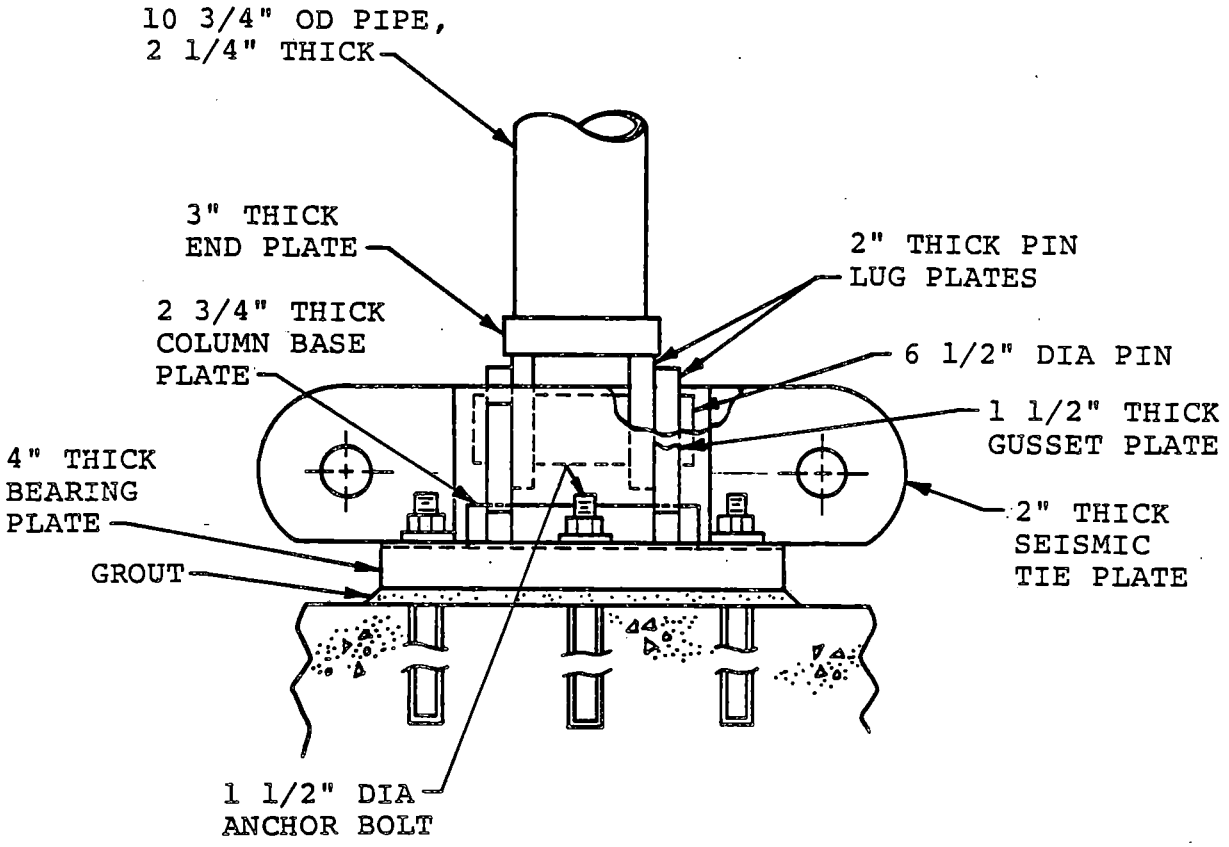

DETAIL G
(FROM FIGURE 2-2.1-11)

Figure 2-2.1-12

SUPPRESSION CHAMBER

OUTSIDE COLUMN ANCHORAGE

nutech ENGINEERS

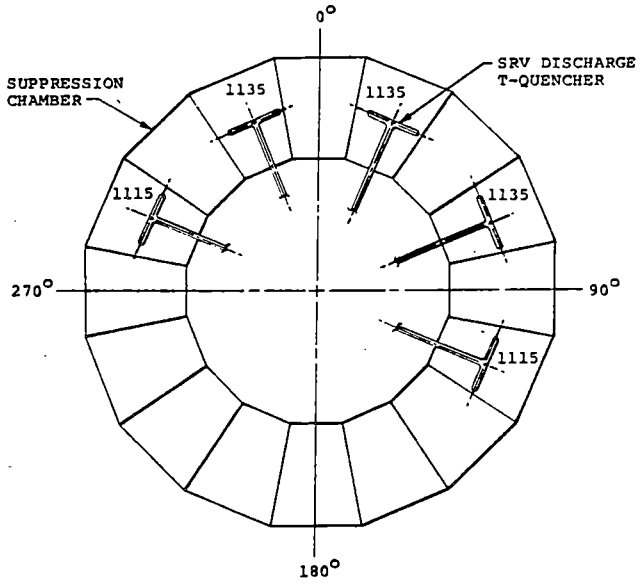

UNIT 2

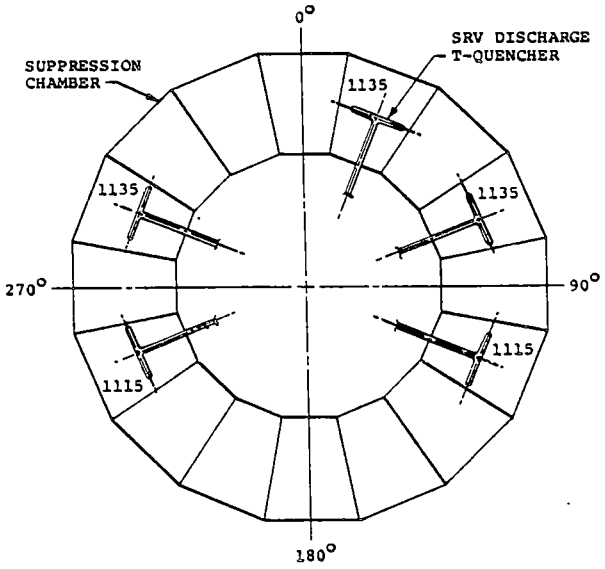

UNIT 3

1. SET POINT PRESSURES SHOWN ARE IN PSI.

Figure 2-2.1-13

T-QUENCHER LOCATIONS AND SRV SET POINT PRESSURES - PLAN VIEW

nutech ENGINEERS

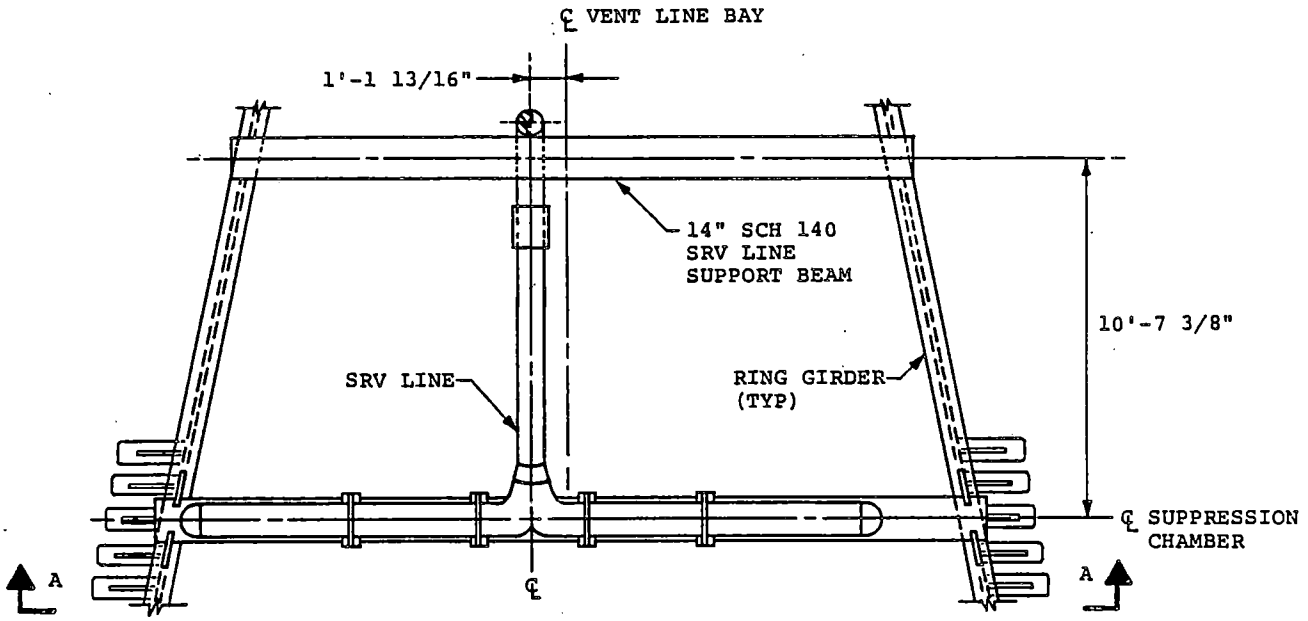

PLAN VIEW

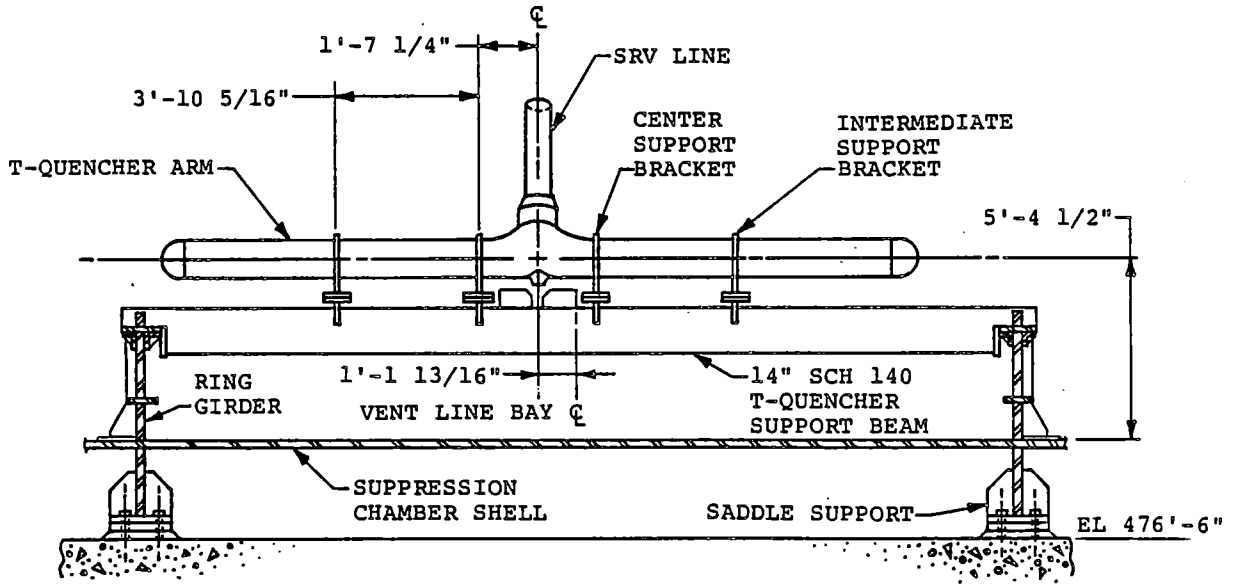

VIEW A-A

Figure 2-2.1-14

T-QUENCHER AND T-QUENCHER SUPPORTS

nutech ENGINEERS

2-2.2 Loads and Load Combinations

The loads for which the Dresden suppression chambers are evaluated are defined in NUREG-0661 on a generic basis for all Mark I plants. The methodology used to develop plant unique suppression chamber loads for each load defined in NUREG-0661 is discussed in Section 1-4.0. The results of applying the methodology to develop specific values for each of the governing loads which act on the suppression chamber are discussed and presented in Section 2-2.2.1.

The controlling load combinations which affect the suppression chamber are formulated using the event combinations and event sequencing defined in NUREG-0661 and discussed in Sections 1-3.2 and 1-4.3. The controlling suppression chamber load combinations are discussed and presented in Section 2-2.2.2.

2-2.2.1 Loads

The loads acting on the suppression chamber are categorized as follows:

1. Dead Weight Loads
2. Seismic Loads
3. Pressure and Temperature Loads
4. Column Preset Loads
5. Pool Swell Loads
6. Condensation Oscillation Loads
7. Chugging Loads
8. Safety Relief Valve Discharge Loads
9. Containment Interaction Loads

Loads in Categories 1 through 3 were considered in the original containment design. Loads in Categories 1 and 3 are documented in the plants' containment data specifications (References 5 and 6) and loads in Category 2 are documented in the plants' design specification (Reference 7). Additional Category 3 pressure and temperature loads result from postulated LOCA and SRV discharge events. Loads in Category 4 are documented in Chicago Bridge and Iron Company (CB&I) Drawing Number 204, (References 11 and 12). Loads in Categories 5 through 7 result from postulated LOCA events; loads in Category 8 result from SRV discharge

events; loads in Category 9 are reactions which result from loads acting on other structures attached to the suppression chamber.

Not all of the loads defined in NUREG-0661 are evaluated in detail, because some are enveloped by others or have a negligible effect on the suppression chamber. Only those loads which maximize the suppression chamber response and lead to controlling stresses are fully evaluated. These loads are referred to as governing loads in subsequent discussions.

Table 2-2.2-1 shows the specific suppression chamber components affected by each of the loadings defined in NUREG-0661. The table also lists the section in Volume 1 which discusses the methodology for developing values for each loading. The magnitudes and characteristics of each governing suppression chamber load in each load category are identified and presented in the following paragraphs.

1. Dead Weight Loads

a. Dead Weight of Steel: The weight of steel used to construct and modify the suppression

chamber and its supports is considered. The nominal component dimensions and a density of steel of 490 lb/ft^3 are used in this calculation.

b. Dead Weight of Water: The weight of water contained in the suppression chamber is considered. A volume of water of 115,655 ft^3, corresponding to a water level of 1-1/2" below the suppression chamber horizontal centerline and a water density of 62.4 lb/ft^3, are used in this calculation. This suppression chamber water volume is the maximum expected during normal operating conditions (NOC).

2. Seismic Loads

a. OBE Loads: The suppression chamber is subjected to horizontal and vertical accelerations during an operating basis earthquake (OBE). This loading is taken from the original design basis earthquake (DBE) for the containment documented in the plants' design specification. The OBE loads have a

maximum horizontal acceleration of 0.25g and a maximum vertical acceleration of 0.07g.

b. SSE Loads: The suppression chamber is subjected to horizontal and vertical accelerations during a safe shutdown earthquake (SSE). This loading is taken from the original DBE for the containment documented in the plant's safety analysis report. The SSE loads have a maximum horizontal acceleration of 0.50g and a maximum vertical acceleration of 0.14g.

3. Pressure and Temperature Loads

a. Normal Operating Internal Pressure Loads: The suppression chamber shell is subjected to internal pressure loads during normal operating conditions. This loading is taken from the original design specifications for the containment documented in the plants' containment data specifications (References 5 and 6). The range of normal operating internal pressures specified is -0.2 to 0.2 psig.

b. LOCA Internal Pressure Loads: The suppression chamber shell is subjected to internal pressure during a SBA, IBA, or DBA event. The procedure used to develop LOCA internal pressures for the primary containment is discussed in Section 1-4.1.1. Figures 2-2.2-1 through 2-2.2-3 present the resulting suppression chamber internal pressure transients and pressure magnitudes at key times during the SBA, IBA, and DBA events.

The pressures specified for each event are assumed to act uniformly over the suppression chamber shell surface, except during the early portion of a DBA event. The effects of internal pressure on the suppression chamber for the initial portion of a DBA event are included in the pool swell torus shell loads, discussed in Load Cases 5a and 5b. The corresponding suppression chamber external or secondary containment pressure for all events is assumed to be 0.0 psig.

c. Normal Operating Temperature Loads: The suppression chamber is subjected to the thermal expansion load associated with normal operating conditions. This loading is taken from the original design specification for the containment documented in the plants' containment data specifications.

Additional suppression chamber normal operating temperatures are taken from the suppression pool temperature response analysis (Reference 4). Table 2-2.2-2 summarizes the maximum bulk pool temperatures.

The range of normal operating temperatures in the suppression chamber during a concurrent SRV discharge event is 70° to 165°F (References 4, 5, and 6).

d. LOCA Temperature Loads: The suppression chamber is subjected to thermal expansion loads associated with the SBA, IBA, and DBA events. The procedure used to develop LOCA containment temperatures is discussed in Section 1-4.1.1. Figures 2-2.2-4 through

2-2.2-6 present the resulting suppression chamber temperature transients and temperature magnitudes at key times during the SBA, IBA, and DBA events.

Additional suppression chamber SBA event temperatures are taken from the suppression pool temperature response analysis. Table 2-2.2-2 summarizes the resulting maximum bulk pool temperatures. The greater of the temperatures specified in Figure 2-2.2-4 and Table 2-2.2-2 is used in evaluating the effects of SBA event temperatures.

The temperatures specified for each event are assumed to be representative of pool temperatures, airspace temperatures, and torus shell metal temperatures throughout the suppression chamber. The ambient temperature for all events is assumed to be equal to the minimum temperature during normal operating conditions.

As the temperature of the torus shell begins to increase, the temperature difference

between the torus shell and the suppression chamber vertical supports will result in differential thermal expansion effects. Temperatures in the suppression chamber vertical supports are obtained from a one-dimensional steady-state heat transfer analysis performed using the thermal characteristics of the suppression chamber. Coefficients are then calculated and temperature profiles are derived (Figure 2-2.2-7).

4. Column Preset Loads

a. The inside column of the suppression chamber is preset 3/16" radially outward and the outside column is preset 11/16" radially outward. The columns are preset at their bases to allow for radial growth due to thermal expansion, pressure, and seismic loads.

5. Pool Swell Loads

The Dresden Units 2 and 3 employ a system to maintain a 1 psi pressure differential between the

drywell and wetwell (References 5 and 6). The purpose of this system is to reduce the downcomer waterleg and thereby mitigate the pressure exerted on the torus shell during a LOCA event.

As required by NUREG-0661, Load Combination Number 16 (defined in Table 2-2.2-3) must be evaluated twice, once assuming the pressure differential is intact, and once assuming the pressure differential is lost. A higher stress allowable is permitted for the latter case.

a. Operating Differential Pressure Pool Swell Torus Shell Loads: During the initial phase of a DBA event, transient pressures are postulated to act on the suppression chamber shell above and below the suppression pool surface. The procedure used to develop local torus shell pressures due to pool swell is discussed in Section 1-4.1.3. Figures 2-2.2-8 and 2-2.2-9 show the resulting pressure-time histories at selected locations on the torus shell. Table 2-2.2-4 shows a sampling of operating ΔP pool swell torus shell pressures at various locations and at key times during the event.

These results are based on plant unique quarter-scale test facility (QSTF) test data contained in the PULD (Reference 3) and include the effects of the generic spatial distribution factors and of the conservatism factors on the peak upward and downward loads. Pool swell torus shell loads consist of a quasi-static internal pressure component and a dynamic pressure component, and include the effects of the DBA internal pressure discussed in Load Case 3b. Pool swell loads occurring during SBA and IBA events are bounded by the DBA case.

b. Zero Differential Pressure Pool Swell Torus Shell Loads: The zero ΔP pool swell load phenomena are the same as those previously described for the operating ΔP conditions. Figures 2-2.2-10 and 2-2.2-11 show the resulting pressure-time histories at selected locations on the torus shell. Table 2-2.2-5 shows a sampling of zero ΔP pool swell torus shell pressures at various locations and at key times during the event. These results were calculated on the same basis as the operating ΔP results.

c. LOCA Water Jet Loads on Submerged Structures: Transient drag pressures are postulated to act on structures that are within four downcomer diameters below the downcomer exit elevation. The structure involved is the ring girder. The procedure used to develop the transient forces of the LOCA water jet loads on the ring girder is discussed in Section 1-4.1.5.

In comparison with other submerged structure loads on the ring girder, these loads have a negligible effect on the final stress levels, and will not be considered in this evaluation.

d. LOCA Bubble-Induced Loads on Submerged Structures: Transient drag pressures are postulated to act on the ring girders and other structures during the air clearing phase of a DBA event. The procedure used to develop the transient forces and spatial distribution of LOCA bubble-induced drag loads on these components is discussed in Section 1-4.1.6.

In comparison with other submerged structure loads on the ring girder, these loads have a negligible effect on the final stress levels, and will not be considered in this evaluation.

6. Condensation Oscillation Loads

a. DBA CO Torus Shell Loads: Harmonic pressures are postulated to act on the submerged portion of the suppression chamber shell during the CO phase of a DBA event. The procedure used to develop DBA CO torus shell pressures is discussed in Section 1-4.1.7. Figure 2-2.2-12 shows the resulting normalized spatial distribution of pressures on a typical suppression chamber shell cross-section. Table 2-2.2-6 shows the amplitudes for each of the 50 harmonics and four DBA CO load case alternates.

The results of each harmonic in the DBA CO loading are combined using the methodology discussed in Section 1-4.1.7.

b. IBA CO Torus Shell Loads: Harmonic pressures are postulated to act on the submerged portion of the suppression chamber shell during an IBA event. In accordance with NUREG-0661, the torus shell loads specified for pre-chug are used in lieu of IBA CO torus shell loads. Pre-chug torus shell loads are discussed in Load Case 7a.

Condensation oscillation loads on the torus shell and submerged structures do not occur during a SBA event.

c. DBA CO Submerged Structure Loads: Harmonic drag pressures are postulated to act on the ring girders during the CO phase of a DBA event. The procedure used to develop the harmonic forces and spatial distribution of DBA CO drag loads on these components is discussed in Section 1-4.1.7.

Loads are developed for the case with the average source strength at all downcomers and for the case with the maximum source strength at the nearest downcomer. The results of

these two cases are evaluated to determine the controlling loads. Table 2-2.2-7 shows the resulting magnitudes and distribution of drag pressures acting on the ring girders for the controlling DBA CO load case.

These results include the effects of velocity drag, acceleration drag, torus shell FSI acceleration drag, interference effects, wall effects, and acceleration drag volumes. Figure 2-2.2-13 shows a typical pool acceleration profile from which the FSI accelerations are derived. The results of each harmonic in the DBA CO loading are combined using the methodology discussed in Section 1-4.1.7.

d. IBA CO Submerged Structure Loads: Harmonic pressures are postulated to act on the submerged suppression chamber components during the CO phase of an IBA event. In accordance with NUREG-0661, the submerged structure loads specified for pre-chug are used in lieu of IBA CO loads on submerged structures. Pre-chug loads on submerged structures are discussed in Load Case 7c.

Condensation oscillation loads do not occur during a SBA event.

7. Chugging Loads

a. Pre-Chug Torus Shell Loads: During the chugging phase of a SBA, an IBA, or a DBA event, harmonic pressures associated with the pre-chug portion of a chugging cycle are postulated to act on the submerged portion of the suppression chamber shell. The procedure used to develop pre-chug torus shell loads is discussed in Section 1-4.1.8.

The loading consists of a single harmonic with a specified frequency range and can act either symmetrically or asymmetrically with respect to the vertical centerline of the containment. Figure 2-2.2-14 shows the circumferential pressure distribution on a typical suppression chamber cross-section for both symmetric and asymmetric pre-chug loads. Figure 2-2.2-15 shows the longitudinal pressure distribution for the asymmetric pre-chug load. The symmetric pre-chug load

results in vertical loads on the suppression chamber; the asymmetric pre-chug load results in lateral loads on the suppression chamber.

b. Post-Chug Torus Shell Loads: During the chugging phase of a SBA, an IBA, or a DBA event, harmonic pressures associated with the postchug portion of a chugging cycle are postulated to act on the submerged portion of the suppression chamber shell. The procedure used to develop post-chug torus shell loads is defined in Section 1-4.1.8. Figure 2-2.2-12 shows the resulting normalized spatial distribution of pressure on a typical suppression chamber cross-section. Table 2-2.2-8 shows the pressure amplitudes for each of the 50 harmonics in the post-chug loading. The results of each harmonic in the post-chug loading are combined using the methodology discussed in Section 1-4.1.8.

c. Pre-Chug Submerged Structure Loads: During the chugging phase of a SBA, an IBA, or a DBA event, harmonic drag pressures associated with the pre-chug portion of a chugging cycle

are postulated to act on the ring girders and other submerged structures. The procedure used to develop the harmonic forces and spatial distribution of pre-chug drag loads on the ring girders is discussed in Section 1-4.1.8.

Loads are developed for the case with the average source strength at all downcomers and for the case with the maximum source strength at the nearest downcomer. The results of these two cases are evaluated to determine the controlling loads.

These results include the effects of velocity drag, acceleration drag, torus shell FSI acceleration drag, interference effects, wall effects, and acceleration drag volumes. Figure 2-2.2-13 shows a typical pool acceleration profile from which the FSI accelerations are derived.

In comparison with other submerged structure loads on the ring girder, these loads have a negligible effect on the final stress levels,

and will not be considered in this evaluation.

d. Post-Chug Submerged Structure Loads: During the chugging phase of a SBA, an IBA, or a DBA event, harmonic drag pressures associated with the post-chug portion of a chugging cycle are postulated to act on the ring girders. The procedure used to develop the harmonic forces and spatial distribution of post-chug drag loads on the ring girders and other submerged structures is discussed in Section 1-4.1.8.

Loads are developed for the case with the maximum source strength at the nearest two downcomers acting both in phase and out of phase. The results of these cases are evaluated to determine the controlling loads. Table 2-2.2-9 shows the resulting magnitudes and distribution of post-chug drag pressures acting on the ring girder for the controlling post-chug drag load case.

These results include the effects of velocity drag, acceleration drag, torus shell FSI acceleration drag, interference effects, wall effects, and acceleration drag volumes. Figure 2-2.2-13 shows a typical pool acceleration profile from which the FSI accelerations are derived. The results of each harmonic in the post-chug loading are combined using the methodology discussed in Section 1-4.1.8.

8. Safety Relief Valve Discharge Loads

a-b. SRV Discharge Torus Shell Loads: Transient pressures are postulated to act on the submerged portion of the suppression chamber shell during the air clearing phase of a SRV discharge event. The procedure used to develop SRV discharge torus shell loads is discussed in Section 1-4.2.3. The maximum torus shell pressures and characteristics of the SRV discharge pressure transients are developed using an attenuated bubble model. Pressure transients which include the addi-

tional load mitigation effects of the 12" diameter T-quenchers are developed.

The SRV actuation cases considered are discussed in Section 1-4.2.1. Figure 2-2.1-13 shows the location of each T-quencher and the corresponding SRV set point pressure.

The case resulting in maximum torus shell pressures is Case A1.2, a SBA/IBA first actuation case with elevated drywell pressure and temperature. This load is conservatively used for the Multiple Valve Case 8b, with actuation occurring in all five SRVDL bays simultaneously. Actuation of the automatic depressurization system (ADS) also creates this Multiple Valve Case 8b.

The Single Valve Case 8a was conservatively derived from the multiple valve case results. Multiple valve results were factored by the ratio of the maximum shell pressure for the single valve load profile to that of the multiple valve load profile. When the ratio of 0.669 is applied to the multiple valve

load profile, the resulting load is a conservative approximation of the single valve load profile at all locations on the suppression chamber shell. In this manner, the single valve results are conservatively obtained.

Figures 2-2.2-16 and 2-2.2-17 show the resulting SRV discharge torus shell loads for the Single Valve Case 8a and Multiple Valve Case 8b, respectively. The results shown include the effects of applying the LDR (Reference 2) pressure attenuation algorithm to obtain the spatial distribution of torus shell pressures, the absolute summation of multiple valve effects with application of the bubble pressure cut-off criteria, use of first actuation pressures with subsequent actuation frequencies, and application of the ±25% and ±40% margins to the first and subsequent actuation frequencies, respectively. This methodology is in accordance with the conservative criteria contained in NUREG-0661.

The distribution of SRV discharge torus shell pressures is asymmetric with respect to the vertical centerline of the containment. The pressure distribution which results in the maximum total vertical and horizontal loads on the suppression chamber occurs for the Multiple Valve Case 8b (Figure 2-2.2-17). Figure 2-2.2-18 shows the longitudinal pressure distribution for Multiple Valve Case 8b.

c. SRV Discharge Water Jet Loads on Submerged Structures: Transient drag pressures are postulated to act on structures which fully or partially intercept the water jets being discharged from the T-quencher. The structure involved is the ring girder. The procedure used to develop the transient forces of the SRV discharge water jet loads on the ring girder is discussed in Section 1-4.2.4.

These results include the effects of velocity drag, interference effects, and wall effects.

In comparison with other submerged structure loads on the ring girder, these loads have a negligible effect on the final stress levels, and will not be considered in this evaluation.

d. SRV Discharge Bubble-Induced Drag Loads on Submerged Structures: Transient drag pressures are postulated to act on the ring girders during the air clearing phase of a SRV discharge event. The procedure used to develop the transient forces and spatial distribution of the SRV discharge bubble-induced drag loads on these structures is discussed in Section 1-4.2.4.

Loads on the ring girder and other submerged structures are developed for the following load cases: four bubbles from a T-quencher are considered to act first in phase and then out of phase with the four bubbles from a T-quencher in the next T-quencher bay (two bays away). The results are evaluated to determine the controlling loads. Table 2-2.2-10 shows the resulting magnitudes and

distribution of drag pressures acting on a ring girder for the controlling SRV discharge bubble-induced drag load case. The results include the effects of velocity drag, acceleration drag, interference effects, wall effects, acceleration drag volumes, and the additional load mitigation effects of the 12" diameter T-quencher.

9. Containment Interaction Loads

a. Containment Structure Reaction Loads: Loads acting on the suppression chamber, vent system, SRVDL support, T-quencher support, ECCS header support, and catwalk cause interaction effects between these structures. These interaction effects result in reaction loads on the suppression chamber shell saddle support and ring girder at the points where these structures attach to the suppression chamber. The effects of these reaction loads on the suppression chamber are considered in the suppression chamber analysis.

The values of the loads presented in the preceding paragraphs envelop those which could occur during the LOCA or SRV discharge events postulated. An evaluation for the effects of these loads results in conservative estimates of the suppression chamber responses and leads to bounding values of suppression chamber stresses.

Table 2-2.2-1

SUPPRESSION CHAMBER COMPONENT LOADING IDENTIFICATION

VOLUME 2 LOAD DESIGNATION			PUAR SECTION REFERENCE	COMPONENT PART LOADED					REMARKS
CATEGORY	LOAD TYPE	CASE NUMBER		TORUS SHELL	RING GIRDER	COLUMNS	COLUMN CONNEC-TIONS	SADDLE	
DEAD WEIGHT LOADS	DEAD WEIGHT STEEL	1a	1-3.1	X	X	X	X	X	AS-MODIFIED GEOMETRY
	DEAD WEIGHT WATER	1b	1-3.1	X					115,655 FT^3 WATER
SEISMIC LOADS	OBE SEISMIC LOADS	2a	1-3.1	X	X	X	X	X	0.25 HORIZONTAL, 0.07 VERTICAL
	SSE SEISMIC LOADS	2b	1-3.1	X	X	X	X	X	0.50 HORIZONTAL, 0.14 VERTICAL
PRESSURE AND TEMPERATURE LOADS	NORMAL OPERATING INTERNAL PRESSURE	3a	1-3.1	X					-0.2 TO 0.2 PSI
	LOCA INTERNAL PRESSURE	3b	1-4.1.1	X					SBA, IBA, & DBA PRESSURES
	NORMAL OPERATING TEMPERATURE LOADS	3c	1-3.1	X	X	X	X	X	70 TO 165°F
	LOCA TEMPERATURE LOADS	3d	1-4.1.1	X	X	X	X	X	SBA, IBA, & DBA TEMPERATURES
PRESET LOADS	COLUMN PRESET	4a	1-1.3.1			X			3/16" INSIDE, 11/16" OUTSIDE COLUMN
POOL SWELL LOADS	OPERATING DELTA P POOL SWELL TORUS SHELL LOADS	5a	1-4.1.3	X					INCLUDES DBA INTERNAL PRESSURES
	ZERO DELTA P POOL SWELL TORUS SHELL LOADS	5b	1-4.1.3	X					INCLUDES DBA INTERNAL PRESSURES
	LOCA WATER JET SUBMERGED STRUCTURE LOADS	5c	1-4.1.5		X				PRIMARILY LOCAL EFFECTS
	LOCA BUBBLE-INDUCED LOADS ON SUBMERGED STRUCTURES	5d	1-4.1.6		X				PRIMARILY LOCAL EFFECTS
CONDENSATION OSCILLATION LOADS	DBA CO TORUS SHELL LOADS	6a	1-4.1.7.1	X					FOUR LOADING ALTERNATES
	IBA CO TORUS SHELL LOADS	6b	1-4.1.7.1	X					ENVELOPED BY LOAD CASE 6a
	DBA CO SUBMERGED STRUCTURE LOADS	6c	1-4.1.7.3		X				PRIMARILY LOCAL EFFECTS
	IBA CO SUBMERGED STRUCTURE LOADS	6d	1-4.1.7.3		X				ENVELOPED BY LOAD CASE 6c
CHUGGING LOADS	PRE-CHUG TORUS SHELL LOADS	7a	1-4.1.8.1	X					SYMMETRIC & ASYMMETRIC LOADINGS
	POST-CHUG TORUS SHELL LOADS	7b	1-4.1.8.1	X					SYMMETRIC LOADING
	PRE-CHUG SUBMERGED STRUCTURE LOADS	7c	1-4.1.8.3		X				PRIMARILY LOCAL EFFECTS
	POST-CHUG SUBMERGED STRUCTURE LOADS	7d	1-4.1.8.3		X				PRIMARILY LOCAL EFFECTS
SRV DISCHARGE LOADS	SRV DISCHARGE TORUS SHELL LOADS	8a-8b	1-4.2.3	X					SINGLE & MULTIPLE VALVE CASES
	SRV DISCHARGE WATER JET SUBMERGED STRUCTURE LOADS	8c	1-4.2.4		X				PRIMARILY LOCAL EFFECTS
	SRV DISCHARGE BUBBLE-INDUCED DRAG LOADS ON SUBMERGED STRUCTURES	8d	1-4.2.4		X				PRIMARILY LOCAL EFFECTS
CONTAINMENT INTERACTION LOADS	CONTAINMENT STRUCTURE REACTION LOADS	9a	VOLUMES 3-5	X	X				SUPPORTED STRUCTURES REACTIONS

Table 2-2.2-2

SUPPRESSION POOL TEMPERATURE RESPONSE ANALYSIS

RESULTS - MAXIMUM TEMPERATURES

CONDITION	CASE[1] NUMBER	NUMBER OF SRV'S ACTUATED	MAXIMUM BULK POOL TEMPERATURE (°F)
NORMAL OPERATING	1A	0	131
	1B	0	129
	2A	1	113
	2B	1	122
	2C	2	115
SBA EVENT	3A	5	154
	3B	5	147

1. SEE SECTION 1-5.1 FOR DESCRIPTION OF SRV DISCHARGE EVENTS CONSIDERED.

Table 2-2.2-3

MARK I CONTAINMENT EVENT COMBINATIONS

EVENT COMBINATIONS			SRV	SRV + EQ		SBA IBA		SBA + EQ IBA + EQ				SBA+SRV IBA+SRV		SBA + SRV + EQ IBA + SRV + EQ				DBA		DBA + EQ						DBA + SRV + EQ			
							CO, CH			CO, CH			CO, CH			CO, CH		PS (2)	CO, CH	PS		CO, CH		PS	CO, CH	PS		CO, CH	
TYPE OF EARTHQUAKE				O	S			O	S	O	S			O	S	O	S			O	S	O	S			O	S	O	S
COMBINATION NUMBER			1	2	3	4	5	6	7	8	9	10	11	12	13	14	15	16	17	18	19	20	21	22	23	24	25	26	27
LOADS	NORMAL	N	X	X	X	X	X	X	X	X	X	X	X	X	X	X	X	X	X	X	X	X	X	X	X	X	X	X	X	X
	EARTHQUAKE	EQ		X	X			X	X	X	X			X	X	X	X			X	X	X	X			X	X	X	X
	SRV DISCHARGE	SRV	X	X	X							X	X	X	X	X	X							X	X	X	X	X	X
	LOCA THERMAL	T_A				X	X	X	X	X	X	X	X	X	X	X	X	X	X	X	X	X	X	X	X	X	X	X	X
	LOCA REACTIONS	R_A				X	X	X	X	X	X	X	X	X	X	X	X	X	X	X	X	X	X	X	X	X	X	X	X
	LOCA QUASI-STATIC PRESSURE	P_A				X	X	X	X	X	X	X	X	X	X	X	X	X	X	X	X	X	X	X	X	X	X	X	X
	LOCA POOL SWELL	P_{PS}																X		X	X			X		X	X		
	LOCA CONDENSATION OSCILLATION	P_{CO}					X			X	X		X			X	X		X			X	X		X			X	X
	LOCA CHUGGING	P_{CH}					X			X	X		X			X	X		X			X	X		X			X	X

1. SEE SECTION 1-3.2 FOR ADDITIONAL EVENT COMBINATION INFORMATION.
2. FOR OPERATING AND ZERO DIFFERENTIAL PRESSURE CASES. ALL OTHER POOL SWELL COMBINATIONS ARE FOR OPERATING CONDITIONS ONLY.

nutech ENGINEERS

Table 2-2.2-4

TORUS SHELL PRESSURES DUE TO OPERATING DIFFERENTIAL PRESSURE
POOL SWELL AT KEY TIMES AND SELECTED LOCATIONS

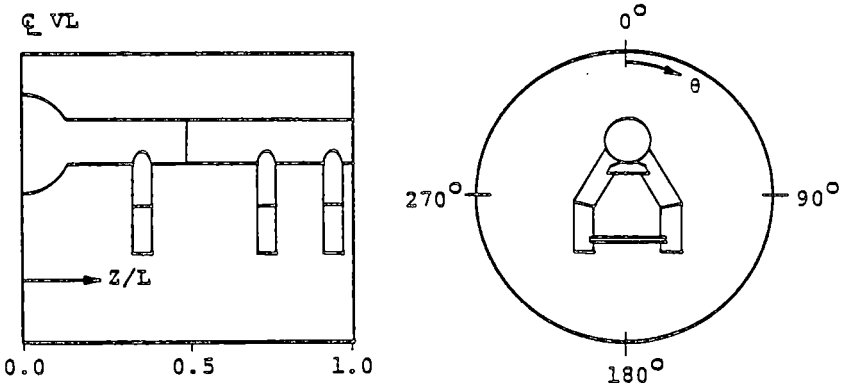

LONGITUDINAL LOCATION (Z/L)	CIRCUMFERENTIAL LOCATION (θ deg)	TORUS SHELL PRESSURE (psi) OPERATING DIFFERENTIAL PRESSURE	
		PEAK DOWNLOAD (t=0.238 sec)	PEAK UPLOAD (t=0.474 sec)
0.000	180	8.4	6.0
0.000	165, 195	8.4	6.2
0.000	150, 210	7.6	6.2
0.000	135, 225	6.2	6.8
0.000	0-120, 240-0	4.5(1)	7.9
0.361	180	9.2	5.4
0.361	165, 195	9.1	5.6
0.361	150, 210	8.3	5.6
0.361	135, 225	6.8	6.1
0.361	0-120, 240-0	4.9(1)	7.1
0.552	180	9.5	5.4
0.552	165, 195	9.4	5.6
0.552	150, 210	8.5	5.6
0.552	135, 225	7.0	6.1
0.552	0-120, 240-0	5.0(1)	7.1
0.895	180	9.9	5.3
0.895	165, 195	9.9	5.4
0.895	150, 210	8.9	5.5
0.895	135, 225	7.3	5.9
0.895	0-120, 240-0	5.3(1)	6.9
1.000	180	10.4	5.1
1.000	165, 195	10.3	5.3
1.000	150, 210	9.3	5.3
1.000	135, 225	7.6	5.8
1.000	0-120, 240-0	5.5(1)	6.7

(1) MAXIMUM IS AT 0.185 SECONDS.

Table 2-2.2-5

TORUS SHELL PRESSURES DUE TO ZERO DIFFERENTIAL PRESSURE
POOL SWELL AT KEY TIMES AND SELECTED LOCATIONS

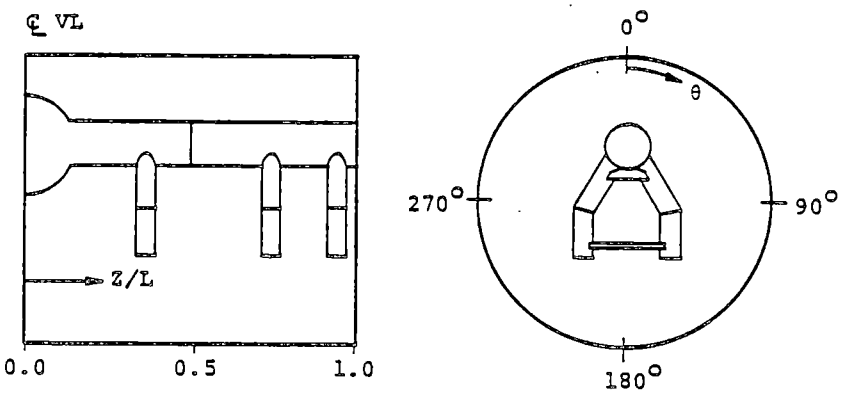

KEY DIAGRAM

LONGITUDINAL LOCATION (Z/L)	CIRCUMFERENTIAL LOCATION (θ deg)	TORUS SHELL PRESSURE (psi) ZERO DIFFERENTIAL PRESSURE	
		PEAK DOWNLOAD (t=0.275 sec)	PEAK UPLOAD (t=0.576 sec)
0.000	180	14.0	7.2
0.000	165, 195	14.0	7.4
0.000	150, 210	12.6	7.5
0.000	135, 225	10.4	8.1
0.000	0-120, 240-0	7.4	9.4
0.361	180	15.3	6.5
0.361	165, 195	15.2	6.7
0.361	150, 210	13.8	6.7
0.361	135, 225	11.3	7.3
0.361	0-120, 240-0	8.1	8.4
0.552	180	15.8	6.5
0.552	165, 195	15.7	6.7
0.552	150, 210	14.2	6.7
0.552	135, 225	11.7	7.3
0.552	0-120, 240-0	8.4	8.5
0.895	180	16.5	6.3
0.895	165, 195	16.4	6.5
0.895	150, 210	14.8	6.4
0.895	135, 225	12.2	7.1
0.895	0-120, 240-0	8.7	8.2
1.000	180	17.2	6.1
1.000	165, 195	17.1	6.3
1.000	150, 210	15.5	6.4
1.000	135, 225	12.7	6.9
1.000	0-120, 240-0	9.1	8.0

Table 2-2.2-6

DBA CONDENSATION OSCILLATION

TORUS SHELL PRESSURE AMPLITUDES

FREQUENCY INTERVALS (Hz)	MAXIMUM PRESSURE AMPLITUDE (psi)(1)			
	ALTERNATE 1	ALTERNATE 2	ALTERNATE 3	ALTERNATE 4
0-1	0.29	0.29	0.29	0.25
1-2	0.25	0.25	0.25	0.28
2-3	0.32	0.32	0.32	0.33
3-4	0.48	0.48	0.48	0.56
4-5	1.86	1.20	0.24	2.71
5-6	1.05	2.73	0.48	1.17
6-7	0.49	0.42	0.99	0.97
7-8	0.59	0.38	0.30	0.47
8-9	0.59	0.38	0.30	0.34
9-10	0.59	0.38	0.30	0.47
10-11	0.34	0.79	0.18	0.49
11-12	0.15	0.45	0.12	0.38
12-13	0.17	0.12	0.11	0.20
13-14	0.12	0.08	0.08	0.10
14-15	0.06	0.07	0.03	0.11
15-16	0.10	0.10	0.02	0.08
16-17	0.04	0.04	0.04	0.04
17-18	0.04	0.04	0.04	0.05
18-19	0.04	0.04	0.04	0.03
19-20	0.27	0.27	0.27	0.34
20-21	0.20	0.20	0.20	0.23
21-22	0.30	0.30	0.30	0.49
22-23	0.34	0.34	0.34	0.37
23-24	0.33	0.33	0.33	0.32
24-25	0.16	0.16	0.16	0.22

Table 2-2.2-6

DBA CONDENSATION OSCILLATION
TORUS SHELL PRESSURE AMPLITUDES
(Concluded)

FREQUENCY INTERVALS (Hz)	MAXIMUM PRESSURE AMPLITUDE (psi)(1)			
	ALTERNATE 1	ALTERNATE 2	ALTERNATE 3	ALTERNATE 4
25-26	0.25	0.25	0.25	0.50
26-27	0.58	0.58	0.58	0.51
27-28	0.13	0.13	0.13	0.39
28-29	0.19	0.19	0.19	0.26
29-30	0.14	0.14	0.14	0.09
30-31	0.08	0.08	0.08	0.08
31-32	0.03	0.03	0.03	0.07
32-33	0.03	0.03	0.03	0.05
33-34	0.03	0.03	0.03	0.04
34-35	0.05	0.05	0.05	0.04
35-36	0.08	0.08	0.08	0.07
36-37	0.10	0.10	0.10	0.11
37-38	0.07	0.07	0.07	0.06
38-39	0.06	0.06	0.06	0.05
39-40	0.09	0.09	0.09	0.02
40-41	0.33	0.33	0.33	0.08
41-42	0.33	0.33	0.33	0.19
42-43	0.33	0.33	0.33	0.19
43-44	0.33	0.33	0.33	0.13
44-45	0.33	0.33	0.33	0.18
45-46	0.33	0.33	0.33	0.30
46-47	0.33	0.33	0.33	0.18
47-48	0.33	0.33	0.33	0.19
48-49	0.33	0.33	0.33	0.16
49-50	0.33	0.33	0.33	0.21

(1) SEE FIGURE 2-2.2-12 FOR SPATIAL DISTRIBUTION OF PRESSURES.

Table 2-2.2-7

RING GIRDER DBA CONDENSATION OSCILLATION SUBMERGED STRUCTURE LOAD DISTRIBUTIONS(1)

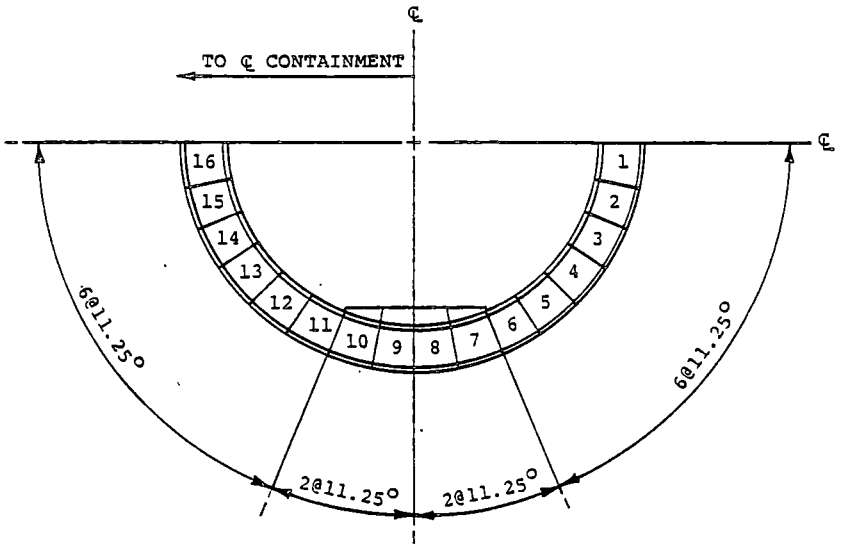

KEY DIAGRAM

SEGMENT NUMBER	WEB PRESSURE (psi) (2)			FLANGE PRESSURE (psi) (3)		
	APPLIED LOAD	FSI	TOTAL	APPLIED LOAD	FSI	TOTAL
1	0.16	0.24	0.40	0.39	6.03	6.42
2	0.44	0.34	0.78	0.73	4.78	5.51
3	0.68	0.78	1.46	0.21	3.14	3.35
4	0.83	0.68	1.51	0.56	2.84	3.40
5	1.25	0.51	1.76	1.11	1.97	3.08
6	1.06	0.68	1.74	1.59	3.34	4.93
7	2.28	0.31	2.59	1.65	4.85	6.50
8	2.98	0.46	3.44	0.77	7.00	7.77
9	2.89	1.01	3.90	0.61	4.31	8.21
10	2.61	2.05	4.66	1.10	8.24	9.34
11	1.52	1.59	3.11	1.72	6.27	7.99
12	1.96	1.42	3.38	1.79	8.43	10.22
13	1.72	1.44	3.16	1.47	7.14	8.61
14	1.18	2.48	3.66	1.48	4.36	5.84
15	0.86	2.42	3.28	0.70	4.33	5.03
16	0.42	0.79	1.21	0.46	1.17	1.63

(1) LOADS SHOWN INCLUDE DLF'S.

(2) OUT-OF-PLANE LOADS.

(3) IN-PLANE LOADS.

Table 2-2.2-8

POST-CHUG TORUS SHELL PRESSURE AMPLITUDES

FREQUENCY INTERVAL (Hz)	MAXIMUM[1] PRESSURE AMPLITUDE (psi)
0 - 1	0.04
1 - 2	0.04
2 - 3	0.05
3 - 4	0.05
4 - 5	0.06
5 - 6	0.05
6 - 7	0.10
7 - 8	0.10
8 - 9	0.10
9 - 10	0.10
10 - 11	0.06
11 - 12	0.05
12 - 13	0.03
13 - 14	0.03
14 - 15	0.02
15 - 16	0.02
16 - 17	0.01
17 - 18	0.01
18 - 19	0.01
19 - 20	0.04
20 - 21	0.03
21 - 22	0.05
22 - 23	0.05
23 - 24	0.05
24 - 25	0.04

Table 2-2.2-8

POST-CHUG TORUS SHELL PRESSURE AMPLITUDES

(Concluded)

FREQUENCY INTERVAL (Hz)	MAXIMUM[1] PRESSURE AMPLITUDE (psi)
25 - 26	0.04
26 - 27	0.28
27 - 28	0.18
28 - 29	0.12
29 - 30	0.09
30 - 31	0.03
31 - 32	0.02
32 - 33	0.02
33 - 34	0.02
34 - 35	0.02
35 - 36	0.03
36 - 37	0.05
37 - 38	0.03
38 - 39	0.04
39 - 40	0.04
40 - 41	0.15
41 - 42	0.15
42 - 43	0.15
43 - 44	0.15
44 - 45	0.15
45 - 46	0.15
46 - 47	0.15
47 - 48	0.15
48 - 49	0.15
49 - 50	0.15

(1) SEE FIGURE 2-2.2-12 FOR SPATIAL DISTRIBUTION OF PRESSURES.

Table 2-2.2-9

RING GIRDER POST-CHUG SUBMERGED STRUCTURE LOAD DISTRIBUTIONS(1)

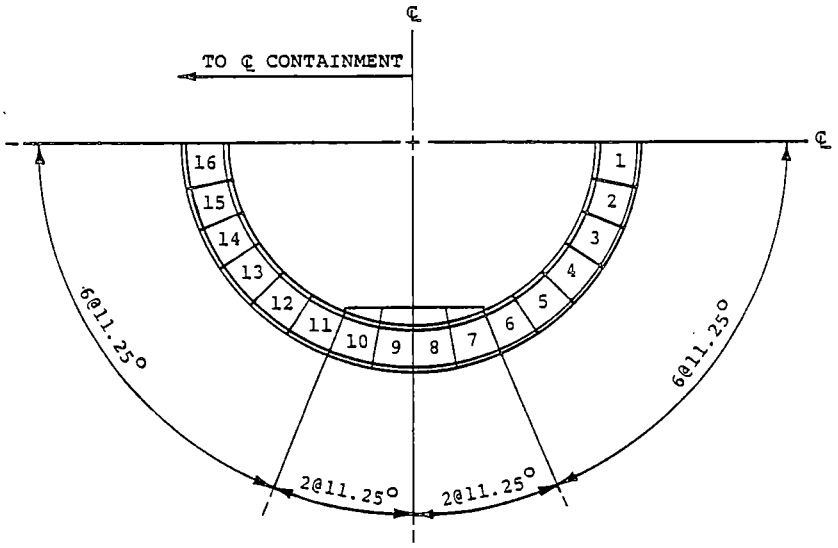

KEY DIAGRAM

SEGMENT NUMBER	WEB PRESSURE (psi)(2)			FLANGE PRESSURE (psi)(3)		
	APPLIED LOAD	FSI	TOTAL	APPLIED LOAD	FSI	TOTAL
1	0.68	0.10	0.78	0.16	0.88	1.04
2	0.68	0.05	0.73	0.66	1.63	2.29
3	1.03	0.11	1.14	1.06	0.68	1.74
4	3.39	0.22	3.61	1.12	0.40	1.52
5	4.45	0.15	4.60	1.24	0.31	1.55
6	1.14	0.09	1.23	2.70	0.75	3.45
7	2.28	0.06	2.34	4.90	1.47	6.37
8	8.06	0.16	8.22	1.05	1.10	2.15
9	7.32	0.26	7.58	0.86	1.15	2.01
10	2.32	0.31	2.63	2.39	1.09	3.48
11	1.44	0.24	1.68	8.13	1.22	9.35
12	7.38	0.34	7.72	2.61	1.22	3.83
13	5.61	0.28	5.89	2.60	1.47	4.07
14	1.40	0.46	1.86	5.56	0.89	6.45
15	0.86	0.41	1.27	0.64	0.59	1.23
16	1.24	0.19	1.43	0.10	0.34	0.44

(1) LOADS SHOWN INCLUDE DLF'S.

(2) OUT-OF-PLANE LOADS.

(3) IN-PLANE LOADS.

Table 2-2.2-10

RING GIRDER SRV SUBMERGED STRUCTURE

LOAD DISTRIBUTIONS

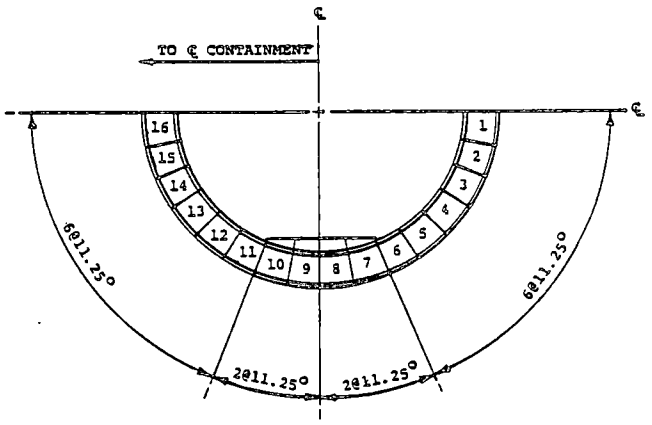

KEY DIAGRAM

SEGMENT NUMBER	SRV AIR BUBBLE (1)	
	WEB (2) PRESSURE (psi)	FLANGE (3) PRESSURE (psi)
1	0.52	0.68
2	1.71	1.65
3	2.70	1.25
4	3.30	0.65
5	4.35	1.83
6	6.21	4.92
7	19.07	12.48
8	15.32	8.82
9	15.32	8.82
10	19.07	12.48
11	6.21	4.92
12	4.35	1.83
13	3.30	0.65
14	2.70	1.25
15	1.71	1.65
16	0.52	0.68

(1) LOADS SHOWN INCLUDE DLF'S.

(2) OUT-OF-PLANE LOADS.

(3) IN-PLANE LOADS.

P_{min} = 0.5 psig

P_{max} = 27.3 psig

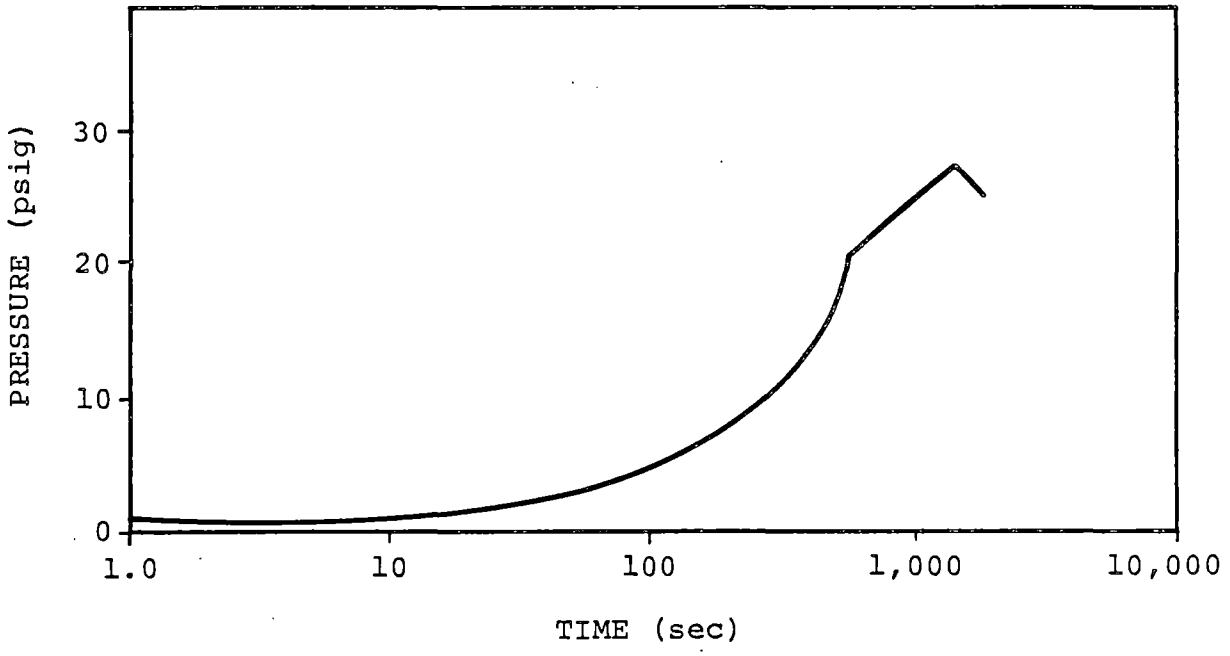

EVENT DESCRIPTION	PRESSURE DESIGNATION	TIME (sec)		PRESSURE (psig)	
		t_{min}	t_{max}	P_{min}	P_{max}
INSTANT OF BREAK TO ONSET OF CHUGGING	P_1	0.0	300.0	0.5	11.0
ONSET OF CHUGGING TO INITIATION OF ADS	P_2	300.0	600.0	11.0	21.5
INITIATION OF ADS TO RPV DEPRESSURIZATION	P_3	600.0	1200.0	21.5	27.3

Figure 2-2.2-1

SUPPRESSION CHAMBER INTERNAL PRESSURES FOR SBA EVENT

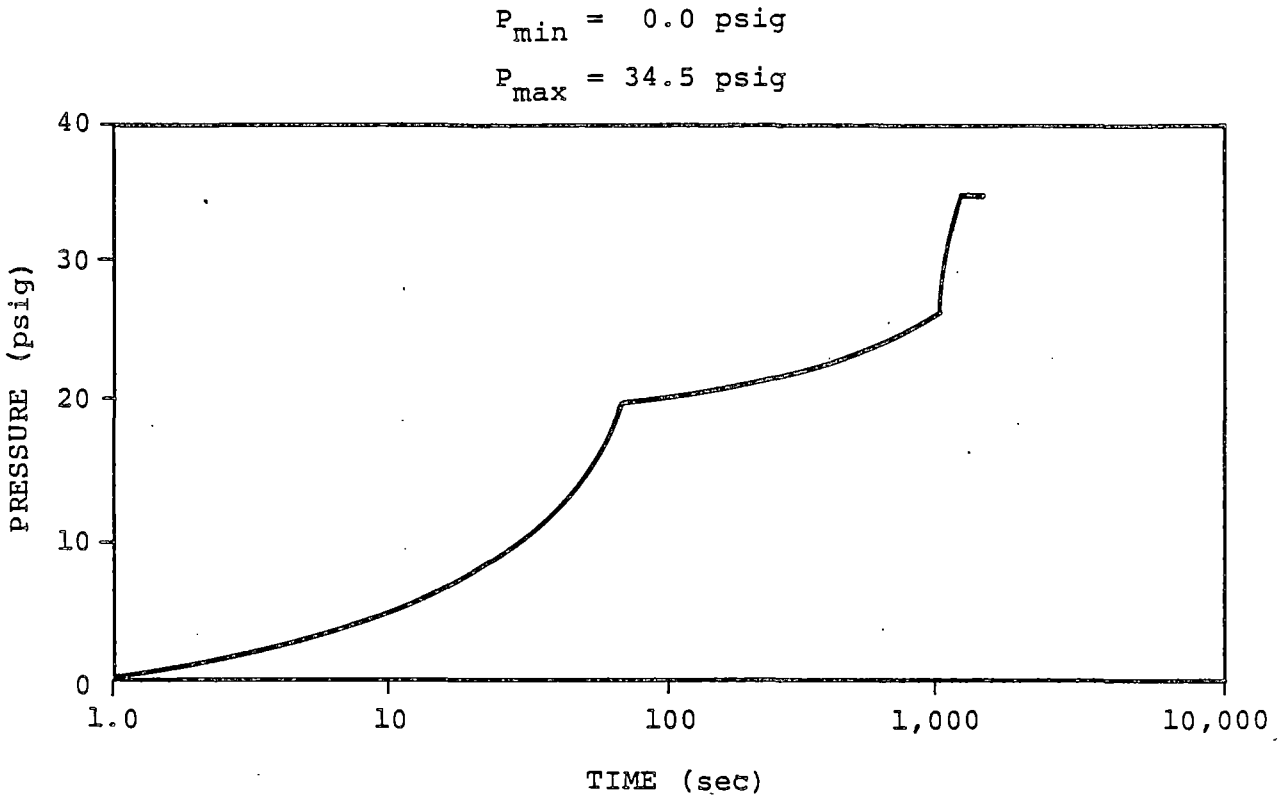

EVENT DESCRIPTION	PRESSURE DESIGNATION	TIME (sec)		PRESSURE (psig)	
		t_{min}	t_{max}	P_{min}	P_{max}
INSTANT OF BREAK TO ONSET OF CO AND CHUGGING	P_1	0.0	5.0	0.0	3.0
ONSET OF CO AND CHUGGING TO INITIATION OF ADS	P_2	5.0	900.0	3.0	25.9
INITIATION OF ADS TO RPV DEPRESSURIZATION	P_3	900.0	1100.0	25.9	34.5

Figure 2-2.2-2

SUPPRESSION CHAMBER INTERNAL PRESSURES FOR IBA EVENT

P_{min} = 0.0 psig

P_{max} = 26.6 psig

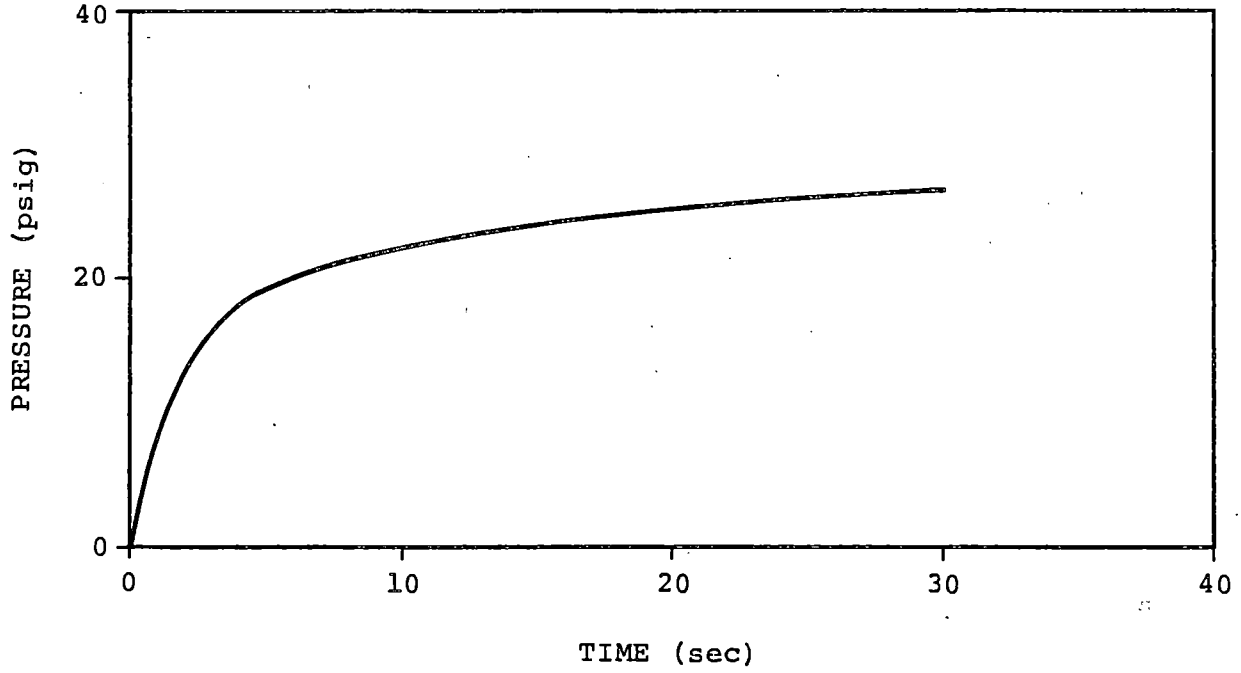

EVENT DESCRIPTION	PRESSURE DESIGNATION	TIME (sec)		PRESSURE (psig)	
		t_{min}	t_{max}	P_{min}	P_{max}
INSTANT OF BREAK TO TERMINATION OF POOL SWELL	P_1	0.0	1.5	0.0	10.0
TERMINATION OF POOL SWELL TO ONSET OF CO	P_2	1.5	5.0	10.0	19.0
ONSET OF CO TO ONSET OF CHUGGING	P_3	5.0	35.0	19.0	26.6
ONSET OF CHUGGING TO RPV DEPRESSURIZATION	P_4	35.0	65.0	26.6	26.6

Figure 2-2.2-3

SUPPRESSION CHAMBER INTERNAL PRESSURES FOR DBA EVENT

$T_{min} = 92^{o}F$

$T_{max} = 139^{o}F$

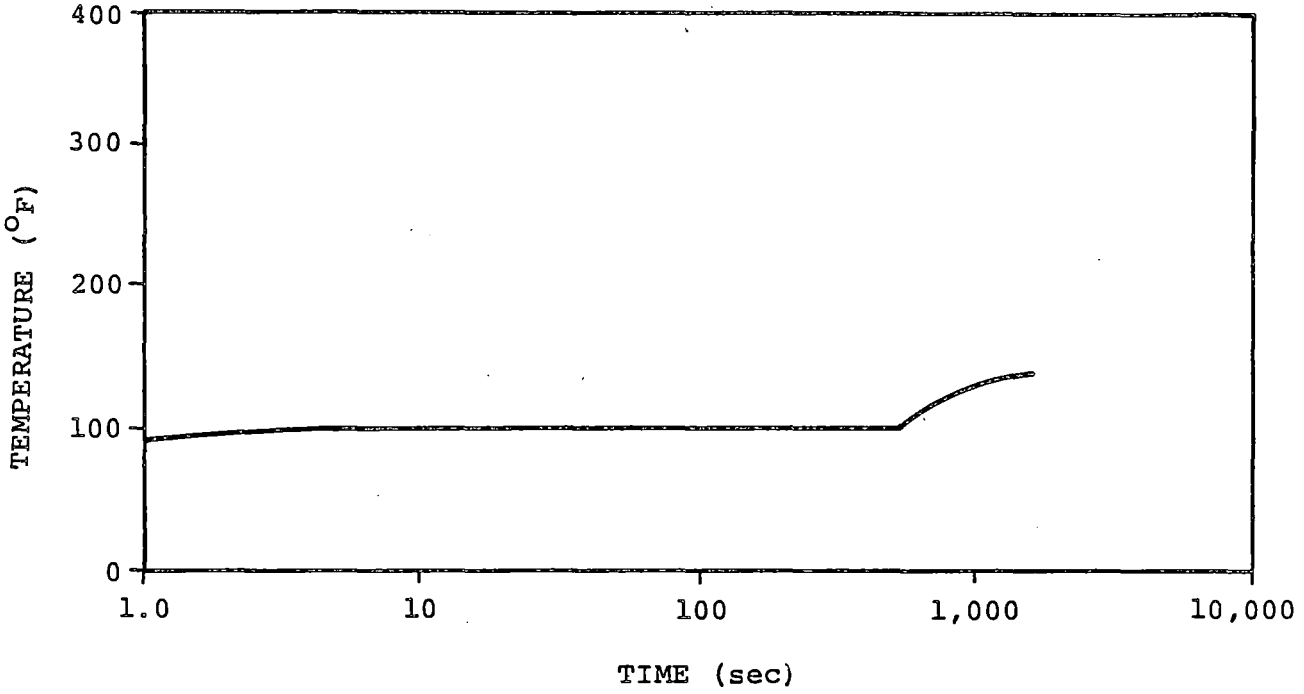

EVENT DESCRIPTION	TEMPERATURE DESIGNATION	TIME (sec)		TEMPERATURE (^{o}F)	
		t_{min}	t_{max}	T_{min}	T_{max}
INSTANT OF BREAK TO ONSET OF CHUGGING	T_1	0.0	300.0	92.0	100.0
ONSET OF CHUGGING TO INITIATION OF ADS	T_2	300.0	600.0	100.0	103.0
INITIATION OF ADS TO RPV DEPRESSURIZATION	T_3	600.0	1200.0	103.0	139.0

Figure 2-2.2-4

SUPPRESSION CHAMBER TEMPERATURES FOR SBA EVENT

$T_{min} = 95^{o}F$
$T_{max} = 165^{o}F$

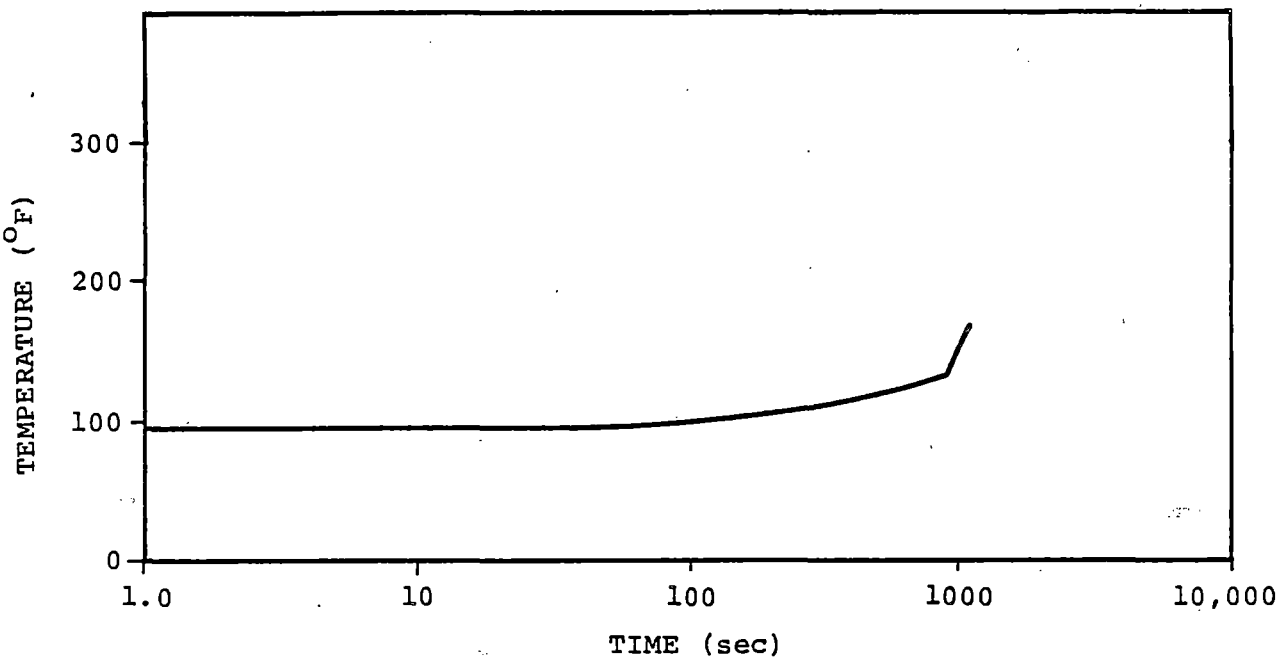

EVENT DESCRIPTION	TEMPERATURE DESIGNATION	TIME (sec)		TEMPERATURE (^{o}F)	
		t_{min}	t_{max}	T_{min}	T_{max}
INSTANT OF BREAK TO ONSET OF CO AND CHUGGING	T_1	0.0	5.0	95.0	95.0
ONSET OF CO AND CHUGGING TO INITIATION OF ADS	T_2	5.0	900.0	95.0	130.0
INITIATION OF ADS TO RPV DEPRESSURIZATION	T_3	900.0	1100.0	130.0	165.0

Figure 2-2.2-5

SUPPRESSION CHAMBER TEMPERATURES FOR IBA EVENT

$T_{min} = 85^{\circ}F$

$T_{max} = 120^{\circ}F$

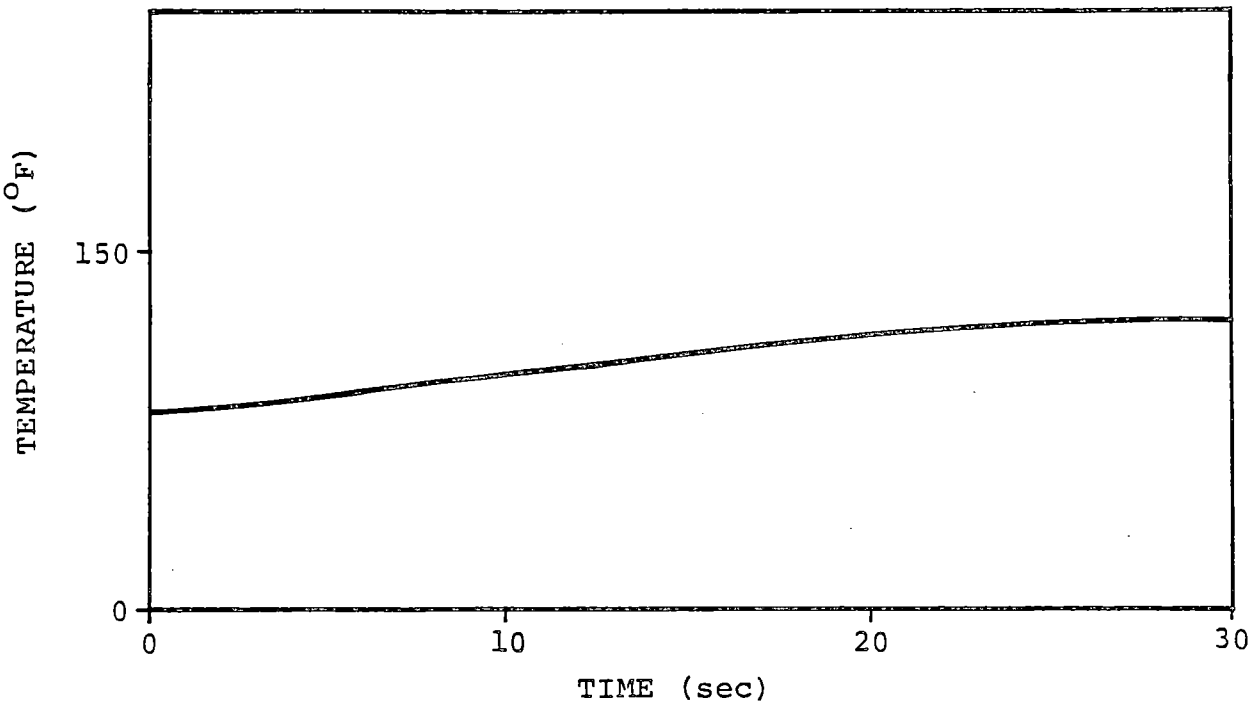

EVENT DESCRIPTION	TEMPERATURE DESIGNATION	TIME (sec)		TEMPERATURE (°F)	
		t_{min}	t_{max}	T_{min}	T_{max}
INSTANT OF BREAK TO TERMINATION OF POOL SWELL	T_1	0.0	1.5	85.0	87.0
TERMINATION OF POOL SWELL TO ONSET OF CO	T_2	1.5	5.0	87.0	91.0
ONSET OF CO TO ONSET OF CHUGGING	T_3	5.0	35.0	91.0	120.0
ONSET OF CHUGGING TO RPV DEPRESSURIZATION	T_4	35.0	65.0	120.0	120.0

Figure 2-2.2-6

SUPPRESSION CHAMBER TEMPERATURES FOR DBA EVENT

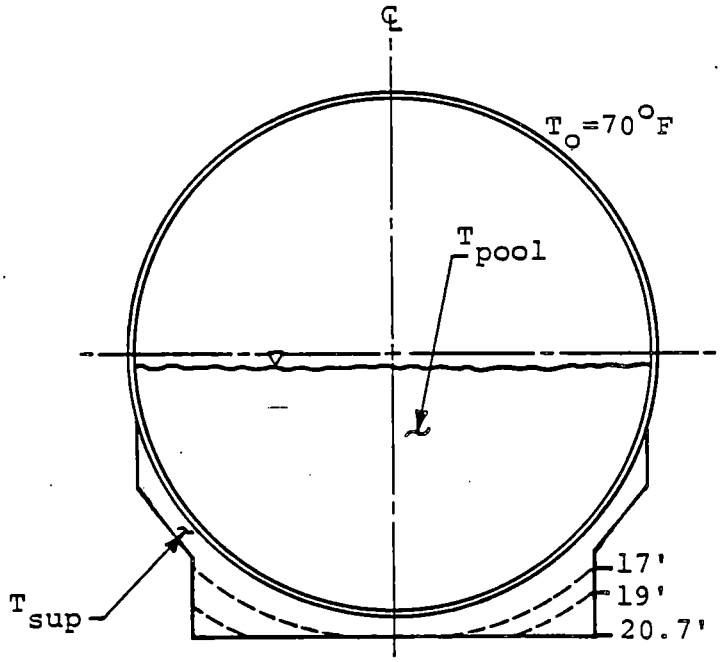

KEY DIAGRAM

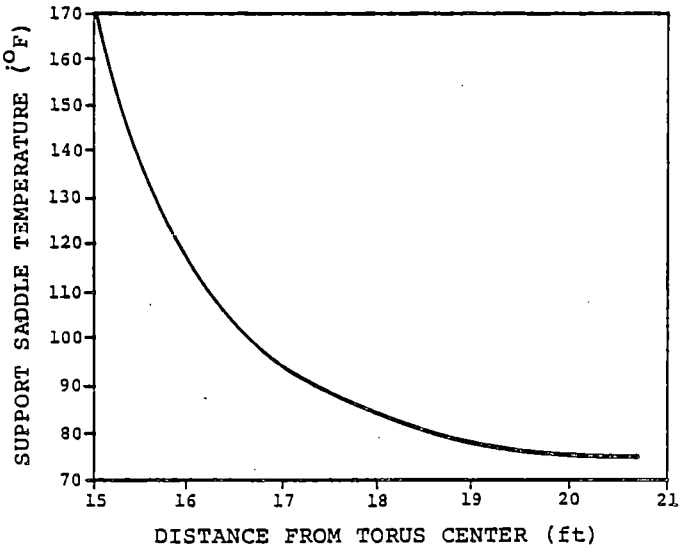

1. SUPPRESSION POOL TEMPERATURES FOR SBA, IBA, AND DBA EVENTS SHOWN IN FIGURES 2-2.2-4 THROUGH 2-2.2-6.

Figure 2-2.2-7

SUPPRESSION CHAMBER SUPPORT DIFFERENTIAL TEMPERATURES

nutech ENGINEERS

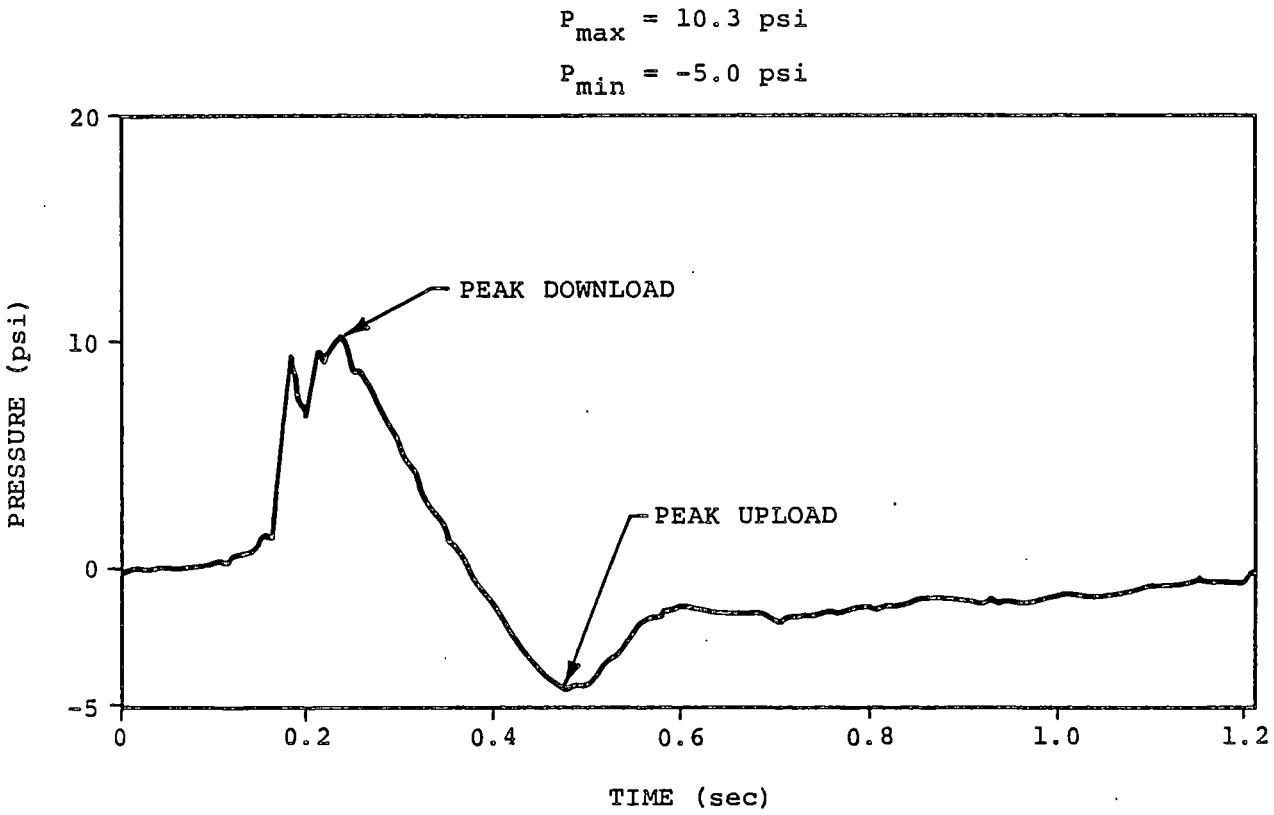

1. PRESSURES SHOWN DO NOT INCLUDE DBA INTERNAL PRESSURE.

Figure 2-2.2-8

POOL SWELL TORUS SHELL PRESSURE TRANSIENT
AT SUPPRESSION CHAMBER MITER JOINT –
BOTTOM DEAD CENTER (OPERATING DIFFERENTIAL PRESSURE)

nutech ENGINEERS

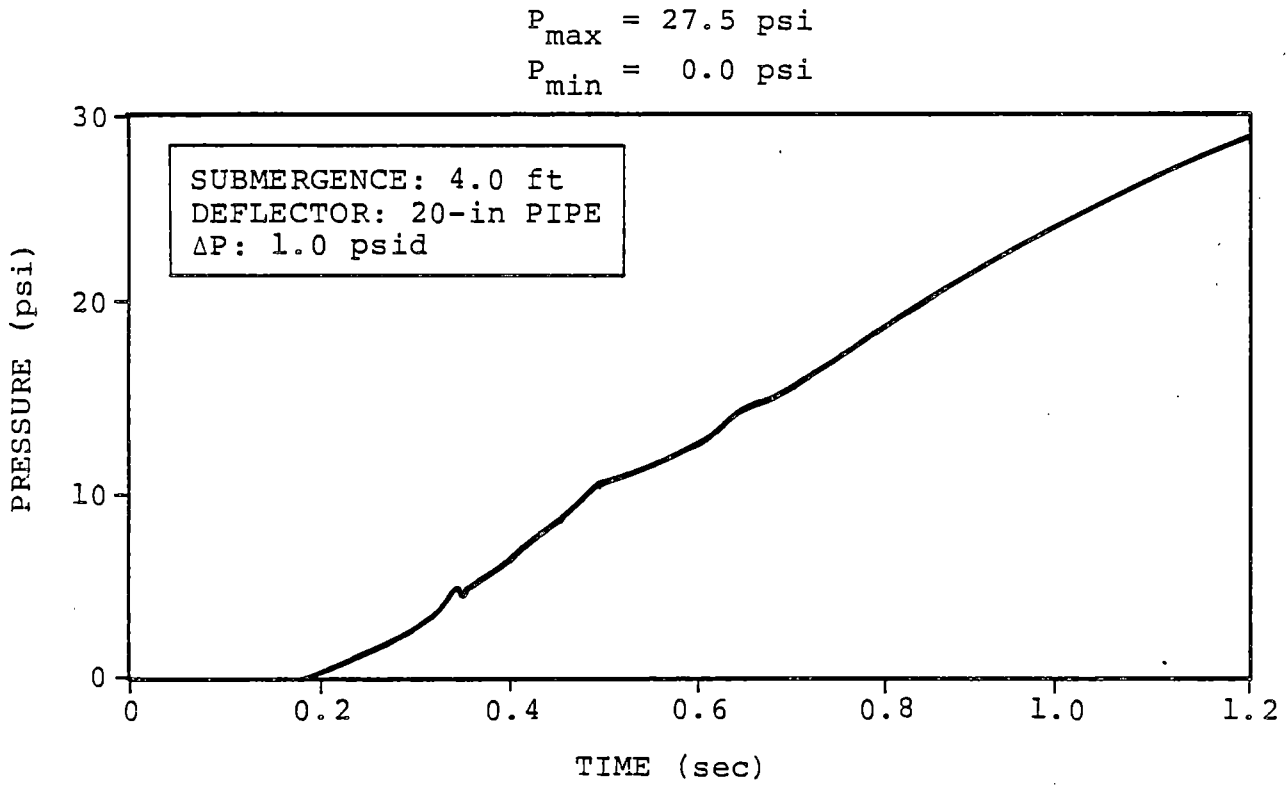

Figure 2-2.2-9

POOL SWELL TORUS SHELL PRESSURE TRANSIENT
FOR SUPPRESSION CHAMBER AIRSPACE
(OPERATING DIFFERENTIAL PRESSURE)

nutech ENGINEERS

P_{max} = 17.2 psi
P_{min} = -6.2 psi

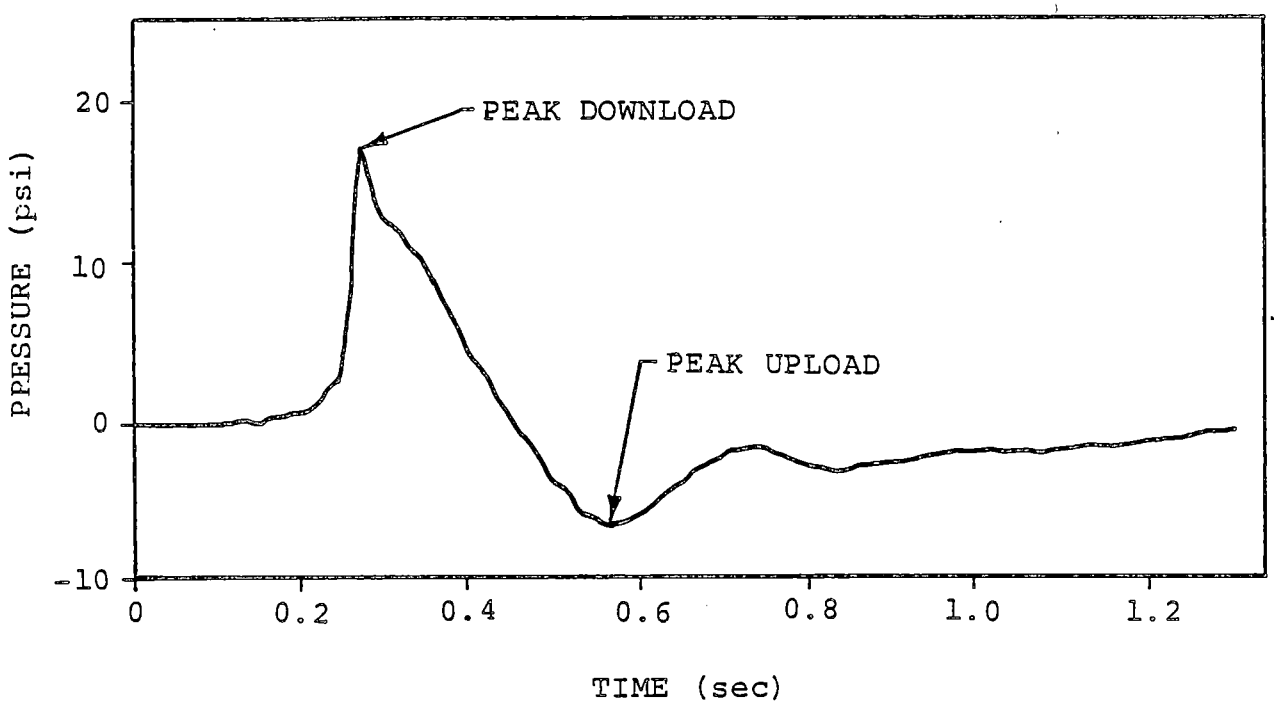

1. PRESSURES SHOWN DO NOT INCLUDE DBA INTERNAL PRESSURE.

Figure 2-2.2-10

POOL SWELL TORUS SHELL PRESSURE TRANSIENT
AT SUPPRESSION CHAMBER MITER JOINT –
BOTTOM DEAD CENTER (ZERO DIFFERENTIAL PRESSURE)

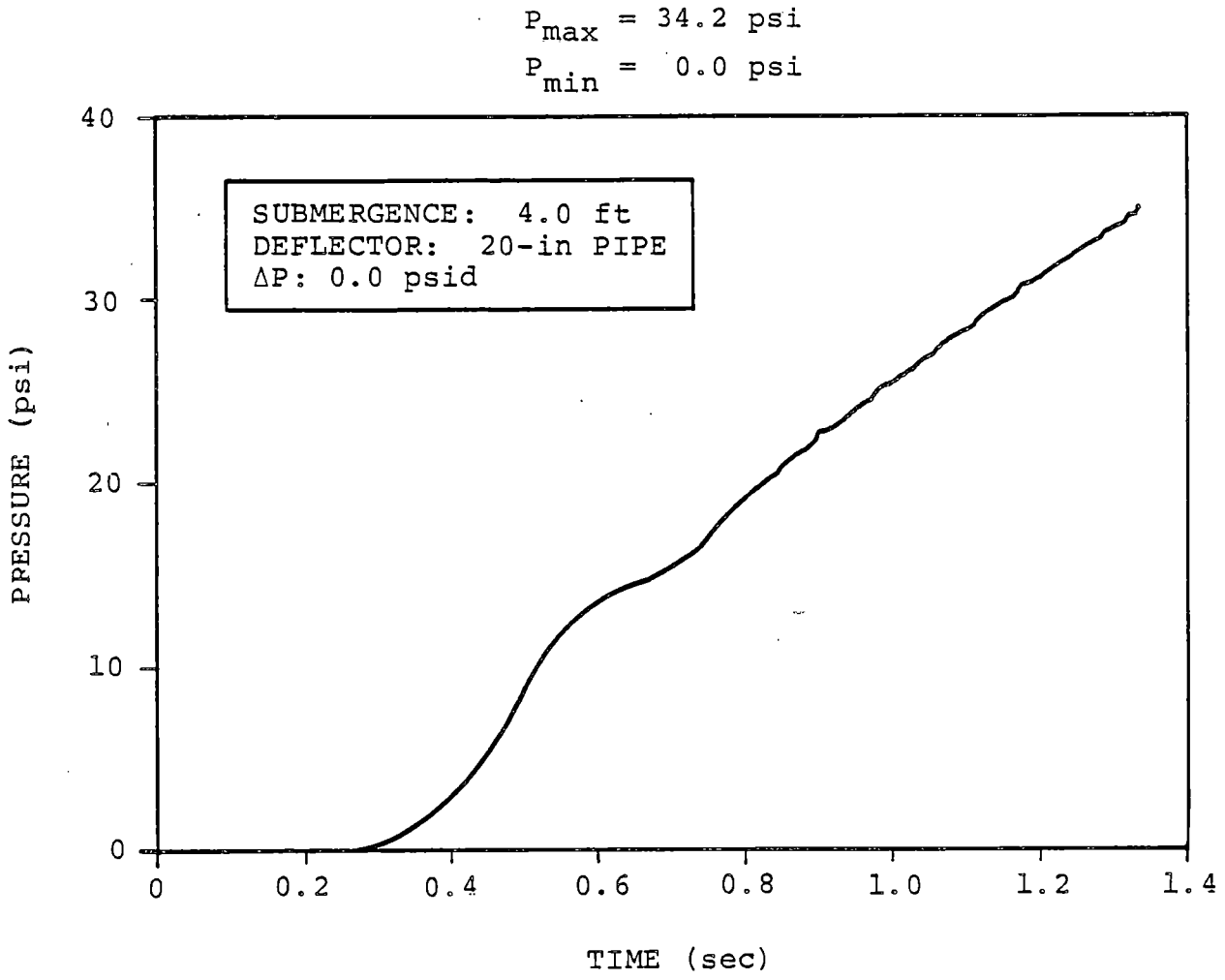

Figure 2-2.2-11

POOL SWELL TORUS SHELL PRESSURE TRANSIENT
FOR SUPPRESSION CHAMBER AIRSPACE
(ZERO DIFFERENTIAL PRESSURE)

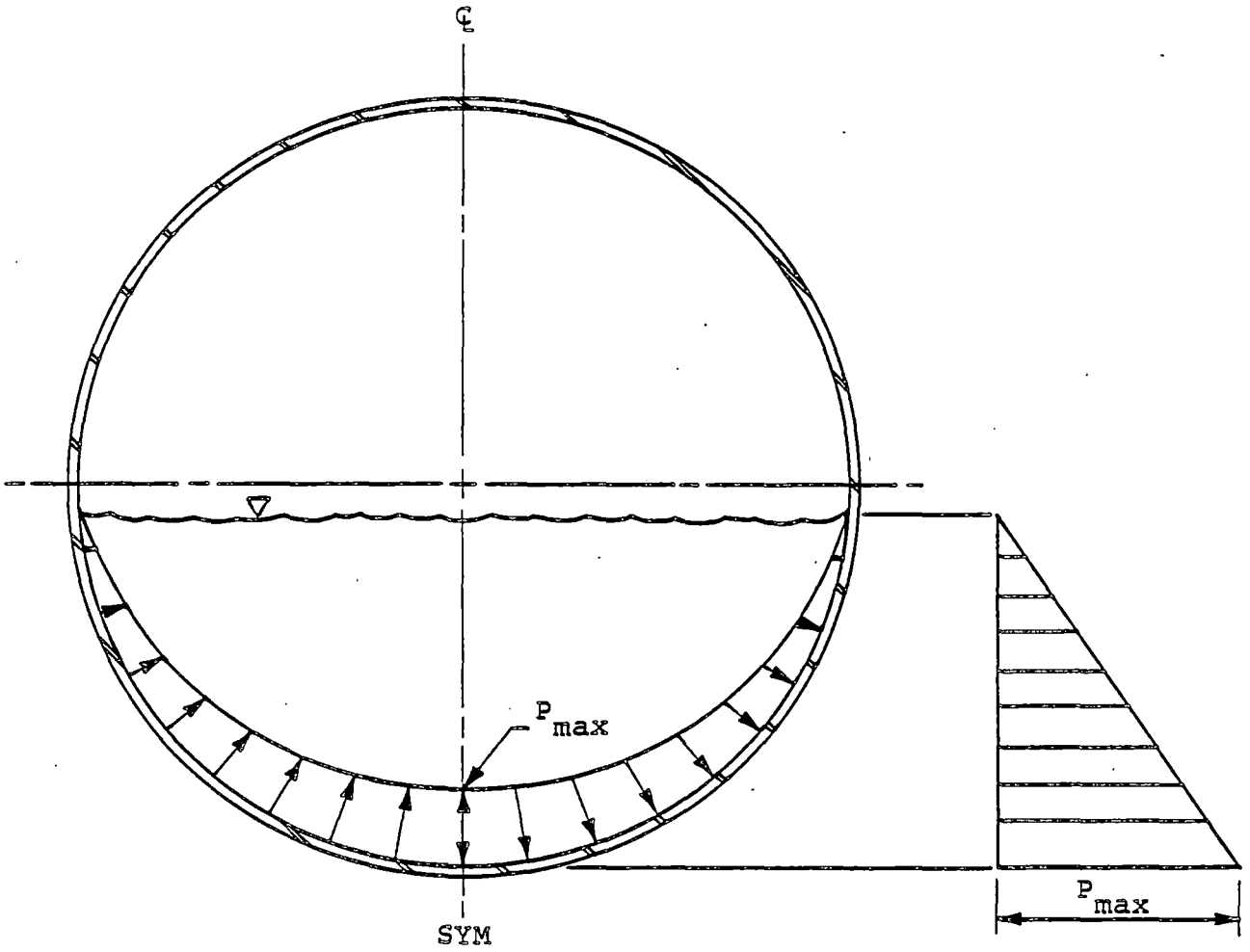

1. PRESSURE AMPLITUDES FOR DBA CONDENSATION OSCILLATION LOADS SHOWN IN TABLE 2-2.2-7.
2. PRESSURE AMPLITUDES FOR POST-CHUG LOADS SHOWN IN TABLE 2-2.2-9.

Figure 2-2.2-12

NORMALIZED TORUS SHELL PRESSURE DISTRIBUTION FOR DBA CONDENSATION OSCILLATION AND POST-CHUG LOADINGS

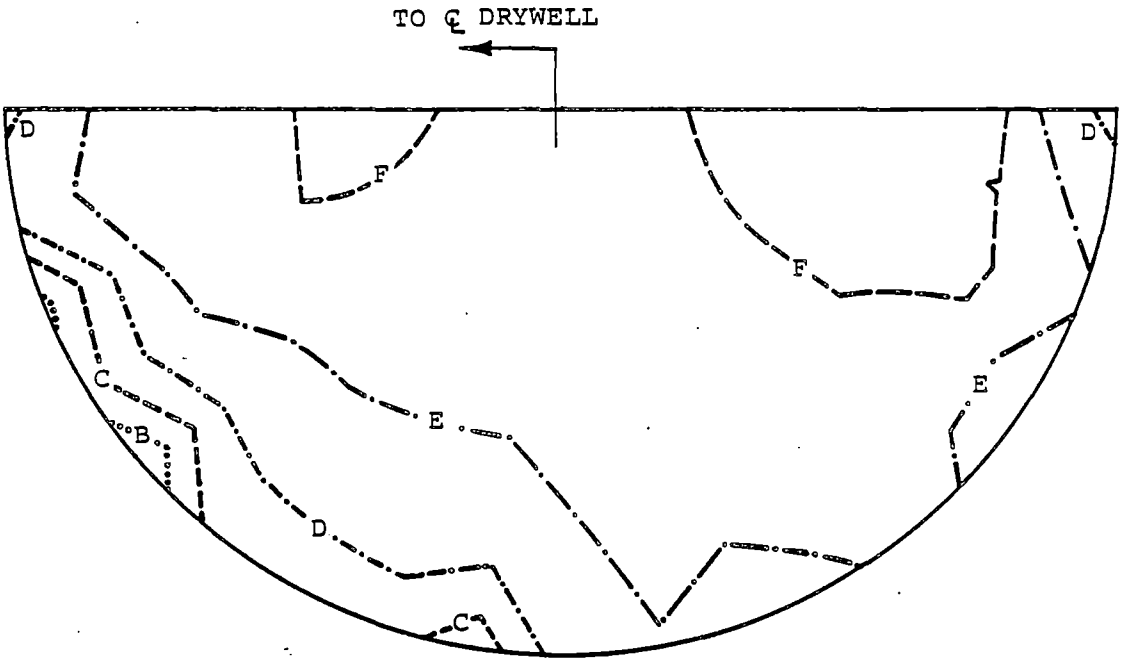

NORMALIZED POOL ACCELERATIONS	
PROFILE	POOL ACCELERATION (ft/sec^2)
A	195.0
B	155.0
C	115.0
D	75.0
E	35.0
F	15.0

1. POOL ACCELERATIONS DUE TO HARMONIC APPLICATION OF TORUS SHELL PRESSURES SHOWN IN FIGURE 2-2.2-12 AT A SUPPRESSION CHAMBER FREQUENCY OF 16.53 HERTZ.

Figure 2-2.2-13

POOL ACCELERATION PROFILE FOR DOMINANT SUPPRESSION CHAMBER FREQUENCY AT MIDCYLINDER LOCATION

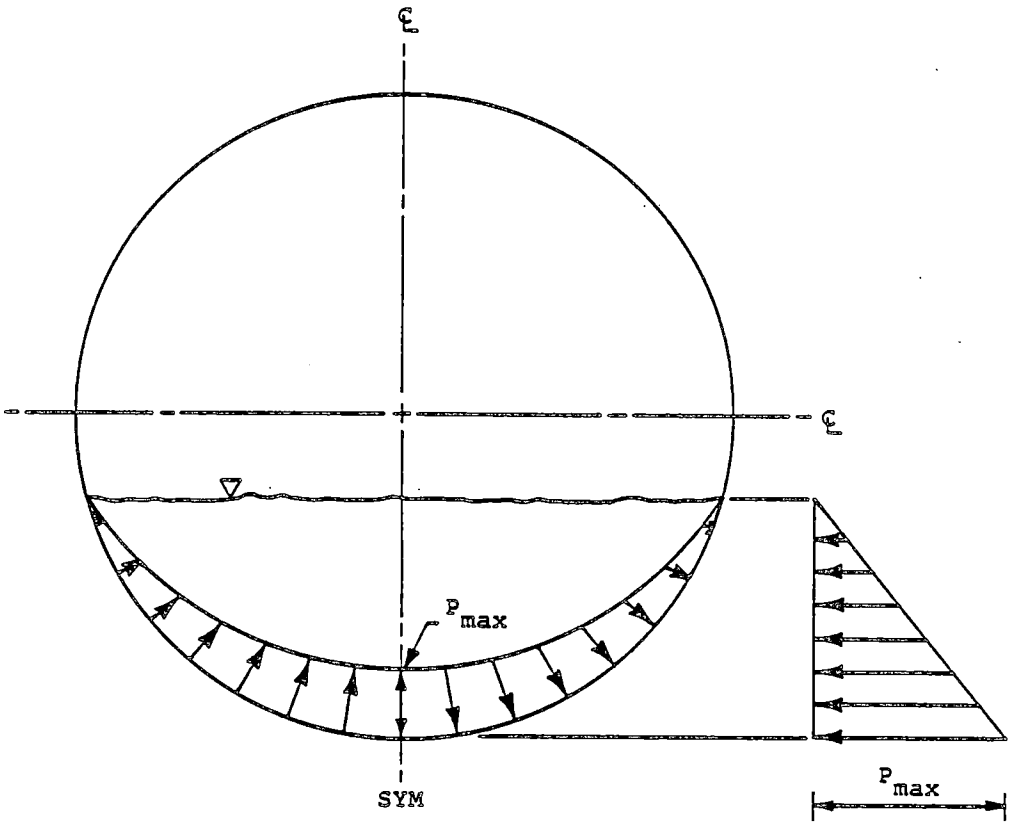

LOADING CHARACTERISTICS
SYMMETRIC DISTRIBUTION P_{max} = ± 2.0 psi AT ALL BOTTOM DEAD CENTER LOCATIONS
ASYMMETRIC DISTRIBUTION: P_{max} = ± 2.0 psi IN ONE BAY WITH LONGITUDINAL ATTENUATION (Figure 2-2.2-15)
FREQUENCY: SINGLE HARMONIC IN 6.9 TO 9.5 Hz RANGE RESULTING IN MAXIMUM RESPONSE
TOTAL INTEGRATED LOAD: SYM DIST: F_{vert} = 146.85 kips PER MITERED CYLINDER ASYM DIST: F_{horz} = 458.94 kips TOTAL HORIZONTAL

Figure 2-2.2-14

CIRCUMFERENTIAL TORUS SHELL PRESSURE DISTRIBUTION FOR SYMMETRIC AND ASYMMETRIC PRE-CHUG LOADINGS

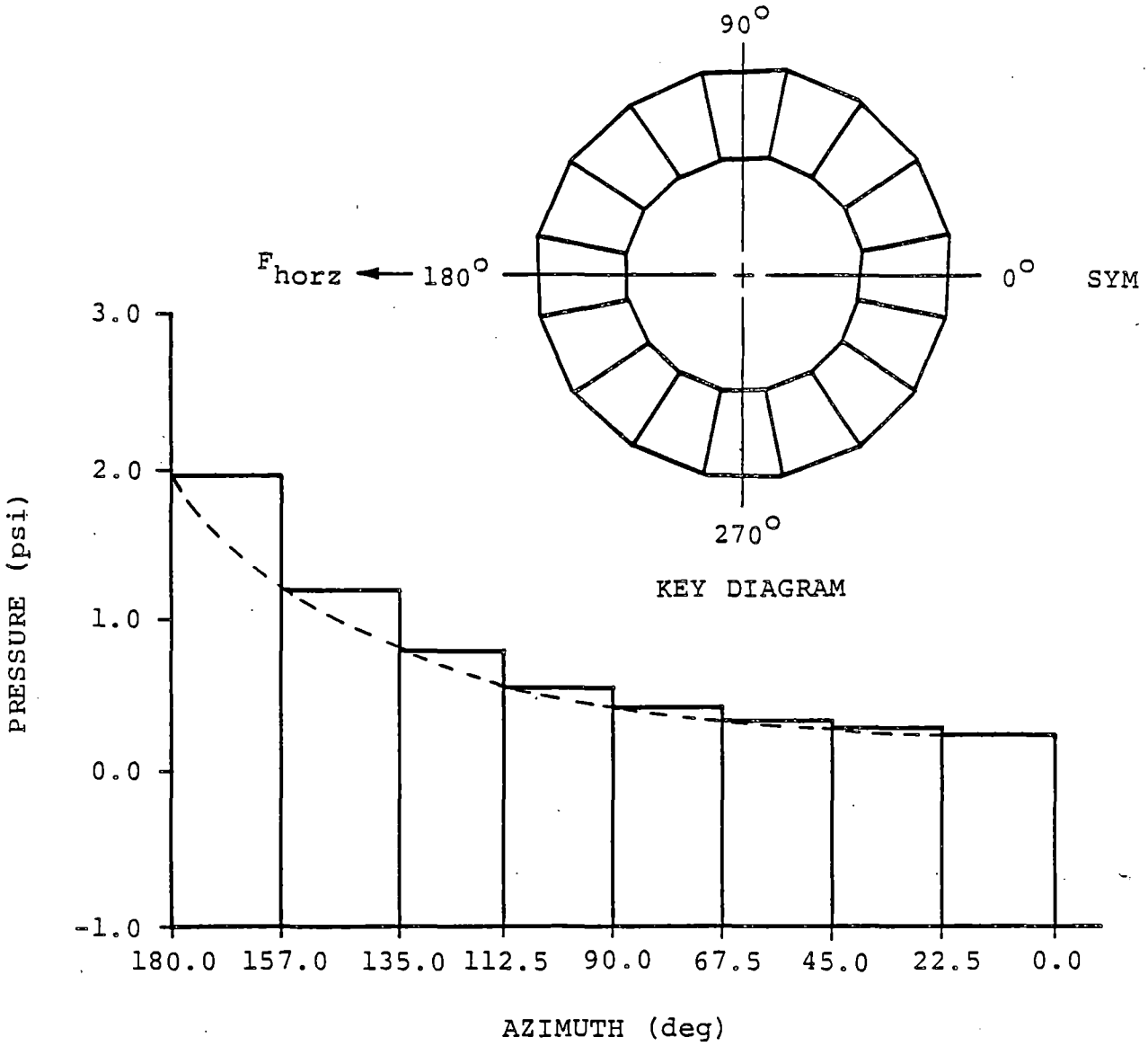

1. SEE FIGURE 2-2.2-14 FOR CIRCUMFERENTIAL TORUS SHELL PRESSURE DISTRIBUTION.

Figure 2-2.2-15

LONGITUDINAL TORUS SHELL PRESSURE
DISTRIBUTION FOR ASYMMETRIC PRE-CHUG LOADINGS

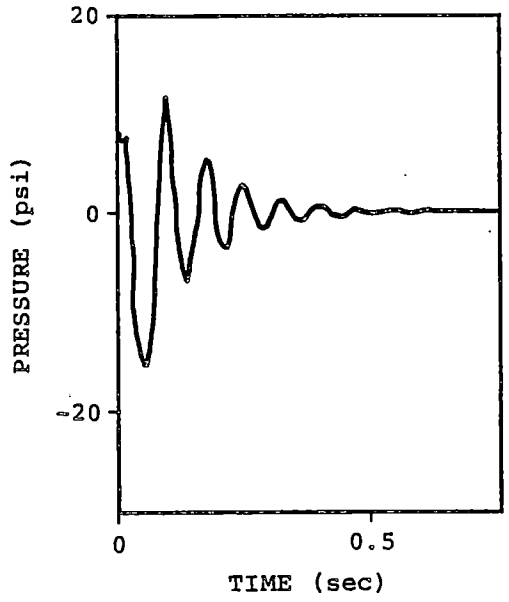

SHELL PRESSURE FORCING FUNCTION

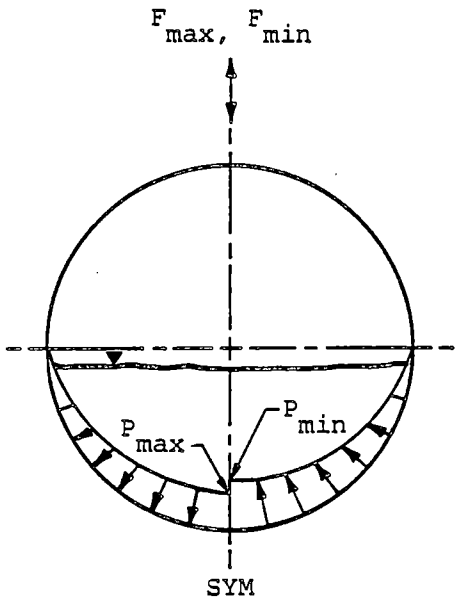

MITER JOINT SPATIAL DISTRIBUTION

LOADING CHARACTERISTICS
SINGLE VALVE
PRESSURE (psi): LONGEST SRVDL BUBBLE:
P_{max} = 19.43 P_{min} = -22.58
SHELL:
P_{max} = 11.84 P_{min} = -12.66
TOTAL APPLIED LOAD (kips):
VERTICAL PER MITERED CYLINDER:
DOWNWARD: F_{max} = 792.8
UPWARD: F_{min} = 847.74
LOAD FREQUENCY (Hz):
RANGE:
$9.94 \leq f_L \leq 16.56$

Figure 2-2.2-16

SRV DISCHARGE TORUS SHELL LOADS FOR SINGLE VALVE ACTUATION

nutech ENGINEERS

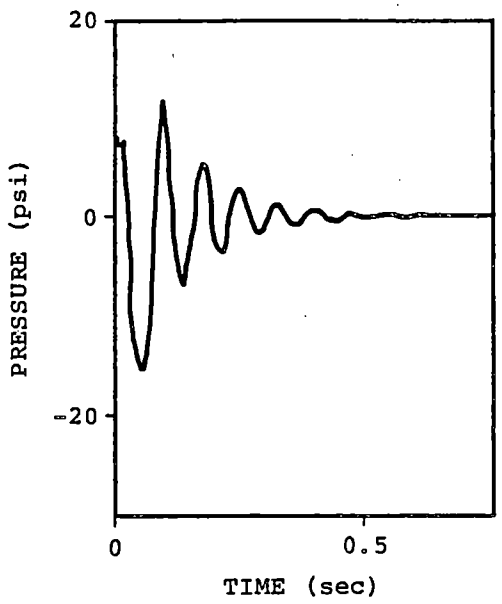

SHELL PRESSURE FORCING FUNCTION

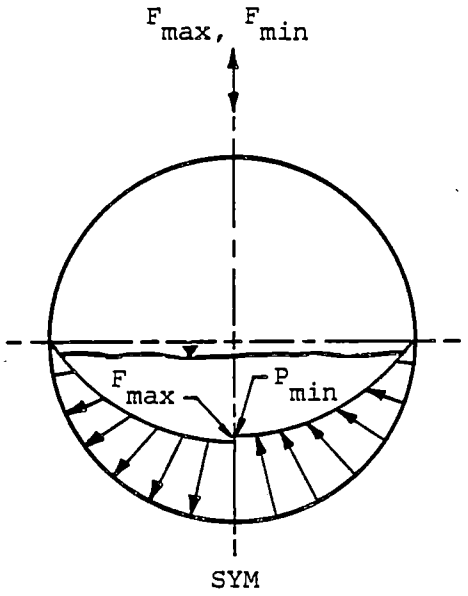

MITER JOINT SPATIAL DISTRIBUTION

LOADING CHARACTERISTICS
MULTIPLE VALVE
PRESSURE (psi): LONGEST SRVDL
BUBBLE:
P_{max} = 19.43 P_{min} = -22.58
SHELL: ONE VALVE
P_{max} = 11.84 P_{min} = -12.66
SHELL: ALL VALVES
P_{max} = 17.70 P_{min} = -18.93
TOTAL APPLIED LOAD (kips):
VERTICAL PER MITERED CYLINDER:
DOWNWARD: F_{max} = 1185.2
UPWARD: F_{min} = 1267.59
LATERAL: F_{max} = 669.3
LOAD FREQUENCY (Hz):
RANGE:
$5.31 \leq f_L \leq 20.90$

Figure 2-2.2-17

SRV DISCHARGE TORUS SHELL LOADS FOR MULTIPLE VALVE ACTUATION

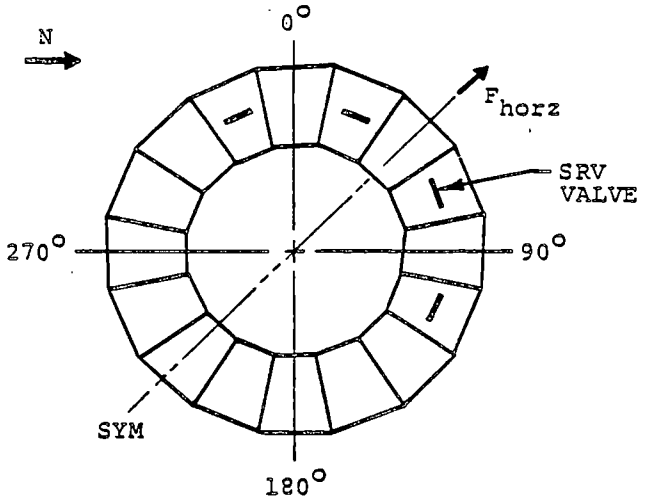

KEY DIAGRAM

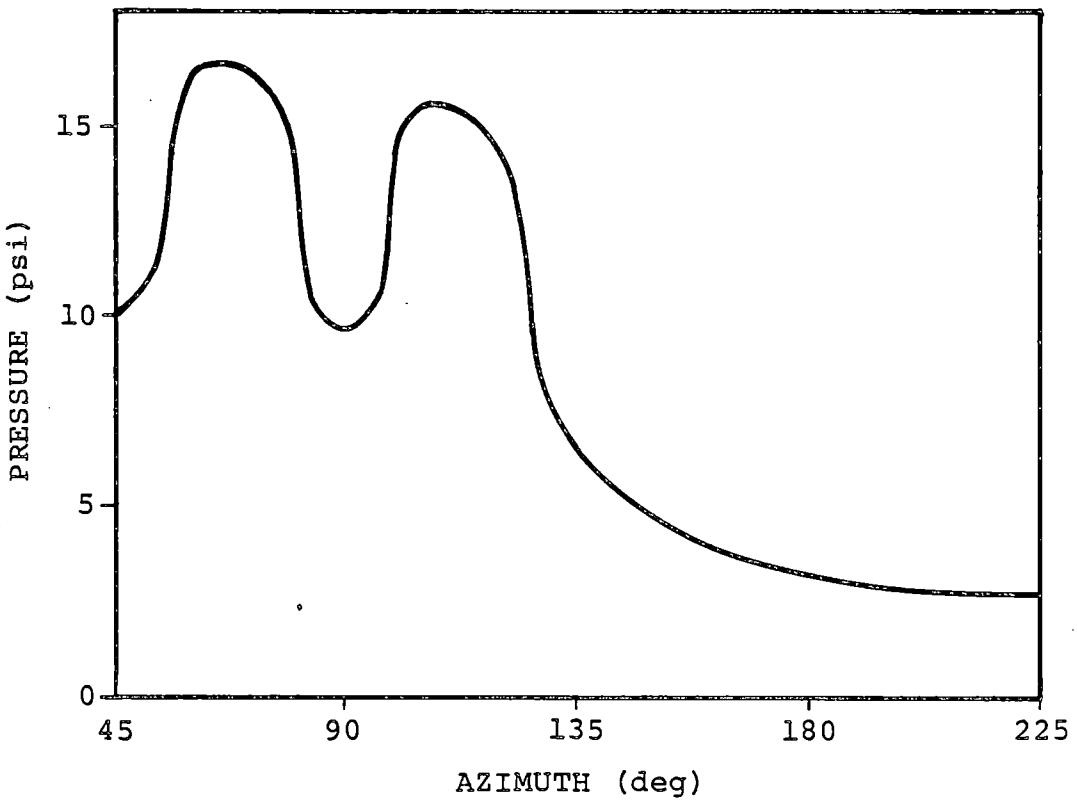

Figure 2-2.2-18

LONGITUDINAL TORUS SHELL PRESSURE DISTRIBUTION FOR SRV DISCHARGE

2-2.2.2 Load Combinations

The load categories and associated load cases for which the suppression chamber is evaluated are presented in Section 2-2.2.1. Table 2-2.2-3 presents the NUREG-0661 criteria for grouping the respective loads and load categories into event combinations.

The 27 general event combinations shown in Table 2-2.2-3 are expanded to form a total of 94 specific suppression chamber load combinations for the Normal Operating, SBA, IBA, and DBA events. The specific load combinations reflect a greater level of detail than the general event combinations, including distinctions between: SBA and IBA, pre-chug and post-chug; SRV actuation cases; zero and operating differential pressure pool swell cases; and consideration of multiple cases of particular loadings. The total number of suppression chamber load combinations consists of 6 for the Normal Operating event, 27 for the SBA event, 36 for the IBA event, and 25 for the DBA event. Several different service level limits and corresponding sets of allowable stresses are associated with these load combinations.

Not all of the possible suppression chamber load combinations are evaluated, since many are enveloped by others and do not lead to controlling suppression chamber stresses. The enveloping load combinations are determined by examining the possible suppression chamber load combinations and comparing the respective load cases and allowable stresses. Table 2-2.2-11 shows the results of this examination. For ease of identification, each enveloping load combination is assigned a number.

The enveloping load combinations are reduced further by examining relative load magnitudes and individual load characteristics to determine which load combinations lead to controlling suppression chamber stresses. The load combinations which have been found to produce controlling suppression chamber stresses are separated into three groups: the SBA III, IBA III, DBA I, DBA III, and DBA IV combinations are used to evaluate the suppression chamber vertical support system (these combinations result in the maximum vertical loads on the suppression chamber); the IBA III, IBA IV, DBA III, and DBA IV combinations are used to evaluate stresses in the suppression chamber shell and ring girders (these combinations result in maximum pressures on the suppression chamber shell); and the IBA III combination

is used to evaluate the effects of lateral loads on the suppression chamber near the seismic restraints. The selection of these controlling suppression chamber load combinations is explained in the following paragraphs. Table 2-2.2-12 summarizes the controlling load combinations and identifies which load combinations are enveloped by each controlling combination.

Many general event combinations have the same allowable stresses and are enveloped by others which contain the same or additional load cases (Table 2-2.2-3). There is no distinction between load combinations with Service Level A or B conditions for the suppression chamber since the allowable stress values for Service Level A and B are the same.

Except for seismic loads, many pairs of load combinations contain identical load cases. One of the load combinations in the pair contains OBE loads and has Service Level A or B allowables; the other contains SSE loads and has Service Level C allowables. Examination of the load magnitudes presented in Section 2-2.2.1 shows that both the OBE and SSE vertical accelerations are small compared to gravity. As a result, suppression chamber stresses and vertical support reactions due to vertical seismic loads are small compared to

those caused by other loads in the load combination. The horizontal seismic loads for OBE and SSE also result in small suppression chamber stresses compared with those caused by other loads in the load combinations. The Service Level C primary stress allowables for the load combinations containing SSE loads are more than 75% higher than the Service Level B allowables for the corresponding load combination containing OBE loads. This margin is due to the higher limits allowed at $1.0S_y$ than at $1.2S_{mc}$ (Reference 9). The controlling load combinations for evaluating suppression chamber stresses and vertical support reactions in these cases, therefore, are those containing OBE loads and Service Level B allowables.

By applying the above reasoning to the total number of suppression chamber load combinations, the number of enveloping load combinations for each event is reduced. Table 2-2.2-11 shows the resulting suppression chamber load combinations for the Normal Operating, SBA, IBA, and DBA events, along with the associated service level assignments. For ease of identification, each load combination in each event is assigned a number. The reduced number of enveloping load combinations shown in Table 2-2.2-11 consists of two for the NOC event, five for the SBA event, five for the IBA event, and seven

for the DBA event. The load case designations for the loads which compose the combinations are the same as those presented in Section 2-2.2.1.

An examination of Table 2-2.2-11 shows that further reductions are possible in the number of suppression chamber load combinations requiring evaluation. Any of the SBA or IBA combinations envelop the NOC I and II combinations since they contain the same loadings as the NOC I and II combinations and, in addition, CO or chugging loads. The effects of the NOC I and II combinations are considered in the suppression chamber fatigue evaluation.

The remaining suppression chamber load combinations can be separated into those which result in: maximum vertical reaction loads, maximum shell pressures, and maximum horizontal reaction loads. The loading combinations which result in maximum vertical reaction loads are discussed first.

Maximum Vertical Reactions

Although there are differences in the SBA III, SBA IV, and IBA IV pressure and temperature loadings, these loadings do not affect net vertical loads in the

suppression chamber. The IBA IV combination was selected to represent these loads since the SBA III, SBA IV and IBA IV load combinations are identical with respect to vertical reactions. According to the reasoning presented earlier for OBE and SSE loads, and because the multiple value SRV vertical loads bound the single value vertical loads, it follows that the IBA IV combination envelops the DBA VII combination and the DBA III combination envelops the DBA V combination for the effects of vertical reaction loads.

Since pre-chug loads are specified in lieu of IBA CO loads, the IBA I combination is the same as the SBA I combination. Thus the SBA I combination can be eliminated from further consideration for combinations affecting vertical reaction loads. The IBA I, IBA II, and IBA III combinations are identical with respect to vertical reactions. The IBA III combination was selected to represent these loads. The differences among some loads in the SBA I, IBA I, IBA II, and IBA III combinations do not affect net vertical loads on the suppression chamber. The IBA III combination also envelops the SBA II combination.

Since the effect of OBE loads on the net vertical reaction is small in comparison to the effect of zero versus operating ΔP, the DBA I combination envelops the DBA II combination for the effects of vertical reaction loads. From the reasoning presented earlier for OBE and SSE loads, it follows that the IBA III combination envelops the SBA V and IBA V combinations for the effects of vertical loads. Similarly, it can be shown that the IBA III combination envelops the DBA VI combination.

Maximum Shell Pressure

The IBA and SBA load combinations which result in the maximum total pressures on the suppression chamber shell include the SBA II, SBA IV, SBA V, IBA II, IBA III, IBA IV, and IBA V combinations. These combinations contain the maximum internal pressures which occur during the SBA and IBA events, and during SRV Discharge Multiple Valve Case 8b. The combined effect of these loadings results in the maximum pressure loads on the suppression chamber shell.

The IBA III combination envelops the SBA II combination, for the effects of maximum pressure loads since the internal pressures for IBA III are larger than

those of SBA II. Since pre-chug loads are specified in lieu of IBA CO loads, the IBA III combination is the same as the IBA II combination. Thus the IBA II combination can be eliminated from further consideration for combinations which result in maximum pressure loads. It also follows, from the reasoning presented earlier for OBE and SSE loads, that the IBA III combination envelops the SBA V and the IBA V combinations. The IBA IV combination envelops the SBA IV for consideration of maximum pressure loads since the internal pressures for IBA IV are larger than those for SBA IV.

The DBA II combination envelops the DBA I combination for pressure loads since the shell stresses are comparable for zero and operating ΔP loads (Load Cases 4a and 4b), while the allowables for the DBA II load combination are more restrictive than for the DBA I combination.

The DBA IV combination envelops the DBA II combination for the effects of vertical reaction loads and pressure loads since it contains the same loadings as the DBA II combination and, in addition, it contains SRV discharge loads. The DBA II combination has Service Level B limits, with allowances for increased allowable

stresses which, when applied, result in allowable stresses which are about the same as the Service Level C allowable stresses for the DBA IV combination.

The DBA III combination envelops the DBA V combination for the effects of vertical reaction loads and pressure loads since SRV discharge loads which occur late in the DBA event have a negligible effect on the suppression chamber. The DBA III combination also has more restrictive allowables than the DBA V combination.

The IBA III combination envelops the DBA VI combination for the effects of maximum pressure loads according to the reasoning mentioned above regarding the DBA SRV loads, and because the internal pressures for IBA III are larger than those for DBA VI. The IBA IV combination envelops the DBA VII combination for the same reasons.

Maximum Horizontal Reactions

The load combinations which result in maximum horizontal reaction loads on the suppression chamber are the SBA II, SBA V, IBA III, and IBA V combinations. All of these combinations contain asymmetric pre-chug loads, SRV Discharge Multiple Valve Case 8b, and either

OBE or SSE loads. The combined effect of these loads results in the maximum possible lateral load on the suppression chamber. The IBA III and SBA II combinations are the same except for differences in internal pressure and temperature loads which do not affect lateral loads on the suppression chamber. The same applies to the IBA V and SBA V combinations.

The reasoning presented earlier for OBE and SSE loads shows that the IBA III combination envelops the IBA V combination.

Summary

The controlling suppression chamber load combinations evaluated in the remaining sections can now be summarized. The IBA III, IBA IV, DBA I, DBA III, and DBA IV combinations are evaluated when the effects of vertical reaction loads on the suppression chamber vertical support system are considered. The IBA III, IBA IV, DBA III, and DBA IV combinations are evaluated when the effects of pressure loads on the suppression chamber shell and ring girders are considered. The IBA III combination is evaluated when the effects of lateral loads on the suppression chamber near the seismic restraints are considered. The DBA I

combination is evaluated as required by the NUREG-0661 acceptance criteria.

To ensure that fatigue in the suppression chamber is not a concern over the life of the plant, the combined effects of fatigue due to Normal Operating plus SBA and Normal Operating plus IBA events are evaluated. Figures 2-2.2-19, 2-2.2-20, and 2-2.2-21 show the relative sequencing and timing of each loading in the SBA, IBA, and DBA events used in this evaluation. The fatigue effects for Normal Operating plus DBA events are enveloped by the Normal Operating plus SBA or IBA events since combined effects of SRV discharge loads and other loads for the SBA and IBA events are more severe than those for DBA events. A summary at the bottom of Table 2-2.2-11 provides additional information used in the suppression chamber fatigue evaluation.

The load combinations and event sequencing described in the preceding paragraphs envelop those postulated to occur during an actual LOCA or SRV discharge event. An evaluation of the above load combinations results in a conservative estimate of the suppression chamber responses and leads to bounding values of suppression chamber stresses and fatigue effects.

Table 2-2.2-11

CONTROLLING SUPPRESSION CHAMBER LOAD COMBINATIONS

SECTION 2-2.2.1 LOAD DESIGNATION	CONDITION/ EVENT	NOC		SBA					IBA					DBA						
	VOLUME 2 LOAD COMBINATION NUMBER	I	II	I	II	III	IV	V	I	II	III	IV	V	I	II	III	IV	V	VI	VII
	TABLE 2-2.2-13 LOAD COMBINATION NUMBER	2	2	14	14	14	14	15	14	14	14	14	15	16	18	20	25	27	27	27
DEAD WEIGHT		1a,1b	←	—	—	—	—	—	—	—	—	—	—	—	—	—	—	—	→	1a,1b
SEISMIC	OBE	2a	←	—	—	—	→ 2a		2a ←	—	—	← 2a			2a	2a				
	SSE							2b					2b				2b ⇒	—	—	← 2b
PRESSURE (1)		P (2)	P (2)	P_2	P_3	P_2	P_3	P_3	P_2	P_3	P_3	P_2	P_3	P_1	P_1	P_3	P_1	P_3	P_4	P_4
TEMPERATURE (3)		T (4)	T (4)	T_2	T_3	T_2	T_3	T_3	T_2	T_3	T_3	T_1	T_3	T_1	T_1	T_3	T_1	T_3	T_4	T_4
POOL SWELL														5b,5c, 5d	5a,5c, 5d		5a,5c, 5d			
CONDENSATION OSCILLATION									6b,6d	6b,6d						6a,6c		6a,6c		
CHUGGING	PRE-CHUG			7a,7c	7a,7c			7a,7c			7a,7c		7a,7c						7a,7c	
	POST-CHUG					7b,7d	7b,7d					7b,7d								7b,7d
SRV DISCHARGE	SINGLE	8a,8c, 8d															8a,8c, 8d	8a,(5) 8c,8d	→	8a,(5) 8c,8d
	MULTIPLE		8b,8c, 8d	←	—	—	—	—	—	—	—	→	8b,8c, 8d							
CONTAINMENT INTERACTION		9a ←	—	—	—	—	—	—	—	—	—	—	—	—	—	—	—	—	—	→ 9a
SERVICE LEVEL		B	B	B	B	B	B	C	B	B	B	B	C	D	B (6)	B	C	C	C	C
NUMBER OF EVENT OCCURENCES (7)		150	150	1 ←	—	—	—	—	—	—	—	—	—	—	—	—	—	—	—	→ 1
NUMBER OF SRV ACTUATIONS (8)		300 (9)		50	←	—	→	50	25	←	—	→	25	0	0	0	1	1	1	1

nutech ENGINEERS

NOTES TO TABLE 2-2.2-11

(1) SEE FIGURES 2-2.2-1 THROUGH 2-2.2-3 FOR SBA, IBA, AND DBA INTERNAL PRESSURE VALUES.

(2) THE RANGE OF NORMAL OPERATING INTERNAL PRESSURES IS -0.2 TO 0.2 PSI AS SPECIFIED BY THE ORIGINAL CONTAINMENT DATA.

(3) SEE FIGURES 2-2.2-4 THROUGH 2-2.2-6 FOR SBA, IBA, AND DBA TEMPERATURE VALUES. SEE TABLE 2-2.2-2 FOR ADDITIONAL SBA EVENT TEMPERATURES.

(4) THE RANGE OF NORMAL OPERATING TEMPERATURES IS 70°F TO 165°F AS SPECIFIED BY THE CONTAINMENT DATA SPECIFICATIONS. SEE TABLE 2-2.2-2 FOR ADDITIONAL NORMAL OPERATING TEMPERATURES.

(5) THE SRV DISCHARGE LOADS WHICH OCCUR DURING THIS PHASE OF THE DBA EVENT HAVE A NEGLIGIBLE EFFECT ON THE SUPPRESSION CHAMBER.

(6) EVALUATION OF SECONDARY STRESS RANGE OR FATIGUE NOT REQUIRED. WHEN EVALUATING TORUS SHELL STRESSES, THE VALUE OF S_{mc} MAY BE INCREASED BY THE DYNAMIC LOAD FACTOR DERIVED FROM THE ANALYTICAL MODEL.

(7) THE NUMBER OF SEISMIC LOAD CYCLES USED FOR FATIGUE IS 600.

(8) THE VALUES SHOWN ARE CONSERVATIVE ESTIMATES OF THE NUMBER OF ACTUATIONS EXPECTED FOR A BWR 3 PLANT WITH A REACTOR VESSEL DIAMETER OF 251".

(9) THE VALUE SHOWN IS THE TOTAL OF THE SINGLE AND MULTIPLE VALVE ACTUATIONS. SINCE THE MULTIPLE VALVE CASE GOVERNS, THE TOTAL NUMBER OF ACTUATIONS IS CONSERVATIVELY APPLIED TO THAT CASE.

Table 2-2.2-12

ENVELOPING LOGIC FOR CONTROLLING SUPPRESSION CHAMBER LOAD COMBINATIONS

CONDITION/EVENT			NOC		SBA					IBA					DBA						
TABLE 2-2.2-12 LOAD COMBINATION NUMBER			2	2	14	14	14	14	15	14	14	14	14	15	16	18	20	25	27	27	27
TABLE 2-2.2-12 LOAD COMBINATIONS ENVELOPED			1	1	4-6, 8, 10-12	4-6, 8 10-12	4-6, 8, 10-12	4-6, 8, 10-12	3,7, 9,13	4-6, 8, 10-12	4-6, 8, 10-12	4-6, 8 10-12	4-6, 8, 10-12	3,7, 9,13	(1)	16 (2)	17	19, 22,24	21, 23,26	21, 23,26	21, 23,26
VOLUME 2 LOAD COMBINATION DESIGNATION			I	II	I	II	III	IV	V	I	II	III	IV	V	I	II	III	IV	V	VI	VII
CONTROLLING LOAD COMBINATIONS EVALUATED	VERTICAL SUPPORT LOADS	IBA III	X	X	X	X			X	X	X			X						X	
		IBA IV	X	X			X	X													X
		DBA I														X					
		DBA III																	X		
		DBA IV														X					
	TORUS SHELL PRESSURES	IBA III	X	X		X			X		X			X						X	
		IBA IV	X	X				X													X
		DBA III																	X		
		DBA IV													X	X					
	LATERAL LOADS	IBA III	X	X		X			X					X							

(1) FOR ZERO DIFFERENTIAL PRESSURE.

(2) FOR OPERATING DIFFERENTIAL PRESSURE.

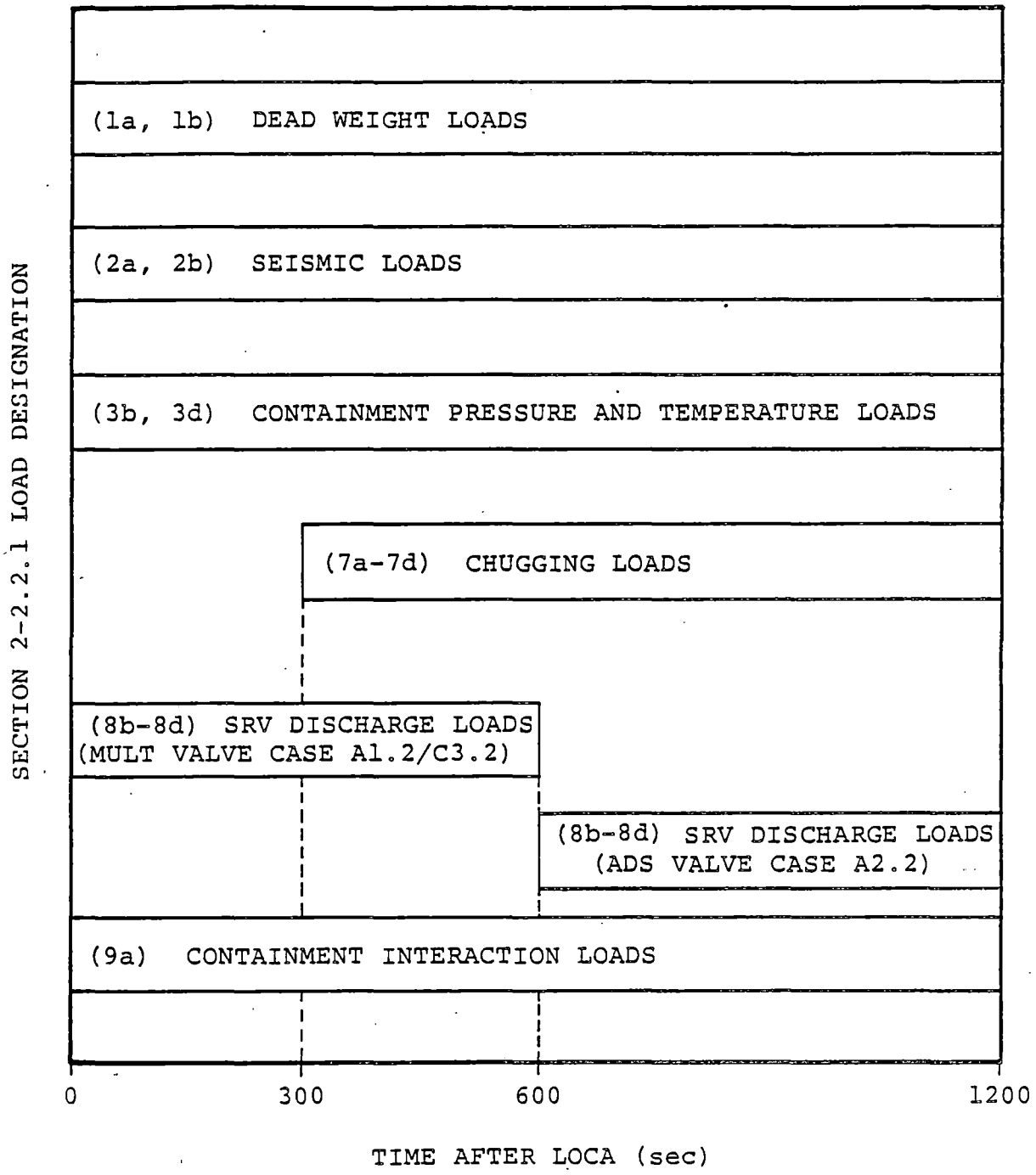

Figure 2-2.2-19

SUPPRESSION CHAMBER SBA EVENT SEQUENCE

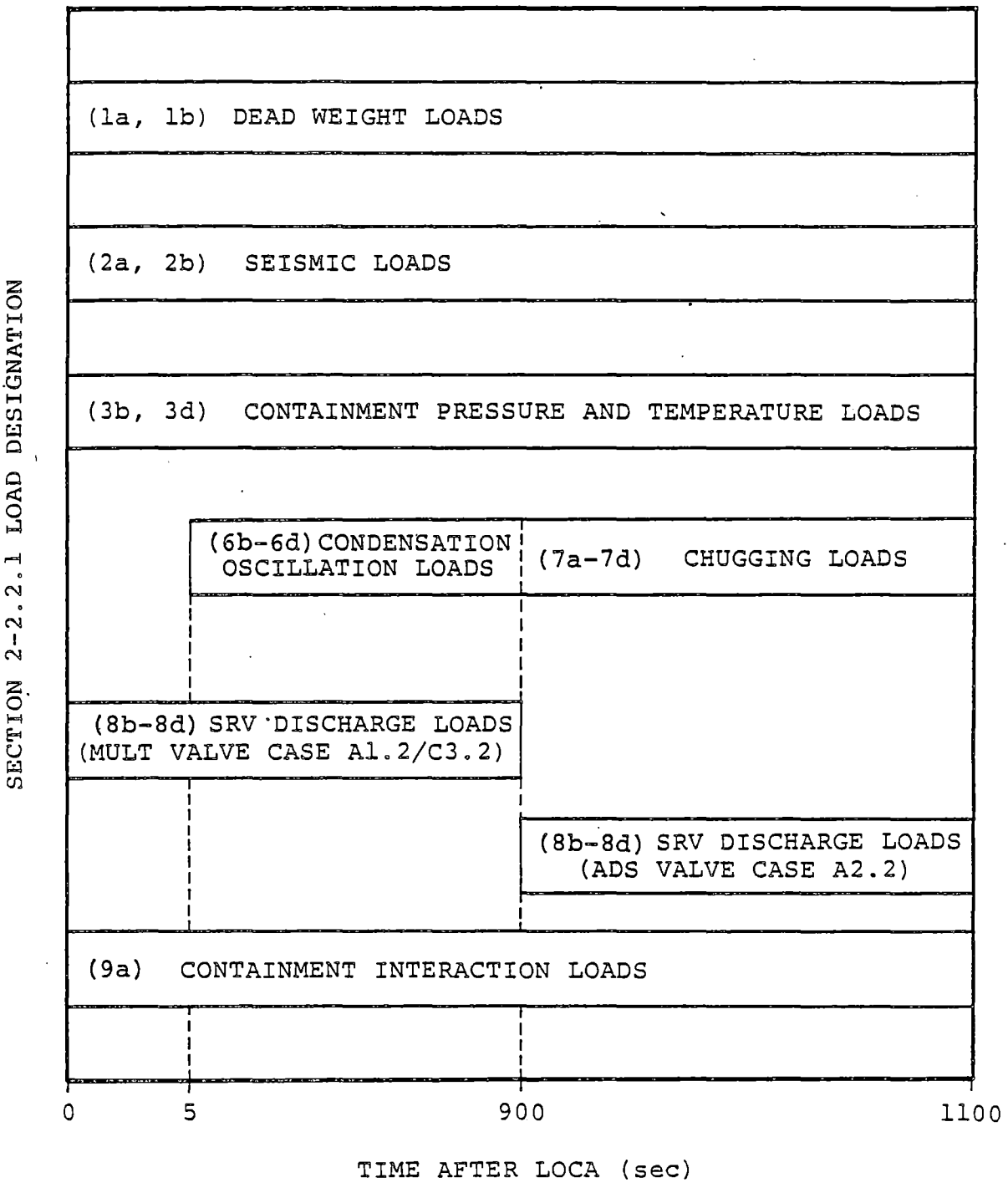

Figure 2-2.2-20

SUPPRESSION CHAMBER IBA EVENT SEQUENCE

nutech ENGINEERS

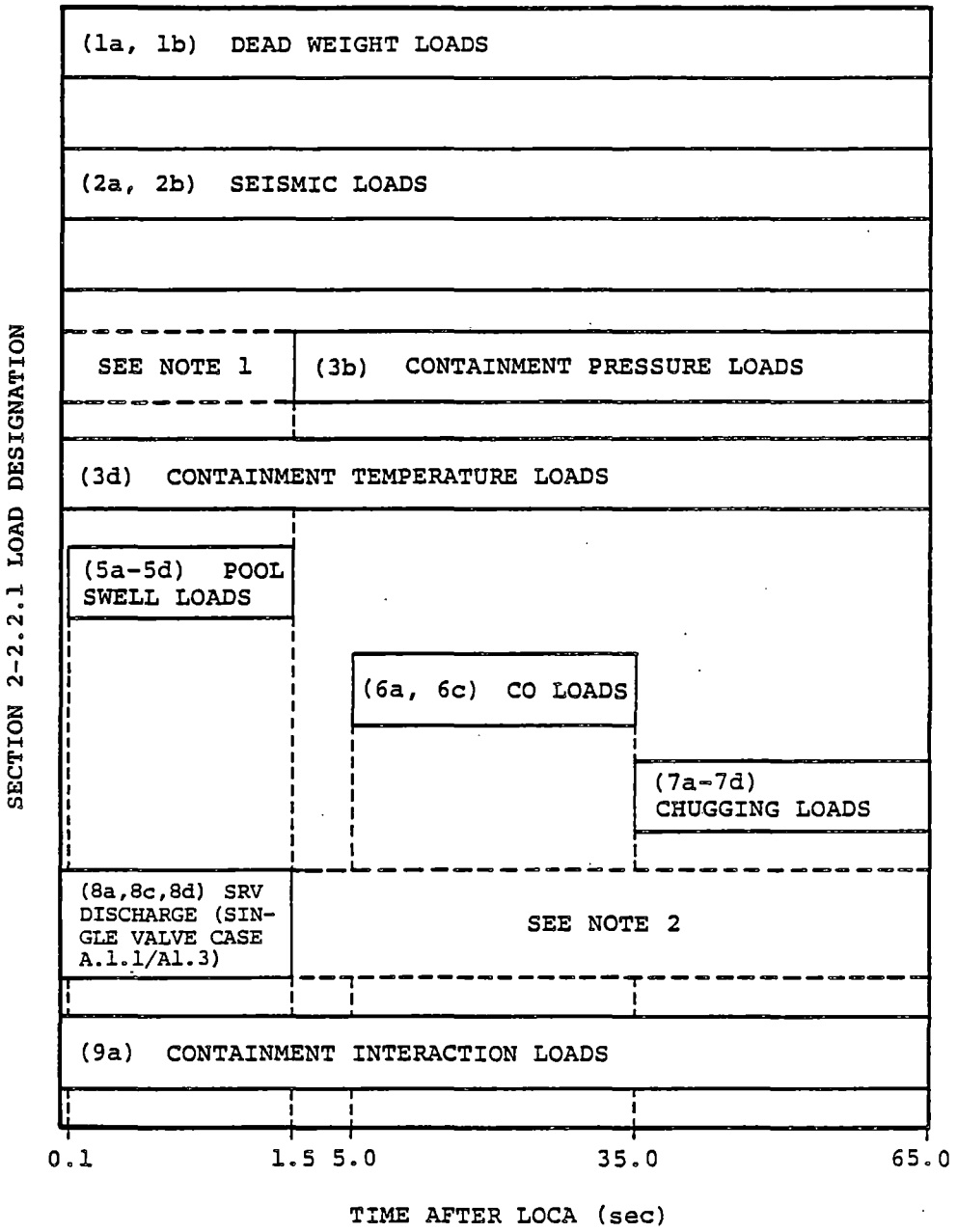

(1) THE EFFECTS OF INTERNAL PRESSURE LOADS ARE INCLUDED IN POOL SWELL TORUS SHELL LOADS.

(2) THE SRV DISCHARGE LOADS WHICH OCCUR DURING THIS PHASE OF THE DBA EVENT ARE NEGLIGIBLE.

Figure 2-2.2-21

SUPPRESSION CHAMBER DBA EVENT SEQUENCE

nutech ENGINEERS

2-2.3 Acceptance Criteria

The NUREG-0661 acceptance criteria on which the Dresden Units 2 and 3 suppression chamber analyses are based are discussed in Section 1-3.2. In general, the acceptance criteria follow the rules contained in the ASME Code, Section III, Division 1, including the Summer 1977 Addenda for Class MC components and component supports (Reference 9). The corresponding service limit assignments, jurisdictional boundaries, allowable stresses, and fatigue requirements are consistent with those contained in the applicable subsections of the ASME Code and the PUAAG. The acceptance criteria used in the analysis of the suppression chamber are summarized in the following paragraphs.

The items examined in the analysis of the suppression chamber include the suppression chamber shell, the ring girder, and the suppression chamber horizontal and vertical support systems. Figures 2-2.1-1 through 2-2.1-14 identify the specific components associated with each of these items.

The suppression chamber shell and ring girder are evaluated in accordance with the requirements for Class MC components contained in Subsection NE of the ASME

Code. Fillet welds and partial penetration welds in which one or both of the joined parts includes the suppression chamber shell and the ring girder are also evaluated in accordance with the requirements for Class MC component attachment welds contained in Subsection NE of the ASME Code.

The suppression chamber columns, column connections, saddle supports, and associated components and welds are evaluated in accordance with the requirements for Class MC component supports contained in Subsection NF of the ASME Code.

Table 2-2.2-11 shows that the SBA III, IBA III, IBA IV, and DBA III combinations all have Service Level B limits, while the DBA IV combination has Service Level C limits and the DBA I combination has Service Level D limits. Since these load combinations have somewhat different maximum temperatures, the allowable stresses for the three load combination groups with Service Level B, C, and D limits are conservatively determined at the highest temperature in each load combination group, unless otherwise indicated.

The allowable stresses for each suppression chamber component and vertical support system component are determined at the maximum SBA temperature of 165°F. The allowable stresses for the vertical support system base plate assemblies are determined at 100°F. Table 2-2.3-1 shows the resulting allowable stresses for the load combinations with Service Level B, C, and D limits.

The saddle and column base plate anchor bolts and associated epoxy grout, shown in Figure 2-2.1-8, are those specified in the torus support modification drawings (References 13 and 14). The minimum allowable uplift load per bolt, based on an average embedment of 3'-1/4", is 113 kips. This is equivalent to 3.12 kips per inch of embedment.

Bearing stresses in the grout and reactor building basemat in the vicinity of the column and saddle base plates are evaluated in accordance with the requirements of the American Concrete Institute (ACI) Code (Reference 15).

The allowable load capacities for the suppression chamber vertical support system are determined by considering the capacities of the individual components

and selecting the critical load. Allowable capacities for the column, saddle, base plates, anchor bolts, and epoxy grout are evaluated. To determine the saddle capacities, a hydrostatic load is applied to the 1/32 segment analytical model and the resulting stresses compared until the first component in the assembly reaches its allowable stress. Table 2-2.3-2 summarizes the resulting allowable load capacities for the suppression chamber vertical supports.

The allowable loads on the suppression chamber seismic sway bars are taken from the stress reports (References 16 and 17). The allowable seismic tension load for each sway bar is 346 kips.

The acceptance criteria described in the preceding paragraphs result in conservative estimates of the existing margins of safety and assure that the original suppression chamber design margins are restored.

Table 2-2.3-1

ALLOWABLE STRESSES FOR SUPPRESSION CHAMBER COMPONENTS AND SUPPORTS

ITEM		MATERIAL	MATERIAL[1] PROPERTIES (ksi)	STRESS TYPE	ALLOWABLE STRESS (ksi)		
					SERVICE[2] LEVEL B	SERVICE[3] LEVEL C	SERVICE[4] LEVEL D
COMPONENTS	SHELL	SA-516 GRADE 70	S_{mc} = 19.30 S_{ml} = 23.17 S_y = 35.86 S_u = 70.00	PRIMARY MEMBRANE	19.30	35.86	41.65
				LOCAL PRIMARY MEMBRANE	28.95	53.79	62.48
				PRIMARY + SECONDARY[5] STRESS RANGE	69.51	N/A	N/A
	RING GIRDER	SA-516 GRADE 70	S_{mc} = 19.30 S_{ml} = 23.17 S_y = 35.86 S_u = 70.00	PRIMARY MEMBRANE	19.30	35.86	41.65
				LOCAL PRIMARY MEMBRANE	28.95	53.79	62.48
				PRIMARY + SECONDARY[5] STRESS RANGE	69.51	N/A	N/A
COMPONENT SUPPORTS	COLUMN[6] CONNECTION	SA-516 GRADE 70	S_y = 35.86	MEMBRANE	21.52	28.69	43.04
				EXTREME FIBER	26.90	35.87	53.80
	SADDLE[6]	SA-516 GRADE 70	S_y = 35.86	MEMBRANE	21.52	28.69	43.04
				EXTREME FIBER	26.90	35.87	53.80
WELDS	RING GIRDER TO SHELL	SA-516 GRADE 70	S_{mc} = 19.30 S_{ml} = 23.17 S_y = 35.86	PRIMARY	15.02	27.89	32.40
				PRIMARY + SECONDARY	54.07	N/A	N/A
	COLUMN CONNECTION TO SHELL	SA-516 GRADE 70	S_{mc} = 19.30 S_{ml} = 23.17 S_y = 35.86	PRIMARY	15.02	27.89	32.40
				PRIMARY + SECONDARY	54.07	N/A	N/A
	SADDLE TO SHELL	SA-516 GRADE 70	S_{mc} = 19.30 S_{ml} = 23.17 S_y = 35.86	PRIMARY	20.47	38.03	44.17
				PRIMARY + SECONDARY	61.42	N/A	N/A

(1) MATERIAL PROPERTIES ARE TAKEN AT THE MAXIMUM EVENT TEMPERATURE.

(2) SERVICE LEVEL B ALLOWABLES ARE USED WHEN EVALUATING SBA III, IBA I, IBA III, IBA IV, AND DBA II LOAD COMBINATION RESULTS.

(3) SERVICE LEVEL C ALLOWABLES ARE USED WHEN EVALUATING IBA V AND DBA IV LOAD COMBINATION RESULTS.

(4) SERVICE LEVEL D ALLOWABLES ARE USED WHEN EVALUATING DBA I LOAD COMBINATION RESULTS.

(5) THERMAL BENDING STRESSES MAY BE EXCLUDED WHEN COMPARING PRIMARY-PLUS-SECONDARY STRESS RANGE VALUES TO ALLOWABLES.

(6) STRESSES DUE TO THERMAL LOADS MAY BE EXCLUDED WHEN EVALUATING COMPONENT SUPPORTS.

Table 2-2.3-2

SUPPRESSION CHAMBER VERTICAL SUPPORT SYSTEM ALLOWABLE LOADS

SUPPORT COMPONENT		LOAD CAPACITY (kips)	
		UPWARD	DOWNWARD(1)
COLUMN	INSIDE	191(1)	1002
	OUTSIDE	352(1)	1300
SADDLE	INSIDE	879(2)	901
	OUTSIDE	879(2)	901
TOTAL PER MITERED CYLINDER		2301	4104

(1) CAPACITIES SHOWN ARE BASED ON SERVICE LEVEL B ALLOWABLES. FOR SERVICE LEVEL C ALLOWABLES, INCREASE VALUES SHOWN BY 1/3. FOR SERVICE LEVEL D ALLOWABLES, MULTIPLY VALUES SHOWN BY A FACTOR OF 2.

(2) CAPACITIES ARE APPLICABLE FOR ALL SERVICE LEVELS.

2-2.4 Method of Analysis

The governing loads for which the Dresden Units 2 and 3 suppression chambers are evaluated are presented in Section 2-2.2.1. The methodology used to evaluate the suppression chamber for the effects of all loads (except those which result in lateral loads on the suppression chamber) is discussed in Section 2-2.4.1. The methodology used to evaluate the suppression chamber for the effects of lateral loads is discussed in Section 2-2.4.2.

The methodology used to formulate results for the controlling load combinations, consider fatigue effects, and evaluate the analysis results for comparison with the applicable acceptance limits is discussed in Section 2-2.4.3.

2-2.4.1 Analysis for Major Loads

The repetitive nature of the suppression chamber geometry is such that the suppression chamber can be divided into 16 identical segments, which extend from midbay of the vent line bay to midbay of the non-vent line bay (Figure 2-2.1-1). The suppression chamber can be further divided into 32 identical segments extending from the miter joint to midbay, provided the offset ring girder and vertical supports are assumed to lie in the plane of the miter joint. The effects of the ring girder and vertical supports offset have been evaluated and found to have a negligible effect on the suppression chamber response. The analysis of the suppression chamber, therefore, is performed for a typical 1/32 segment.

A finite element model of a 1/32 segment of the suppression chamber is used to obtain the suppression chamber response to all loads except those on submerged structures (Figure 2-2.4-1). This analytical model includes the suppression chamber shell, the ring girder modeled with beam elements, the column connections and associated column members, the saddle support and associated base plates, and miscellaneous stiffener plates.

This analytical model is composed of 955 nodes, 298 elastic beam elements, and 1,147 plate bending and stretching elements. The suppression chamber shell has a circumferential node spacing of 8° at midbay, with additional mesh refinement near discontinuities to facilitate examination of local stresses. Additional refinement is also included in modeling of the column connections and saddle support at locations where higher local stresses occur. The stiffness and mass properties used in the model are based on the nominal dimensions and densities of the materials used to construct the suppression chamber (Figures 2-2.1-1 through 2-2.1-12). Small displacement linear-elastic behavior is assumed throughout.

The boundary conditions used in this analytical model are both physical and mathematical in nature. The physical boundary conditions consist of vertical restraints at each of the column and saddle base plate locations. The mathematical boundary conditions consist of symmetry, anti-symmetry, or a combination of both (depending on the characteristics of the load being evaluated) at the miter joint and midcylinder planes.

A second finite element model is developed to obtain detailed ring girder responses to suppression chamber shell hydrodynamic loads and ring girder-torus shell interaction responses to loads on submerged structures. This model consists of a detailed plate model of the ring girder and ring girder stiffeners, a partial 1/32 segment torus shell model on each side of the miter joint, the column connections and associated column members, the saddle support with associated flanges, and the stiffener plates. The column, column connection, and saddle support are positioned 4" from the miter joint in this analytical model to accurately represent the as-built torus support system. Figures 2-2.4-2 and 2-2.4-3 show the ring girder analytical model.

The model reflects the modified ring girders, reinforced to withstand Mark I loads. These modifications are lateral reinforcement stiffeners to prevent ring girder bending due to out-of-plane loads. Upon installation of the final Mark I related modifications, both Dresden units will have five ring girder stiffeners in the SRV bays (Figure 2-2.1-4); however, they differ in the number of ring girder stiffeners in the non-SRV bays. Unit 2 has zero, and Unit 3 has two (Figure 2-2.4-4). Two analytical models

were generated to address the submerged structure loads, one each for the SRV and non-SRV bays. These are the five-stiffener model and the zero-stiffener model. The zero stiffener ring girder configuration was conservatively chosen for analysis of the non-SRV bay loads.

The zero stiffener model is composed of 1,467 nodes, 307 elastic beam elements, and 2,068 plate bending and stretching elements. The five-stiffener model has an additional 30 nodes, 4 elastic beam elements, and 37 plate bending and stretching elements. The five stiffener shell mesh refinement of this model is the same as that of the previously described torus shell model. A spoke system is constructed at the shell boundaries on each side of the miter joint and a rigid beam extended to midbay, where symmetry boundary conditions are imposed. The vertical restraints for this analytical model are the same as those previously discussed for the suppression chamber model.

For each of the hydrodynamic torus shell loads, a displacement set is statically applied to the ring girder-torus shell intersection on the ring girder model, along with appropriate dynamic amplification factors. This displacement set is selected from the response

time-history at the time of maximum strain energy. These loads thus applied determine the state of stress in the ring girder due to hydrodynamic torus shell loads.

For each of the submerged structure loads, a set of forces is applied to the ring girder below the pool surface in the out-of-plane direction. A dynamic load factor (DLF) is developed for each load, depending upon the natural frequency of the ring girder and that of the load itself. With the application of this factor, the state of stress is determined in the ring girder, the ring girder stiffener plates, and the local torus shell due to the submerged structure loads.

When computing the response of the suppression chamber to dynamic loadings, the fluid-structure interaction effects of the suppression chamber shell and contained fluid (water) are considered. This is accomplished through use of a finite element model of the fluid (Figure 2-2.4-5). The analytical fluid model is used to develop a coupled mass matrix, which is added to the submerged nodes of the suppression chamber analytical model to represent the fluid. A water volume corresponding to a water level 3-1/2" below the suppression chamber horizontal centerline is used in

this calculation. This is the average water volume expected during normal operating conditions.

A frequency analysis is performed using the suppression chamber analytical model from which all structural modes in the range of 0 to 50 hertz are extracted. Table 2-2.4-1 shows the resulting frequencies and vertical mass participation factors. The dominant suppression chamber frequency occurs at 18.87 hertz, which is above the dominant frequencies of most major hydrodynamic loadings.

Using the analytical model of the suppression chamber, a dynamic analysis is performed for each of the hydrodynamic torus shell load cases specified in Section 2-2.2.1. The analysis consists of either a transient or a harmonic analysis, depending on the characteristics of the torus shell load being considered. The modal superposition technique with 2% of critical damping, as recommended by Regulatory Guide 1.61 (Reference 18), is utilized in both transient and harmonic analyses.

The remaining suppression chamber load cases specified in Section 2-2.2.1 involve either static or dynamic loads which are evaluated using an equivalent static

approach. For the latter, conservative dynamic amplification factors are developed and applied to the maximum spatial distributions of the individual dynamic loadings.

The specific treatment of each load in the load categories identified in Section 2-2.2.1 is discussed in the following paragraphs.

1. Dead Weight Loads

   a. Dead Weight of Steel: A static analysis is performed for a unit vertical acceleration applied to the weight of suppression chamber steel.

   b. Dead Weight of Water: A static analysis is performed for hydrostatic pressures applied to the submerged portion of the suppression chamber shell.

2. Seismic Loads

   a. OBE Loads: A static analysis is performed for a 0.07g vertical acceleration applied to the combined weight of suppression chamber

steel and water. The effects of horizontal OBE accelerations are evaluated in Section 2-2.4.2.

b. SSE Loads: A static analysis is performed for a 0.14g vertical acceleration applied to the combined weight of suppression chamber steel and water. The effects of horizontal SSE accelerations are evaluated in Section 2-2.4.2.

3. Containment Pressure and Temperature

a. Normal Operating Internal Pressure: A static analysis is performed for a 0.2 psi internal pressure uniformly applied to the suppression chamber shell.

b. LOCA Internal Pressure Loads: A static analysis is performed for the SBA, IBA, and DBA internal pressures (Figures 2-2.2-1 through 2-2.2-3). These pressures are uniformly applied to the suppression chamber shell at selected times during each event.

c. Normal Operating Temperature Loads: A static analysis is performed for a 165°F temperature uniformly applied to the suppression chamber shell, ring girder, saddle, and columns. An additional static analysis is performed for the maximum normal operating temperature listed in Table 2-2.2-2. Discrete temperatures for the suppression chamber vertical supports are obtained from Figure 2-2.2-7.

d. LOCA Temperature Loads: A static analysis is performed for the SBA, IBA, and DBA temperatures uniformly applied to the suppression chamber shell, ring girder, saddle, and columns. The SBA, IBA, and DBA event temperatures (Figures 2-2.2-4 through 2-2.2-6) are applied at selected times during each event. The greater of the temperatures specified in Figure 2-2.2-4 and Table 2-2.2-2 is used in the analysis for SBA temperatures. Discrete temperatures for the suppression chamber vertical supports are obtained from Figure 2-2.2-7.

4. Column Preset Loads

A static analysis is performed on the suppression chamber with a preset of 3/16" at the inside column and a preset of 11/16" at the outside column.

5. Pool Swell Loads

a-b. Pool Swell Torus Shell Loads: A dynamic analysis is performed for both the vent and non-vent line bays for both the operating and zero ΔP pool swell load conditions (Figures 2-2.2-8 through 2-2.2-11 and Tables 2-2.2-4 and 2-2.2-5). The loads are applied to a 1/32 torus model with symmetric boundary conditions at the miter joint and to one with asymmetric boundary conditions at the miter joint. These results are then combined to represent the effect of differential loads across the miter.

c. LOCA Water Jet Loads on Submerged Structures: In comparison with other submerged structure loads on the ring girder, these loads have a negligible effect on the final stress levels,

and will not be considered in this evaluation.

d. LOCA Bubble-Induced Loads on Submerged Structures: In comparison with other submerged structure loads on the ring girder, these loads have a negligible effect on the final stress levels, and will not be considered in this evaluation.

6. Condensation Oscillation Loads

a. DBA CO Torus Shell Loads: A dynamic analysis is performed for the four CO load alternates (Table 2-2.2-6). Figure 2-2.4-6 provides a typical response obtained from the suppression chamber harmonic analysis for the normalized spatial distribution of pressures (Figure 2-2.2-12). During harmonic summation, the amplitudes for each CO load frequency interval are conservatively applied to the maximum response amplitudes obtained from the suppression chamber harmonic analysis results in the same frequency interval.

b. IBA CO Torus Shell Loads: Pre-chug loads described in Load Case 7a are specified in lieu of IBA CO loads.

c. DBA CO Submerged Structure Loads: An equivalent static analysis is performed for the ring girder DBA CO loads on submerged structures (Table 2-2.2-7). The values of the loads shown are derived using the methodology discussed in Section 1-4.1.7.3 and include dynamic amplication factors.

d. IBA CO Submerged Structure Loads: Pre-chug loads described in Load Case 7c are specified in lieu of IBA CO loads.

7. Chugging Loads

a. Pre-Chug Torus Shell Loads: A dynamic analysis is performed for the symmetric pre-chug loads (Figure 2-2.2-14). The harmonic analysis results show that the maximum suppression chamber response in the 6.9 to 9.5 hertz range occurs at the structural frequency of 9.5 hertz (Table 2-2.4-1). The

effects of lateral loads caused by asymmetric pre-chug are examined in Section 2-2.4.2.

b. Post-Chug Torus Shell Loads: A dynamic analysis is performed for post-chug torus shell loads (Table 2-2.2-8). Figure 2-2.4-6 provides a typical response obtained from the suppression chamber harmonic analysis for the normalized spatial distribution of pressures (Figure 2-2.2-12). During harmonic summation, the amplitudes for each post-chug load frequency interval are conservatively applied to the maximum response amplitudes obtained from the suppression chamber harmonic analysis results in the same frequency interval.

c. Pre-Chug Submerged Structure Loads: In comparison with other submerged structure loads on the ring girder, these loads have a negligible effect on the final stress levels, and will not be considered in this evaluation.

d. Post-Chug Submerged Structure Loads: An equivalent static analysis is performed for

the ring girder loads on submerged structures (Table 2-2.2-9). The values of the loads shown are derived using the methodology discussed in Section 1-4.1.8.3 and include dynamic amplification factors.

8. Safety Relief Valve Discharge Loads

a-b. SRV Discharge Torus Shell Loads: A dynamic analysis is performed for SRV Discharge Torus Shell Load Cases 8a and 8b (Figures 2-2.2-16 and 2-2.2-17). Several frequencies within the range of the SRV discharge load frequencies are evaluated to determine the maximum suppression chamber response. The effects of lateral loads on the suppression chamber caused by SRV Discharge Load Case 8b are evaluated in Section 2-2.4.2.

The suppression chamber analytical model used in the analysis is calibrated using the methodology discussed in Section 1-4.2.3. The methodology involves use of modal correction factors which are applied to the response associated with each suppression

chamber frequency. Figure 2-2.4-7 shows the resulting correction factors used in evaluating the effects of SRV discharge torus shell loads.

c. SRV Discharge Water Jet Loads on Submerged Structures: In comparison with other submerged structure loads on the ring girder, these loads have a negligible effect on the final stress levels, and will not be considered in this evaluation.

d. SRV Discharge Bubble-Induced Drag Loads on Submerged Structures: An equivalent static analysis is performed for the ring girder SRV discharge drag loads (Table 2-2.2-10). The values of the loads shown are derived using the methodology discussed in Section 1-4.2.4 and include dynamic amplification factors.

9. Containment Interaction Loads

a. Containment Structures Reaction Loads: An equivalent static analysis is performed for the vent system support column, SRVDL

support, T-quencher support, ECCS header support, spray header, and catwalk support reaction loads taken from the evaluations of these components described in Volumes 3 through 5 of this report.

The methodology described in the preceding paragraphs results in a conservative evaluation of the suppression chamber response and associated stresses for the governing loads. Use of the analysis results obtained by applying this methodology leads to a conservative evaluation of the suppression chamber design margins.

Table 2-2.4-1

SUPPRESSION CHAMBER FREQUENCY ANALYSIS RESULTS

MODE NUMBER	FREQUENCY (Hz)	VERTICAL MASS PARTICIPATION FACTOR (lb)
1	9.45	304.5
2	9.74	7.1
3	11.55	686.3
4	11.56	181.7
5	12.58	448.5
6	13.36	1700.2
7	14.09	961.8
8	14.96	21725.4
9	15.81	992.6
10	16.53	25783.6
11	17.83	3507.6
12	18.87	95847.4
13	19.64	52145.1
14	20.11	9522.8
15	21.44	9342.4
16	21.78	3528.2
17	22.54	10186.4
18	24.22	196.9
19	24.92	27.9
20	25.58	79.1
21	25.68	4684.7
22	26.22	973.3
23	26.94	3209.2
24	28.27	281.2
25	28.70	1.5

Table 2-2.4-1

SUPPRESSION CHAMBER FREQUENCY ANALYSIS RESULTS

(Continued)

MODE NUMBER	FREQUENCY (Hz)	VERTICAL MASS PARTICIPATION FACTOR (lb)
26	28.92	846.8
27	29.33	2776.2
28	29.85	845.8
29	30.82	4514.0
30	31.21	279.2
31	31.81	762.2
32	31.99	1771.6
33	32.58	5.0
34	33.82	29.9
35	33.90	1.0
36	34.52	154.7
37	34.78	105.5
38	35.14	164.3
39	36.10	118.4
40	36.53	6.0
41	36.92	163.6
42	37.38	115.7
43	37.91	137.5
44	38.45	28.9
45	38.57	184.8
46	39.17	27.4
47	39.50	15.2
48	40.16	60.7
49	40.76	3.6
50	41.24	95.2

Table 2-2.4-1

SUPPRESSION CHAMBER FREQUENCY ANALYSIS RESULTS

(Concluded)

MODE NUMBER	FREQUENCY (Hz)	VERTICAL MASS PARTICIPATION FACTOR (lb)
51	41.60	182.7
52	41.93	66.0
53	42.26	2.2
54	42.60	1.2
55	43.03	2.8
56	44.22	0.1
57	44.51	0.4
58	44.86	2.0
59	45.34	65.4
60	45.74	5.8
61	46.30	0.0
62	46.73	0.0
63	47.78	1.7
64	48.56	23.4
65	48.65	8.4
66	48.68	0.3
67	48.88	9.7
68	49.12	0.3
69	49.44	4.1
70	49.70	20.0
71	50.39	1.5
72	50.83	10.3

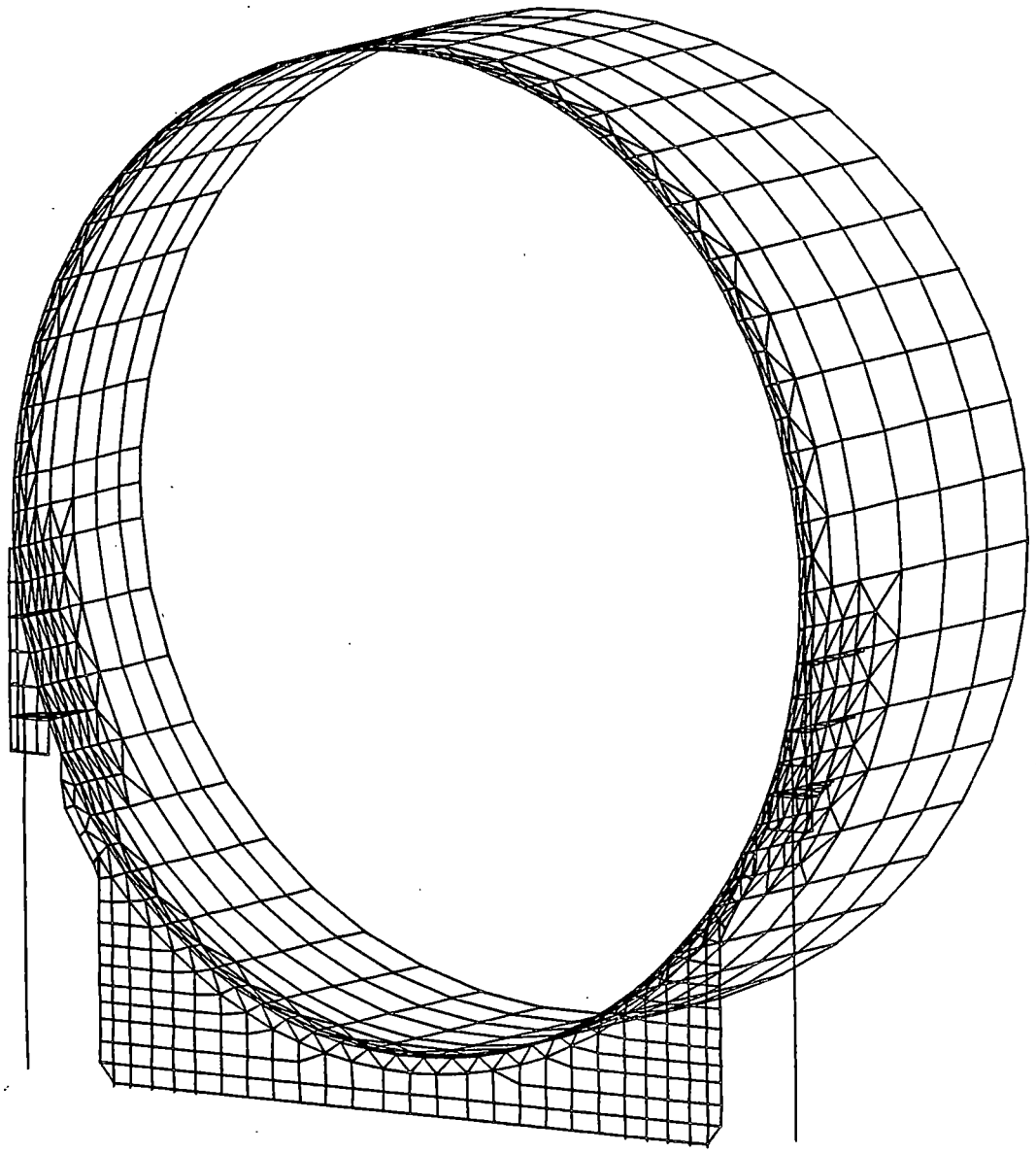

Figure 2-2.4-1

SUPPRESSION CHAMBER 1/32 SEGMENT FINITE ELEMENT MODEL - ISOMETRIC VIEW

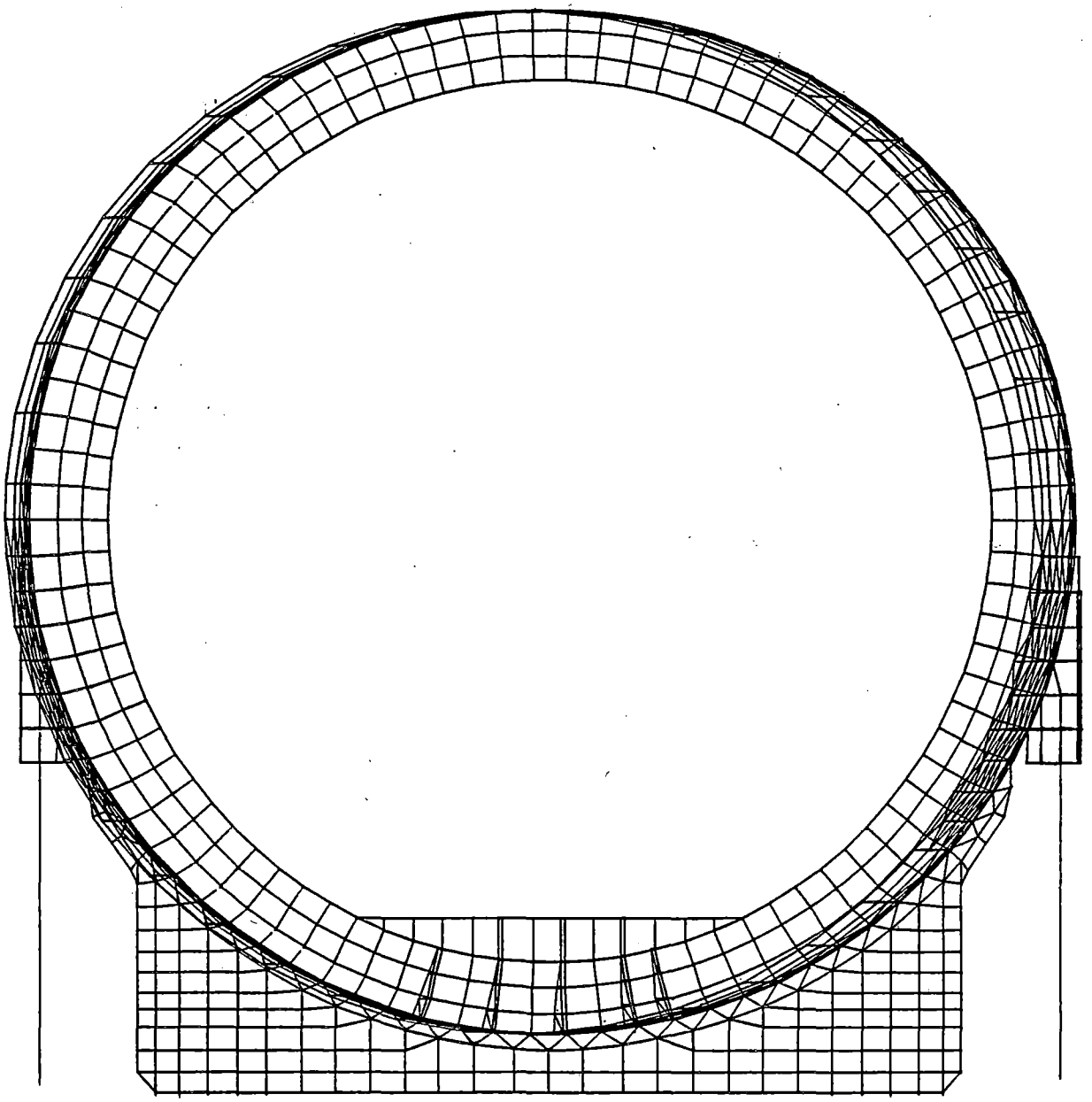

Figure 2-2.4-2

RING GIRDER MODEL - VIEW FROM THE MITER JOINT

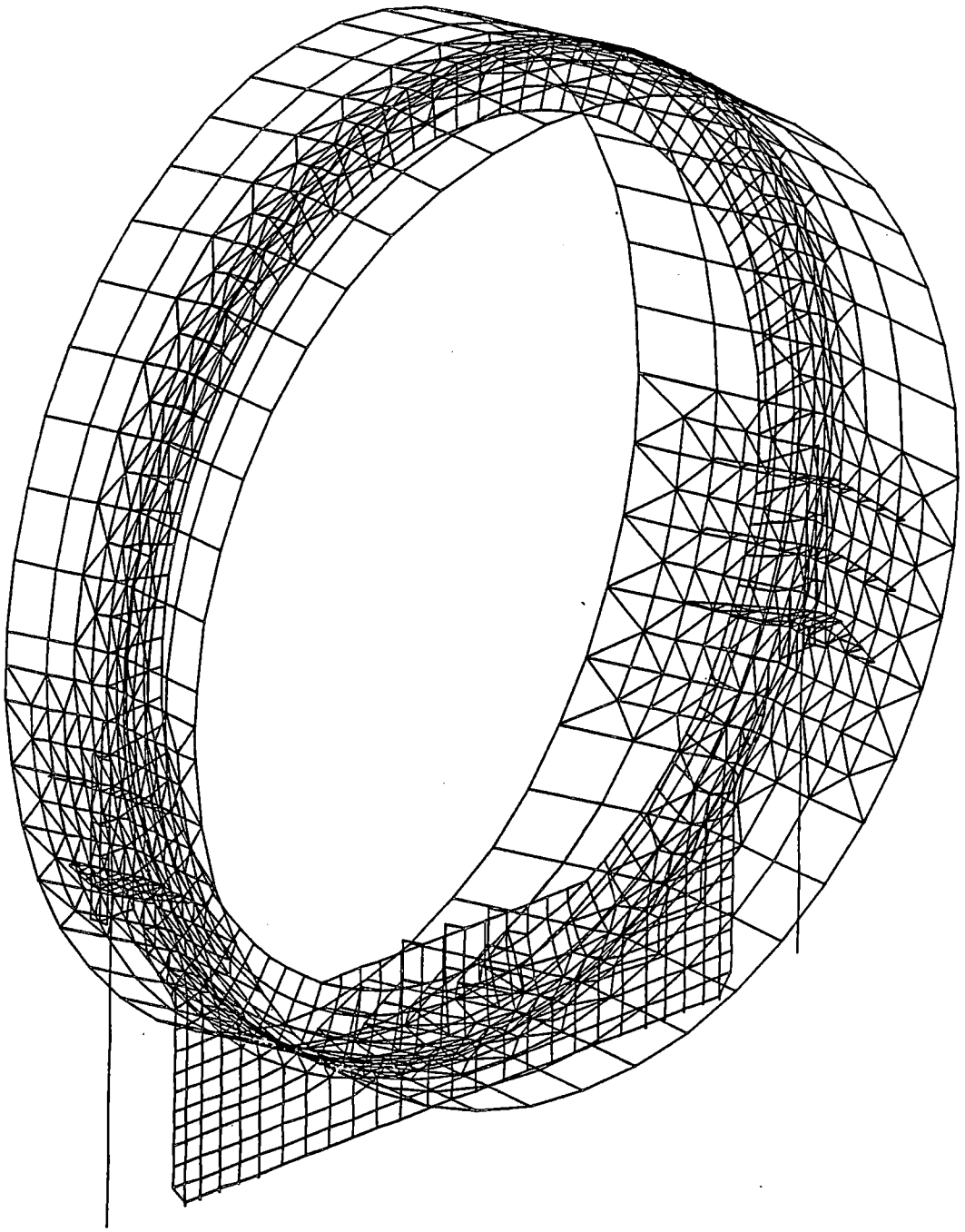

Figure 2-2.4-3

RING GIRDER MODEL - ISOMETRIC VIEW

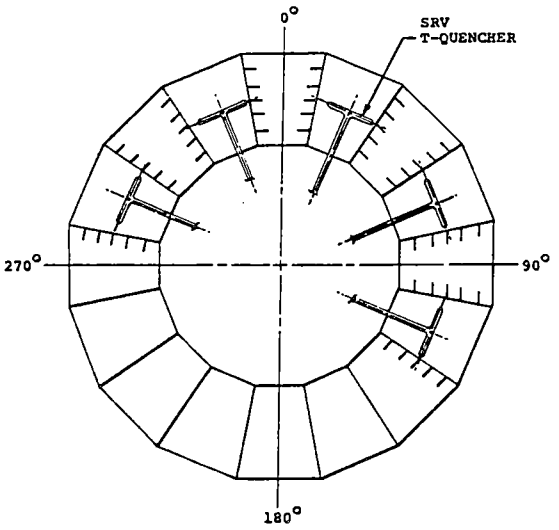

DRESDEN 2

(10 ring girders with 5 stiffeners;
6 ring girders without stiffeners)

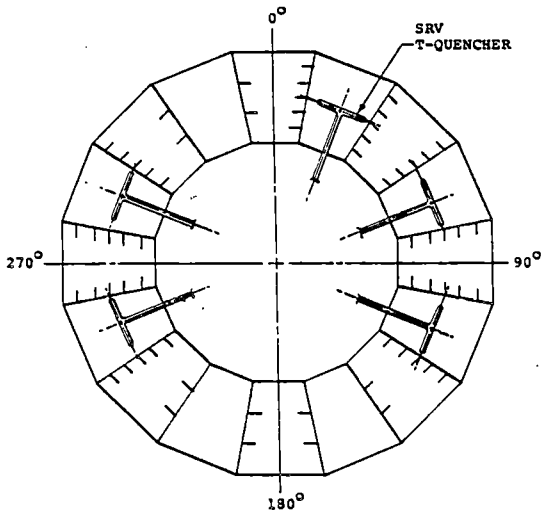

DRESDEN 3

(10 ring girders with 5 stiffeners;
6 ring girders with 2 stiffeners)

Figure 2-2.4-4

FINAL RING GIRDER STIFFENER CONFIGURATION

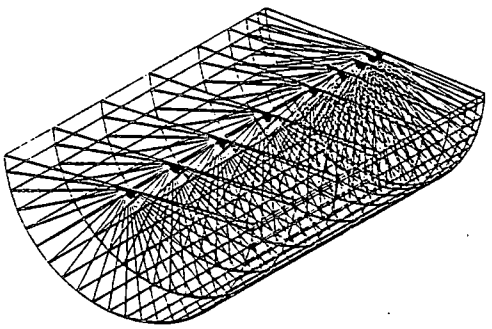

FLUID MODEL CORE

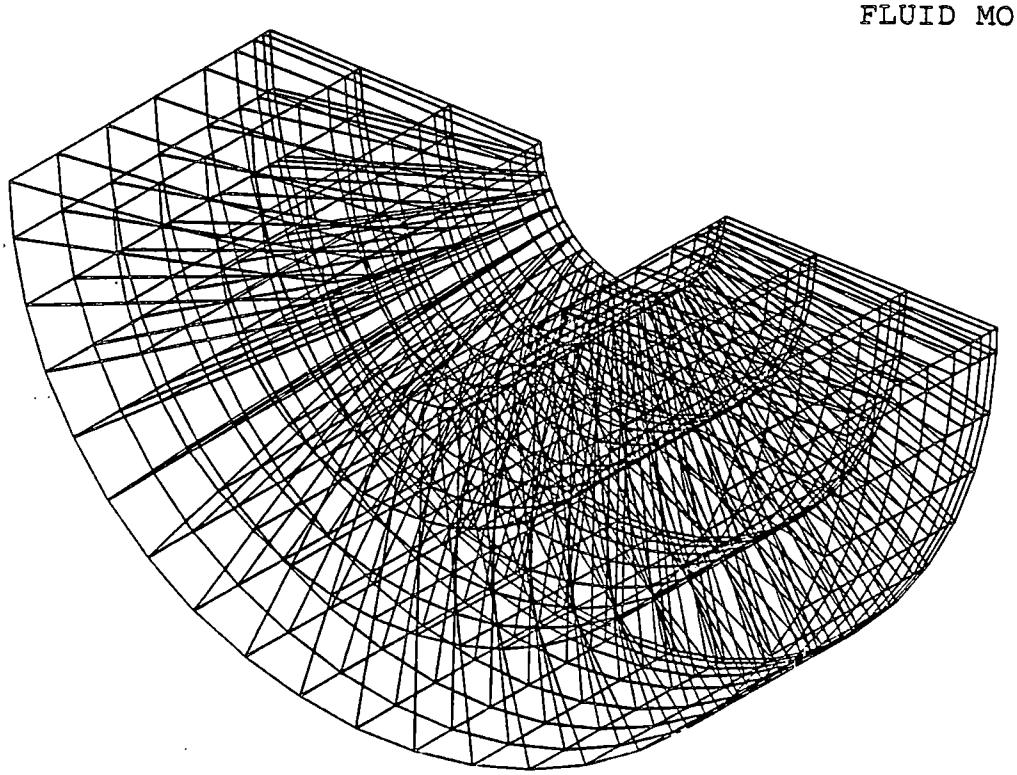

Figure 2-2.4-5

SUPPRESSION CHAMBER FLUID MODEL - ISOMETRIC VIEW

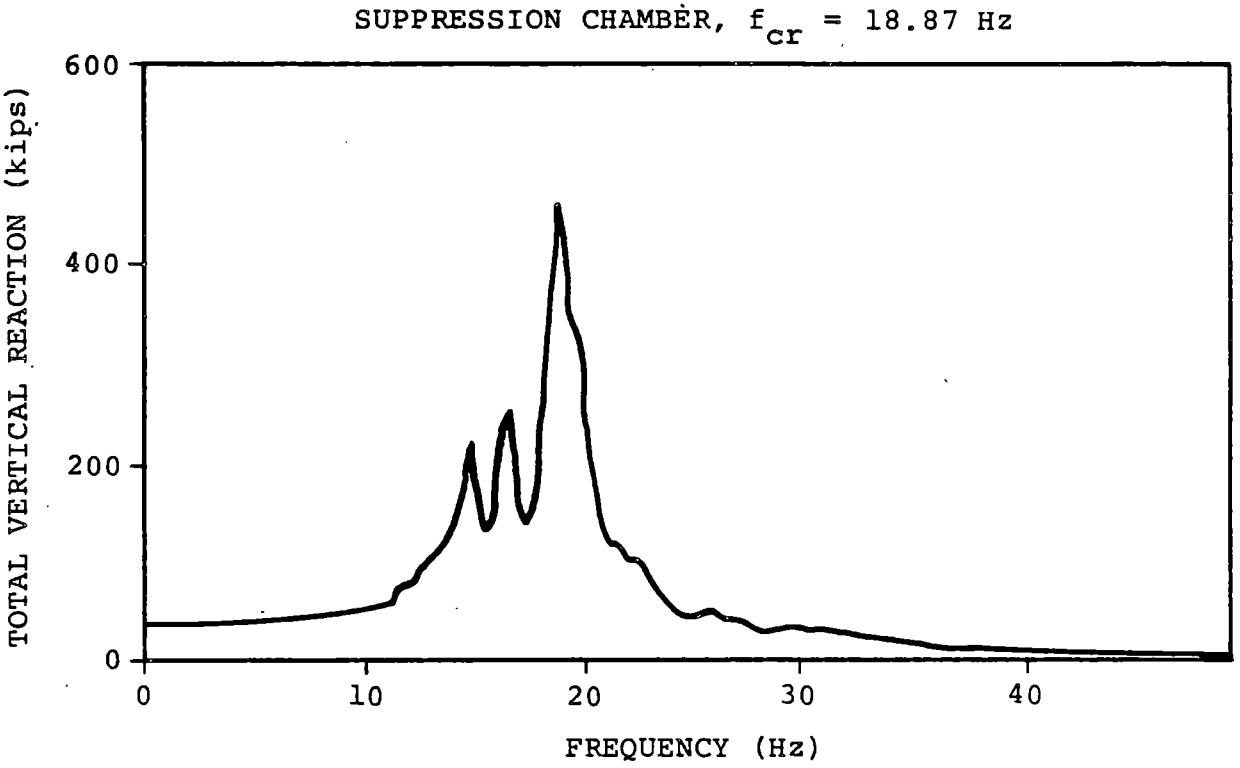

1. SEE FIGURE 2-2.2-10 FOR SPATIAL DISTRIBUTION OF LOADING.

Figure 2-2.4-6

SUPPRESSION CHAMBER HARMONIC ANALYSIS RESULTS FOR NORMALIZED HYDROSTATIC LOAD

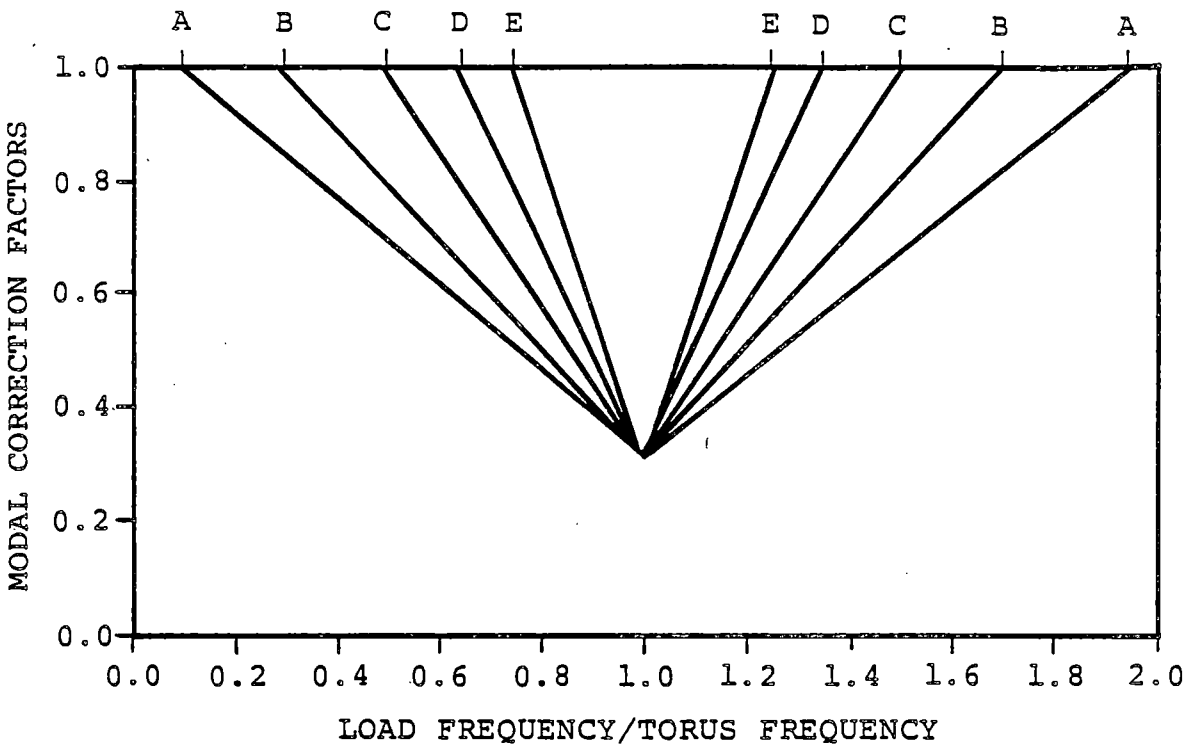

MODE NUMBER	FREQUENCY (Hz)	CORRECTION FACTOR CASE A1.2 (fℓ=13.25)
1	9.45	0.64
2	9.74	0.60
3	11.55	0.42
4	11.56	0.41
5	12.58	0.32
6	13.36	0.32
7	14.09	0.37
8	14.96	0.52
9	15.81	0.57
10	16.53	0.64
11	17.83	0.81
12	18.87	0.90
13	19.64	0.95
14	20.11	0.98
15	21.44	1.00
16-72	≥ 21.78	1.00

LEGEND	
CURVE	TORUS FREQUENCY (Hz)
A	8
B	11
C	14
D	17-23
E	26-32

Figure 2-2.4-7

MODAL CORRECTION FACTORS USED FOR ANALYSIS OF SRV DISCHARGE TORUS SHELL LOADS

2-2.4.2 Analysis for Lateral Loads

In addition to vertical loads, a few of the governing loads acting on the suppression chamber result in net lateral loads, as discussed in Section 2-2.2.1. These lateral loads are transferred to the reactor building basemat by the seismic sway rods and outside column base plate described in Section 2-2.1.

The general methodology used to evaluate the effects of lateral loads consists of establishing an upper bound value of the lateral load for each applicable load case. The results for each load case are then grouped in accordance with the controlling load combinations described in Section 2-2.2.2, and the maximum total lateral load acting on the suppression chamber is determined.

The direction of each lateral load acting on the suppression chamber is taken as the azimuth (Figure 2-2.1-1) causing the maximum tensile stress in the seismic sway rods. Depending on the load, the direction of the azimuth is aligned either with a miter joint or with the midbay of a 1/16th sector of the suppression chamber. A 360° beam model of the torus, supports, and seismic sway rods was used in this deter-

mination of the distribution of the lateral loads. Once the seismic restraint loads are known, these values are compared with the allowable seismic restraint loads contained in Section 2-2.3.

Tensile loads in the seismic sway rods result in concentrated forces acting on the suppression chamber. These forces act in the direction of the sway rods at the point of attachment to the outside column wing plates. The effect of these forces on the suppression chamber shell are evaluated using the analytical model described in Section 2-2.4.1 as the ring girder model. Figure 2-2.4-8 shows the application and distribution of the lateral loads. The resulting shell stresses are then combined with the other loads contained in the controlling load combination being evaluated, and the shell stresses in the vicinity of the seismic restraints are determined.

The magnitudes and characteristics of the governing loads which result in lateral loads on the suppression chamber are presented and discussed in Section 2-2.2.1. The specific treatment of each load which results in lateral loads on the suppression chamber is discussed in the following paragraphs.

2. Seismic Loads

a. OBE Loads: The total lateral load due to OBE loads is equal to the maximum horizontal acceleration of 0.25g applied to the weight of suppression chamber steel and the effective weight of suppression chamber water in the horizontal direction.

The effective weight of suppression chamber water in the horizontal direction used in this evaluation is derived from generic small-scale tests performed on Mark I suppression chambers. These test results have been confirmed analytically using a model of the suppression chamber fluid (water) similar to the one shown in Figure 2-2.4-5.

As recommended in the "Mark I Torus Seismic Slosh Evaluation" (Reference 19), the effective weight of suppression chamber water is taken as 20% of the total weight of water contained in the suppression chamber. This value represents the amount of water acting with the suppression chamber as added mass

during horizontal dynamic events. The effective weight of water exhibits itself in tension loads on the seismic sway bars. The remaining 80% of suppression chamber water acts in sloshing modes at frequencies near zero. Only a portion of the total sloshing mass acting at considerably lower seismic accelerations results in reaction loads on the seismic restraints. The total sloshing mass is conservatively applied at the maximum OBE acceleration in the range of the sloshing frequencies.

b. SSE Loads: The total lateral load due to SSE loads is equal to the maximum horizontal acceleration of 0.50g applied to the weight of suppression chamber steel and the effective weight of suppression chamber water in the horizontal direction. The methodology used to evaluate horizontal SSE loads is discussed in Load Case 2a.

7. Chugging Loads

a. Pre-Chug Torus Shell Loads: The spatial distribution of asymmetric pre-chug pressures is

integrated, and the total lateral load is determined (Figures 2-2.2-14 and 2-2.2-15). A dynamic amplification factor is computed using first principles and characteristics of the chugging cycle transient (Figure 2-2.4-9). The maximum dynamic amplification factor possible, regardless of structural frequency, is conservatively used.

8. Safety Relief Valve Discharge Loads

c. SRV Discharge Torus Shell Loads: The spatial distribution of pressures for SRV Discharge Load Case 8b is integrated and the total lateral load is determined (Figures 2-2.2-17 and 2-2.2-18). It was determined that, due to the positioning of these T-quenchers, a larger lateral load is created by the multiple actuation of four safety relief valves than by all five. The maximum load due to the actuation of four valves was used. A dynamic amplification factor is computed using the methodology discussed in Section 2-2.4.1 for SRV discharge torus shell loads analysis. The maximum dynamic amplification factor possible, regardless of

structural frequency, is conservatively used (Figure 2-2.4-10).

Use of the methodology described in the preceding paragraphs results in a conservative evaluation of suppression chamber shell stresses. These stresses are due to the governing loads which result in lateral loads on the suppression chamber.

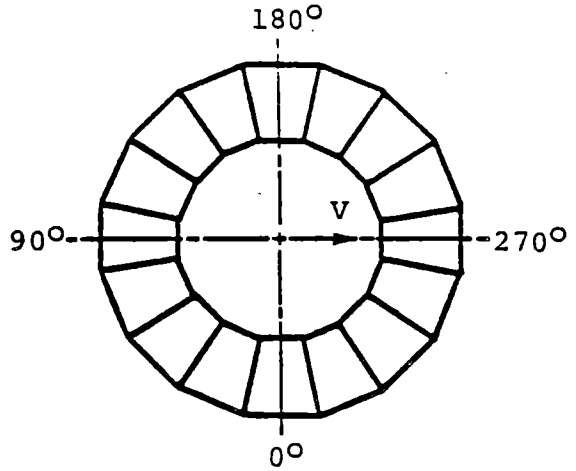

PLAN VIEW

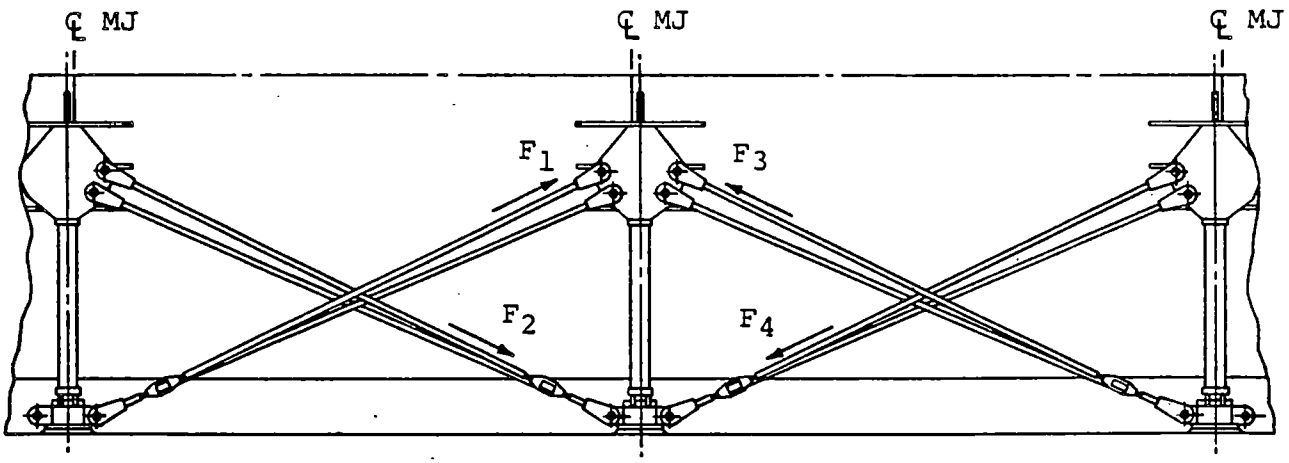

PARTIAL ELEVATION VIEW

FOR V_{tot} = 2,018 kip(1)

F_1 = 123.12 kip TENSION F_3 = 0.00 kip TENSION

F_2 = 0.00 kip TENSION F_4 = 114.42 kip TENSION

(1) THIS TOTAL LOAD REPRESENTS THE SUM OF OBE PRE-CHUG AND SRV LATERAL LOADS.

Figure 2-2.4-8

METHODOLOGY FOR SUPPRESSION CHAMBER LATERAL LOAD APPLICATION

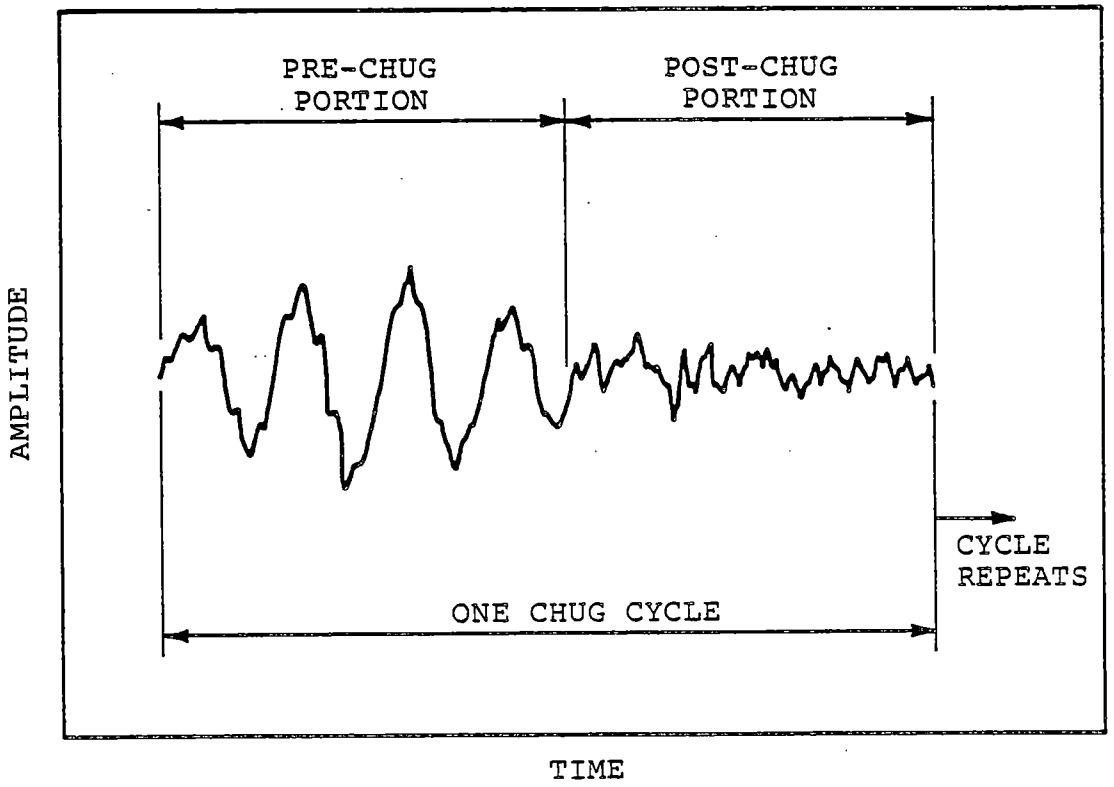

Figure 2-2.4-9

TYPICAL CHUGGING LOAD TRANSIENT USED FOR ASYMMETRIC PRE-CHUG DYNAMIC AMPLIFICATION FACTOR DETERMINATION

DLF_{max} = 2.42

TORUS FREQUENCY (f_t) (Hz)	LOAD FREQUENCY RANGE (f_ℓ) (Hz)	FREQUENCY RATIO (f_ℓ/f_t)	FORCED VIBRATION DLF RANGE	MODAL CORRECTION FACTOR (MCF)	DLF X MCF
8.	7.800	0.975	4.324	0.358	1.549
	18.200	2.275	0.973	1.000	0.973
11.0	7.800	0.709	2.396	0.614	1.472
	18.200	1.655	1.947	0.957	1.864
14.0	7.800	0.557	1.911	0.925	1.767
	18.200	1.300	3.292	0.736	2.423
17.0	7.800	0.459	1.528	1.000	1.528
	18.200	1.071	4.523	0.473	2.140
23.0	7.800	0.339	1.285	1.000	1.285
	18.200	0.791	2.633	0.734	1.932
26.0	7.800	0.300	1.282	1.000	1.282
	18.200	0.700	2.375	1.000	2.375
32.0	7.800	0.244	1.424	1.000	1.424
	18.200	0.569	1.941	1.000	1.941

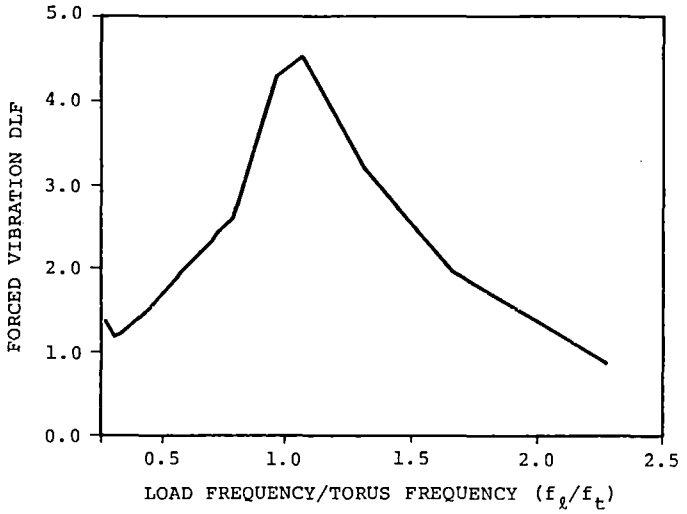

1. SEE FIGURE 2-2.2-17 FOR FORCED VIBRATION LOADING TRANSIENT AND FREQUENCY RANGE.
2. SEE FIGURE 2-2.4-7 FOR MODAL CORRECTION FACTORS.

Figure 2-2.4-10

DYNAMIC LOAD FACTOR DETERMINATION FOR SUPPRESSION CHAMBER UNBALANCED LATERAL LOAD DUE TO SRV DISCHARGE MULTIPLE VALVE ACTUATION

2-2.4.3 Methods for Evaluating Analysis Results

The methodology discussed in Sections 2-2.4.1 and 2-2.4.2 is used to determine element forces and component stresses in the suppression chamber components. The methodology used to evaluate the analysis results, determine the controlling stresses in the suppression chamber components and component supports, and examine fatigue effects is discussed in the following paragraphs.

Membrane and extreme fiber stress intensities are computed when the analysis results for the suppression chamber Class MC components are evaluated. The values of the membrane stress intensities away from discontinuities are compared with the primary membrane stress allowables contained in Table 2-2.3-1. The values of membrane stress intensities near discontinuities are compared with local primary membrane stress allowables contained in Table 2-2.3-1. Primary stresses in suppression chamber Class MC component welds are computed using the maximum primary stress or resultant force acting on the associated weld throat. The results are compared to the primary weld stress allowables contained in Table 2-2.3-1.

In each of the controlling load combinations there are many dynamic loads resulting in stresses which cycle with time, and which are partially or fully reversible. The maximum stress intensity range for all suppression chamber Class MC components is calculated using the maximum values of the extreme fiber stress differences which occur near discontinuities. These values are compared with primary plus secondary stress range allowables contained in Table 2-2.3-1. A similar procedure is used to compute the stress range for the suppression chamber Class MC component welds. The results are compared to the primary plus secondary weld stress allowables contained in Table 2-2.3-1.

When analysis results for the suppression chamber saddle supports are evaluated, membrane and extreme fiber principal stresses are computed and compared with the Class MC component support allowable stresses contained in Table 2-2.3-1. The reaction loads acting on the suppression chamber vertical support system column and saddle base plate assemblies are compared to the allowable support loads shown in Table 2-2.3-2. Stresses in suppression chamber Class MC component support welds are computed using the maximum resultant force acting on the associated weld throat. The

results are compared to the weld stress limits discussed in Section 2-2.3.

The controlling suppression chamber load combinations evaluated are defined in Section 2-2.2.2. During load combination formulation, the maximum stress components in a particular suppression chamber component are combined for the individual loads contained in each combination. The stress components for dynamic loadings are combined to obtain the maximum stress intensity.

For evaluating fatigue effects in the suppression chamber Class MC components and associated welds, extreme fiber alternating stress intensity histograms are determined for each load in each event or combination of events. Stress intensity histograms are developed for the suppression chamber components and welds with the highest stress intensity ranges. Fatigue strength reduction factors of 2.0 for major component stresses and 4.0 for component weld stresses are conservatively used. For each combination of events, a load combination stress intensity histogram is formulated, and the corresponding fatigue usage factors are determined using the curve shown in Figure

2-2.4-11. The usage factors for each event are then summed to obtain the total fatigue usage.

Use of the methodology described above results in a conservative evaluation of the suppression chamber design margins.

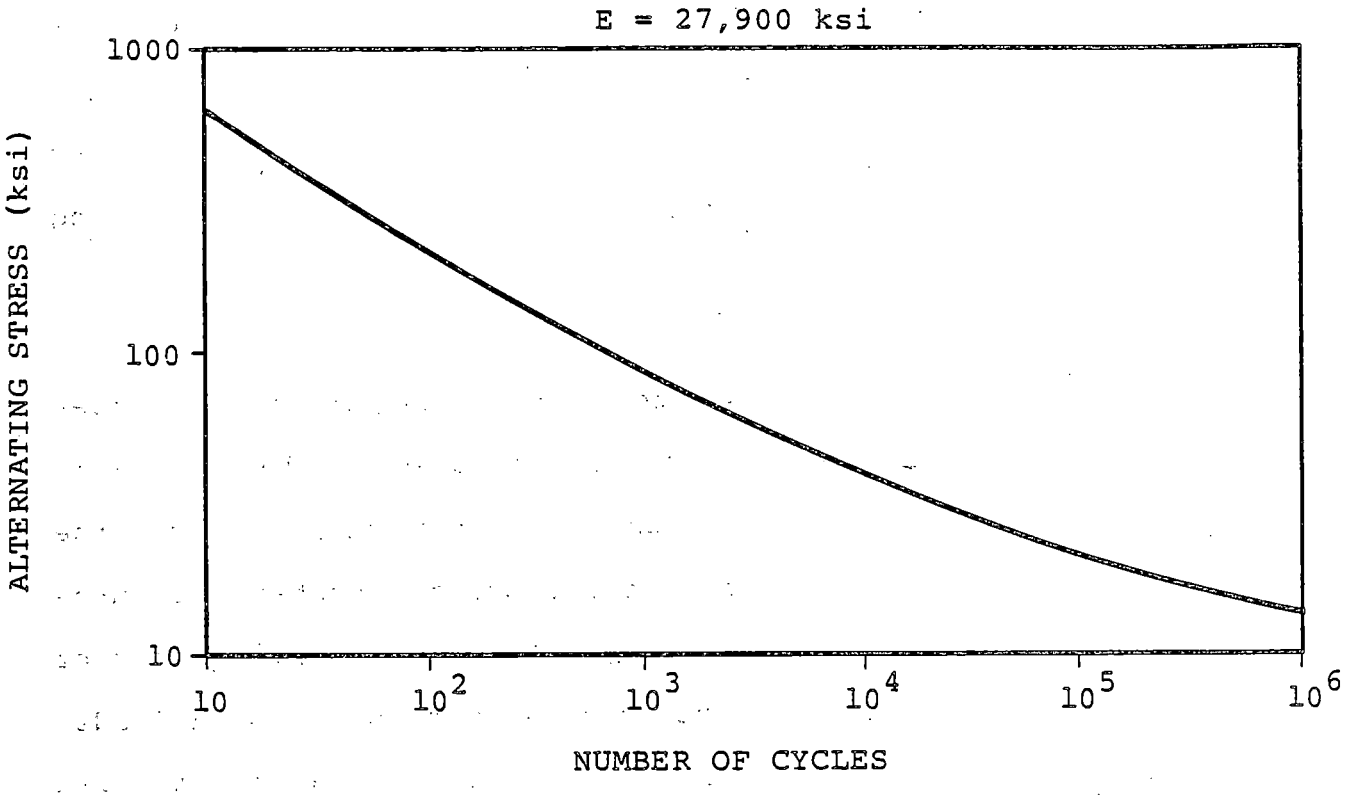

Figure 2-2.4-11

ALLOWABLE NUMBER OF STRESS CYCLES FOR SUPPRESSION CHAMBER FATIGUE EVALUATION

nutech ENGINEERS

2-2.5 Analysis Results

The geometry, loads and load combinations, acceptance criteria, and analysis methods used in the evaluation of the Dresden Units 2 and 3 suppression chambers are presented and discussed in the preceding sections. The results and conclusions derived from the evaluation of the suppression chamber are presented in the following paragraphs.

Table 2-2.5-1 shows the maximum suppression chamber shell stresses for each of the governing loads. Table 2-2.5-2 shows the corresponding reaction loads for the suppression chamber vertical support system. Figures 2-2.5-1 through 2-2.5-4 show the transient responses of the suppression chamber for selected torus shell loads, expressed in terms of total vertical load per mitered cylinder.

Table 2-2.5-5 shows the maximum suppression chamber shell stresses adjacent to the seismic restraints for each of the governing loads resulting in lateral loads on the suppression chamber. Table 2-2.5-6 shows the corresponding reaction loads on the suppression chamber seismic restraints.

Table 2-2.5-3 shows the maximum stresses and associated design margins for the major suppression chamber components and welds for the IBA III, IBA IV, DBA III, and DBA IV load combinations. Table 2-2.5-4 shows the maximum reaction loads and associated design margins for the suppression chamber vertical support system for the IBA III, IBA IV, DBA I, DBA III, and DBA IV load combinations. Table 2-2.5-7 shows the maximum suppression chamber seismic restraint reactions and associated shell stresses adjacent to the seismic restraints for the IBA III combination.

Table 2-2.5-8 shows the fatigue usage factors for the controlling suppression chamber component and weld. These usage factors are obtained by evaluating the Normal Operating plus SBA events and the Normal Operating plus IBA events.

Section 2-2.5.1 describes the suppression chamber evaluation results presented in the preceding paragraphs.

Table 2-2.5-1

MAXIMUM SUPPRESSION CHAMBER SHELL STRESSES FOR GOVERNING LOADS

SECTION 2-2.2.1 LOAD DESIGNATION		SHELL STRESS TYPE[1] (ksi)		
LOAD TYPE	LOAD CASE NUMBER	PRIMARY MEMBRANE	LOCAL PRIMARY MEMBRANE	PRIMARY + SECONDARY STRESS RANGE
DEAD WEIGHT	1a + 1b	2.74	5.62	6.56
SEISMIC	2a	0.29	1.64	6.15
	2b	0.58	3.29	12.30
PRESSURE AND TEMPERATURE	3b	10.77	10.59	19.29
	3d	0.79	5.91	10.15
POOL SWELL[2]	5b (VB)	10.79	11.40	22.41
	5b (NVB)	10.84	12.98	22.51
CONDENSATION OSCILLATION	6a	6.50	10.88	23.44
	6c	0.44	1.05	3.13
CHUGGING	7a	1.63	3.86	10.00
	7b	1.17	1.78	4.08
	7d	0.61	1.59	4.68
SRV DISCHARGE	8a	8.92	10.28	39.24
	8b	13.34	15.37	58.67
	8d	1.48	4.25	12.00

(1) VALUES SHOWN ARE MAXIMUMS IRRESPECTIVE OF TIME AND LOCATIONS AND MAY NOT BE ADDED TO OBTAIN LOAD COMBINATION RESULTS.

(2) ZERO DIFFERENTIAL PRESSURE.

Table 2-2.5-2

MAXIMUM VERTICAL SUPPORT REACTIONS FOR GOVERNING SUPPRESSION CHAMBER LOADINGS

SECTION 2-2.2.1 LOAD DESIGNATION				VERTICAL REACTION LOAD (kips)				
LOAD TYPE		LOAD CASE NUMBER	DIRECTION	COLUMN		SADDLE		TOTAL (1)
				INSIDE	OUTSIDE	INSIDE	OUTSIDE	
DEAD WEIGHT		1a + 1b	UPWARD	251.82	300.92	(2)	(2)	552.74
SEISMIC	OBE	2a	DOWNWARD	6.69	7.46	10.70	13.79	38.64
			UPWARD	6.69	7.46	10.70	13.79	38.64
	SSE	2b	DOWNWARD	13.38	14.92	21.40	27.58	77.28
			UPWARD	13.38	14.92	21.40	27.58	77.28
INTERNAL PRESSURE		3b	UP (-) / DOWN (+)	+21.39	-17.94	-16.28	+12.63	-0.20
THERMAL		3d	UP (-) / DOWN (+)	+30.40	+29.99	-32.18	-28.22	-0.01
POOL SWELL (3)		5b	DOWNWARD	238.60	323.40	160.84	204.30	927.14
			UPWARD	373.20	469.20	525.52	645.92	2013.84
CONDENSATION OSCILLATION		6a	DOWNWARD	170.49	166.66	325.87	332.27	995.29
			UPWARD	196.82	201.31	413.97	476.27	1288.37
CHUGGING	PRE-CHUG	7a	DOWNWARD	33.76	37.60	55.12	85.35	211.83
			UPWARD	33.68	37.56	55.19	85.52	211.95
	POST-CHUG	7b	DOWNWARD	29.94	31.69	59.66	68.24	189.53
			UPWARD	33.96	35.45	66.90	75.40	211.72
SRV DISCHARGE	SINGLE VALVE	8a	DOWNWARD	81.22	94.74	297.80	333.78	807.54
			UPWARD	94.86	109.23	292.41	375.27	871.77
	MULTIPLE VALVE	8b	DOWNWARD	121.41	141.62	445.14	498.92	1207.09
			UPWARD	141.79	163.27	437.08	560.94	1303.08

(1) REACTIONS ARE ADDED IN TIME FOR DYNAMIC LOADS.

(2) SADDLE DOES NOT REACT TO DEAD WEIGHT LOADS.

(3) ZERO DIFFERENTIAL PRESSURE.

Table 2-2.5-3

MAXIMUM SUPPRESSION CHAMBER STRESSES FOR CONTROLLING LOAD COMBINATIONS

ITEM		STRESS TYPE	LOAD COMBINATION STRESSES (ksi)							
			IBA III		IBA IV		DBA III		DBA IV	
			CALCULATED STRESS	CALCULATED ALLOWABLE	CALCULATED STRESS	CALCULATED ALLOWABLE	CALCULATED STRESS	CALCULATED ALLOWABLE	CALCULATED STRESS	CALCULATED ALLOWABLE
COMPONENTS	SHELL(1)	PRIMARY MEMBRANE	16.96	0.88	17.28	0.89	15.93	0.82	22.18	0.62
		LOCAL PRIMARY MEMBRANE	21.24	0.73	20.22	0.70	15.09	0.52	27.04	0.50
		PRIMARY + SECONDARY STRESS RANGE	63.05	0.91	64.22	0.92	30.18	0.43	N/A	N/A
	RING GIRDER	PRIMARY MEMBRANE	19.24	0.99	18.84	0.98	19.09(2)	0.99	24.62	0.69
		LOCAL PRIMARY MEMBRANE	25.53	0.88	23.24	0.80	28.17(2)	0.97	26.02	0.48
		PRIMARY + SECONDARY STRESS RANGE	45.92	0.66	47.20	0.68	57.41(2)	0.83	N/A	N/A
COMPONENT SUPPORTS	COLUMN CONNECTION	MEMBRANE	17.25	0.80	17.62	0.82	8.72	0.41	19.24	0.67
		EXTREME FIBER	20.09	0.75	20.61	0.77	8.72	0.32	20.87	0.58
	SADDLE	MEMBRANE	18.29	0.85	18.25	0.85	10.16	0.47	27.47	0.96
		EXTREME FIBER	18.29	0.68	18.25	0.68	10.16	0.38	27.47	0.77
WELDS	RING GIRDER TO SHELL	PRIMARY	19.70(3)	0.87	17.76(3)	0.79	21.62(2)(3)	0.96	24.40	0.87
		SECONDARY	45.94	0.85	42.57	0.79	50.30(2)	0.93	N/A	N/A
	COLUMN CONNECTION TO SHELL	PRIMARY	20.25	0.91	21.90	0.97	11.92	0.79	40.59	0.97
		SECONDARY	27.88	0.52	29.39	0.54	14.21	0.26	N/A	N/A
	SADDLE TO SHELL	PRIMARY	19.05	0.93	18.36	0.90	11.81	0.58	30.65	0.81
		SECONDARY	19.05	0.31	18.36	0.30	11.81	0.19	N/A	N/A

(1) A STRESS INTENSIFICATION FACTOR OF 1.10 HAS BEEN USED TO ACCOUNT FOR PITTING IN THE TORUS SHELL.

(2) THESE RESULTS ARE GOVERNED BY THE ZERO RING GIRDER STIFFENER MODEL.

(3) THIS LOCAL PRIMARY MEMBRANE STRESS HAS AN ALLOWABLE BASED ON 1.5 Smc.

Table 2-2.5-4

MAXIMUM VERTICAL SUPPORT REACTIONS FOR CONTROLLING SUPPRESSION CHAMBER LOAD COMBINATIONS

VERTICAL SUPPORT COMPONENT		DIRECTION	LOAD COMBINATION REACTIONS (kips)									
			IBA III[1]		IBA IV[1]		DBA I[1]		DBA III[1]		DBA IV[1]	
			CALCULATED LOAD	CALCULATED / ALLOWABLE[2]	CALCULATED LOAD	CALCULATED / ALLOWABLE[2]	CALCULATED LOAD	CALCULATED / ALLOWABLE[2]	CALCULATED LOAD	CALCULATED / ALLOWABLE[2]	CALCULATED LOAD	CALCULATED / ALLOWABLE[2]
COLUMN	INSIDE	DOWNWARD	(3)	N/A	(3)	N/A	98.22	0.51	(3)	N/A	133.17	0.70
		UPWARD	382.19	0.38	382.47	0.38	594.62	0.30	403.54	0.40	534.06	0.40
	OUTSIDE	DOWNWARD	(3)	N/A	(3)	N/A	115.38	0.33	(3)	N/A	144.19	0.41
		UPWARD	497.46	0.38	495.35	0.38	740.63	0.28	497.84	0.38	628.78	0.36
SADDLE	INSIDE	DOWNWARD	634.27	0.72	639.26	0.73	486.56	0.55	432.57	0.49	731.09	0.83
		UPWARD	698.48	0.77	708.16	0.79	841.91	0.47	611.31	0.68	952.11	0.79
	OUTSIDE	DOWNWARD	751.35	0.85	732.53	0.83	558.66	0.64	470.78	0.54	841.08	0.96
		UPWARD	770.46	0.86	754.64	0.84	927.14	0.51	594.90	0.66	1034.07	0.86
TOTAL[4]		DOWNWARD	1280.12	0.56	1255.58	0.55	1258.82	0.55	800.88	0.35	1850.33	0.80
		UPWARD	2348.59	0.57	2340.62	0.57	3104.33	0.38	2107.59	0.51	3149.02	0.57

(1) SEE TABLE 2-2.2-13 FOR LOAD COMBINATION DESIGNATION.

(2) SEE TABLE 2-2.3-2 FOR ALLOWABLE SUPPORT LOADS.

(3) THERE IS NO UPLIFT ON THIS MEMBER.

(4) TOTALS REFLECT FULL MITER JOINT LOAD.

Table 2-2.5-5

MAXIMUM SUPPRESSION CHAMBER SHELL STRESSES DUE TO LATERAL LOADS

SECTION 2-2.2-1 LOAD DESIGNATION			SHELL STRESS TYPE (ksi) (1)	
LOAD TYPE		LOAD CASE NUMBER	LOCAL PRIMARY MEMBRANE	PRIMARY AND SECONDARY STRESS RANGE
SEISMIC	OBE	2a	1.64	5.25
	SSE	2b	3.29	N/A
PRE-CHUG		7a	1.04	3.32
SRV DISCHARGE		8b	0.55	1.76

(1) STRESSES SHOWN ARE IN SUPPRESSION CHAMBER SHELL ADJACENT TO OUTSIDE COLUMN ATTACHMENT LOCATION.

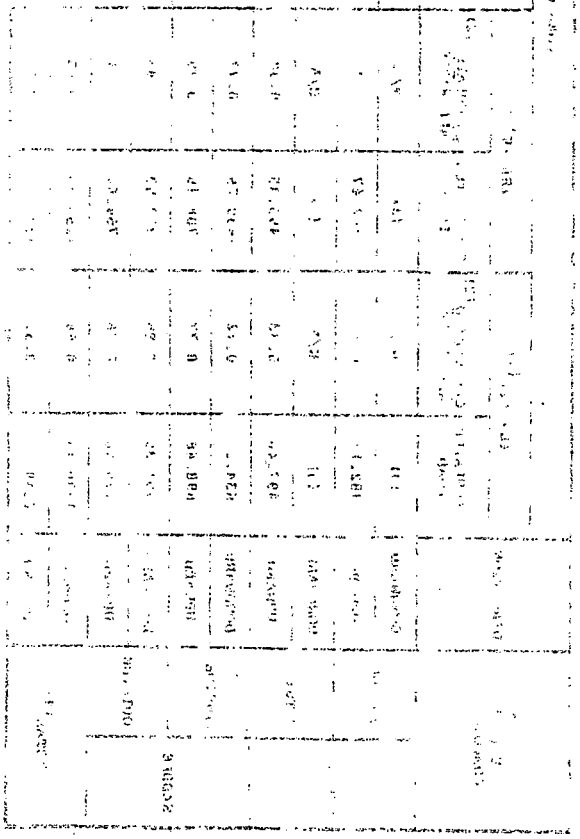

Table 2-2.5-6

MAXIMUM SEISMIC RESTRAINT REACTIONS

DUE TO LATERAL LOADS

SECTION 2-2.2.1 LOAD DESIGNATION			HORIZONTAL REACTION LOAD (kips)		
LOAD TYPE		LOAD CASE NUMBER	MAXIMUM SWAY ROD REACTION	TOTAL HORIZONTAL LOAD	DYNAMIC LOAD FACTOR
SEISMIC	OBE	2a	62.56	890.00	N/A
	SSE	2b	125.12	1780.00	N/A
PRE-CHUG		7a	39.60	459.00	13.77
SRV DISCHARGE		8b	20.96	669.00	2.42

nutech ENGINEERS

Table 2-2.5-7

MAXIMUM SUPPRESSION CHAMBER SHELL STRESSES AND SEISMIC RESTRAINT REACTIONS FOR CONTROLLING LOAD COMBINATION WITH LATERAL LOADS

ITEM	STRESS/REACTION TYPE	LOAD COMBINATION(2,3) STRESSES/REACTIONS (ksi,kips) IBA III	
		CALCULATED VALUE	CALCULATED / ALLOWABLE
SHELL(1)	LOCAL PRIMARY MEMBRANE	24.51	0.85
	PRIMARY AND SECONDARY STRESS RANGE	61.34	0.88
SWAY ROD	MAXIMUM REACTION LOAD	123.12	0.36

(1) STRESSES SHOWN ARE IN THE SUPPRESSION CHAMBER SHELL, ADJACENT TO THE OUTSIDE COLUMN ATTACHMENT LOCATION.

(2) SEE TABLE 2-2.2-13 FOR THE LOAD COMBINATION DESIGNATION.

(3) SEE SECTION 2-2.3 FOR THE ALLOWABLE SEISMIC RESTRAINT LOADS.

Table 2-2.5-8

MAXIMUM FATIGUE USAGE FACTORS FOR SUPPRESSION CHAMBER COMPONENTS AND WELDS

EVENT SEQUENCE (1)	LOAD CASE CYCLES (1)					EVENT USAGE FACTOR (8)	
	SEISMIC	PRESSURE	TEMPERATURE	SRV DISCHARGE	PRE + POST CHUG (sec)	TORUS SHELL	WELD
NOC W/SINGLE SRV	0	150 (2)	150 (2)	300 (3,9)	N/A	0.34	0.08
NOC W/MULTIPLE SRV	0	0	0				
SBA 0. TO 600. SEC	600 (2)	1	1	50 (4)	300. (6)	0.14	0.37
SBA 600. TO 1200. SEC	0	0	0	2 (5)	600. (6)	0.02	0.35
IBA 0. TO 900. SEC	600 (2)	1	1	25 (4)	900. (7)	0.03	0.33
IBA 900. TO 1100. SEC	0	0	0	2 (5)	200. (6)	0.01	0.12
MAXIMUM CUMULATIVE USAGE FACTORS				NOC + SBA		0.50	0.80
				NOC + IBA		0.38	0.53

(1) SEE TABLE 2-2.2-11 AND FIGURES 2-2.2-19 AND 2-2.2-20 FOR LOAD CYCLES AND EVENT SEQUENCING INFORMATION.

(2) ENTIRE NUMBER OF LOAD CYCLES CONSERVATIVELY ASSUMED TO OCCUR DURING TIME OF MAXIMUM EVENT USAGE.

(3) TOTAL NUMBER OF SRV ACTUATIONS SHOWN ARE CONSERVATIVELY ASSUMED TO OCCUR IN SAME SUPPRESSION CHAMBER BAY.

(4) VALUE SHOWN IS CONSERVATIVELY ASSUMED TO BE EQUAL TO THE NUMBER OF MULTIPLE VALVE ACTUATIONS WHICH OCCURS DURING THE EVENT.

(5) NUMBER OF ADS ACTUATIONS ASSUMED TO OCCUR DURING THE EVENT.

(6) EACH CHUG-CYCLE HAS A DURATION OF 1.4 SEC.

(7) CO LOADS, WHICH ARE THE SAME AS PRE-CHUG LOADS, OCCUR DURING THIS PHASE OF THE IBA EVENT.

(8) USAGE FACTORS ARE COMPUTED FOR THE COMPONENT AND WELD WHICH RESULT IN THE MAXIMUM CUMULATIVE USAGE.

(9) ALL ACTUATIONS CONSERVATIVELY ASSUMED TO BE MULTIPLE VALVE.

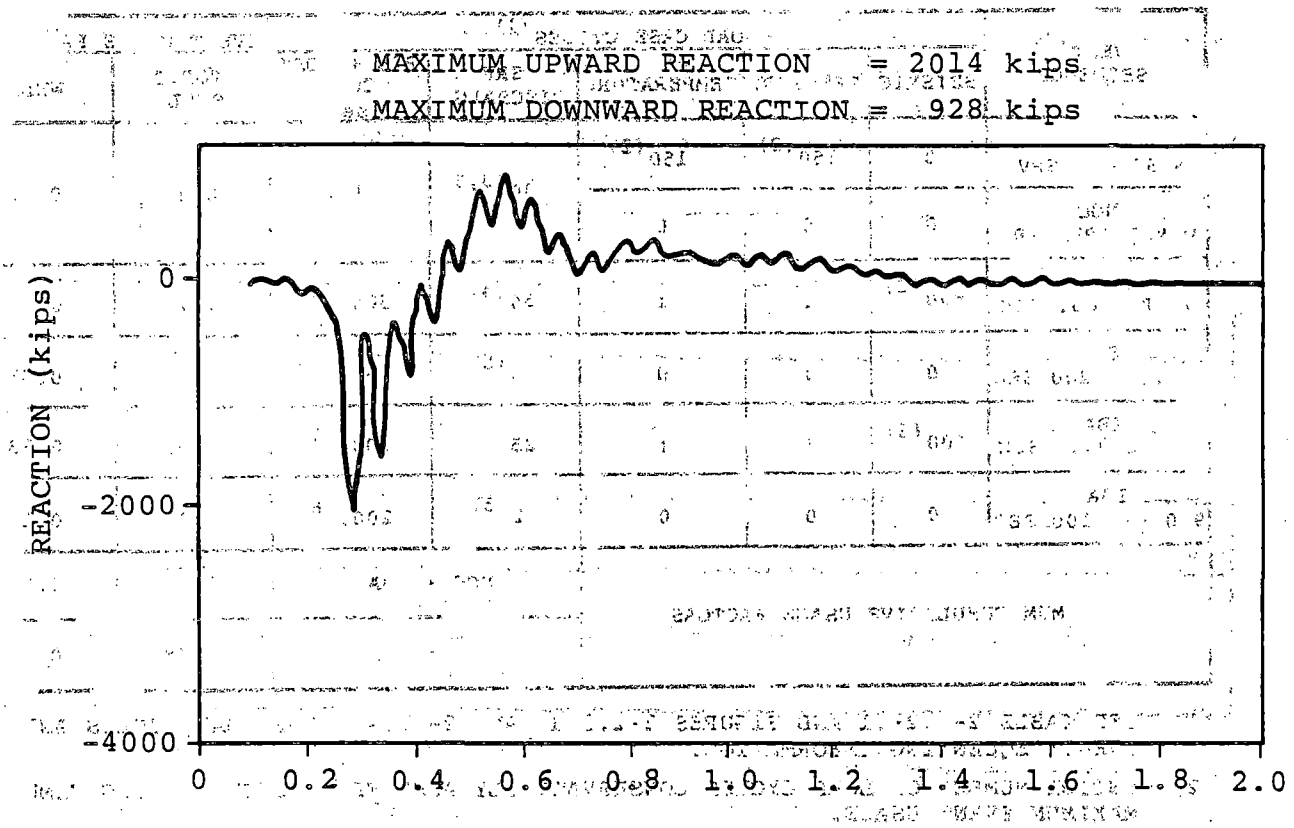

1. SEE TABLE 2-2.2-5 AND FIGURES 2-2.2-10 AND 2-2.2-11 FOR LOADING INFORMATION.

Figure 2-2.5-1

SUPPRESSION CHAMBER RESPONSE DUE TO POOL SWELL LOADS - TOTAL VERTICAL LOAD PER MITERED CYLINDER (ZERO DIFFERENTIAL PRESSURE)

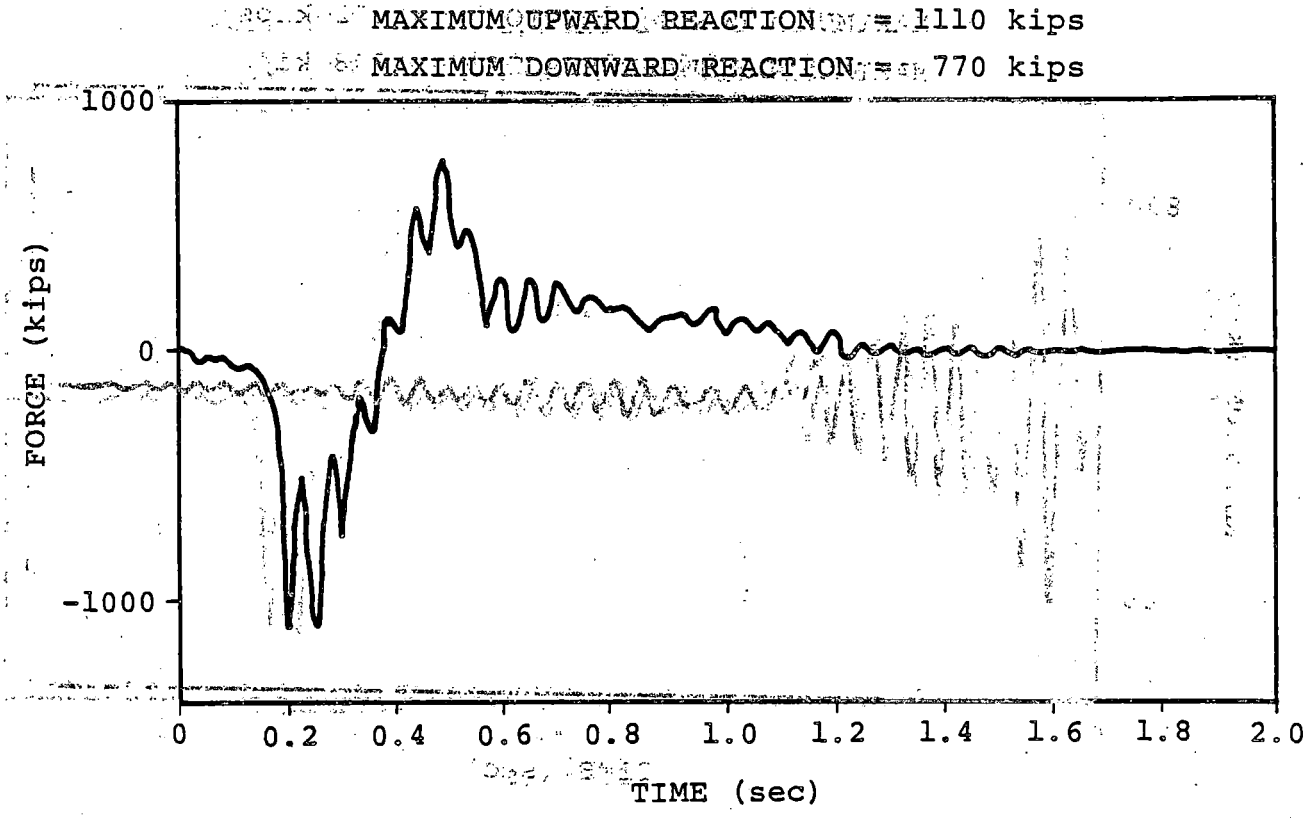

1. SEE TABLE 2-2.4-2 AND FIGURES 2-2.2-8 AND 2-2.2-9 FOR LOADING INFORMATION.

Figure 2-2.5-2

SUPPRESSION CHAMBER RESPONSE DUE TO POOL SWELL LOADS - TOTAL VERTICAL LOAD PER MITERED CYLINDER (OPERATING DIFFERENTIAL PRESSURE)

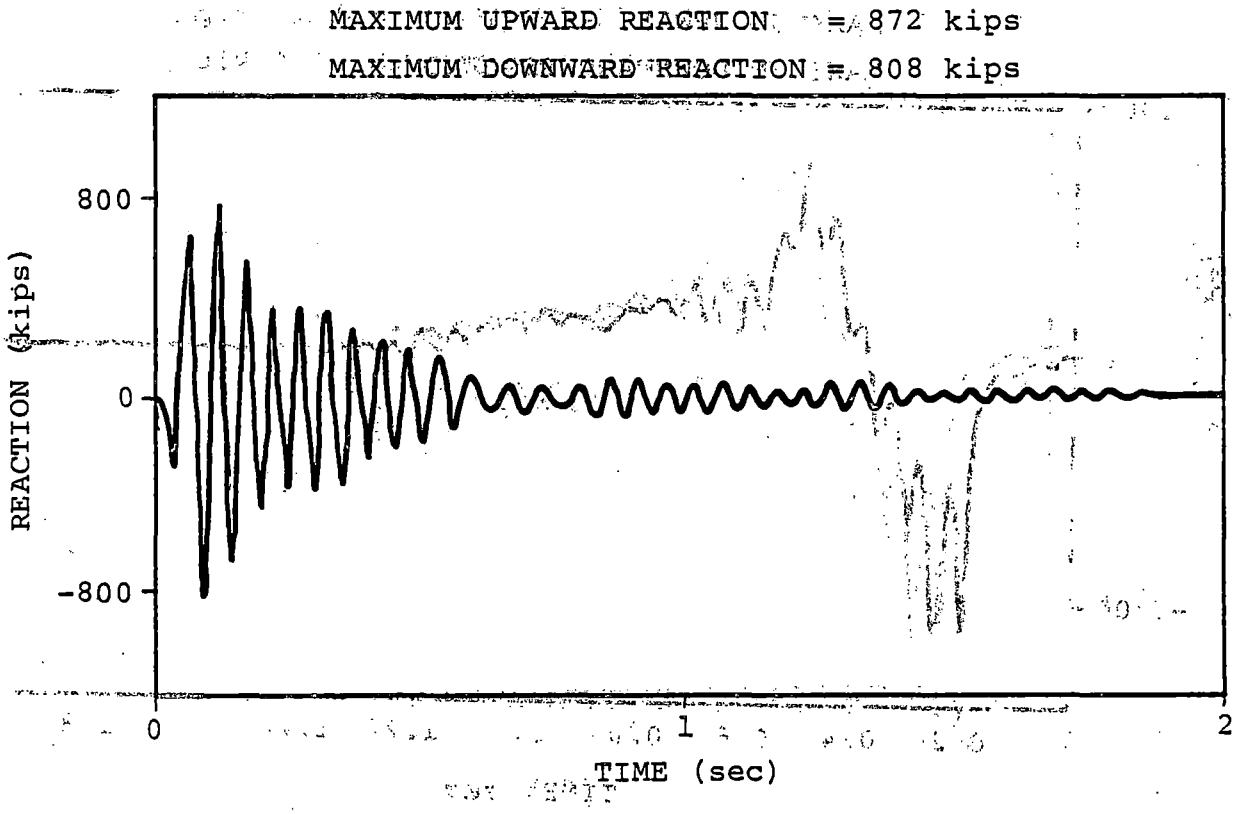

1. SEE FIGURE 2-2.2-16 FOR LOADING INFORMATION.
2. SEE TABLE 2-2.5-2 FOR MAXIMUM UPWARD REACTION.

Figure 2-2.5-3

SUPPRESSION CHAMBER RESPONSE DUE TO SINGLE VALVE SRV DISCHARGE TORUS SHELL LOADS - TOTAL VERTICAL LOAD PER MITERED CYLINDER

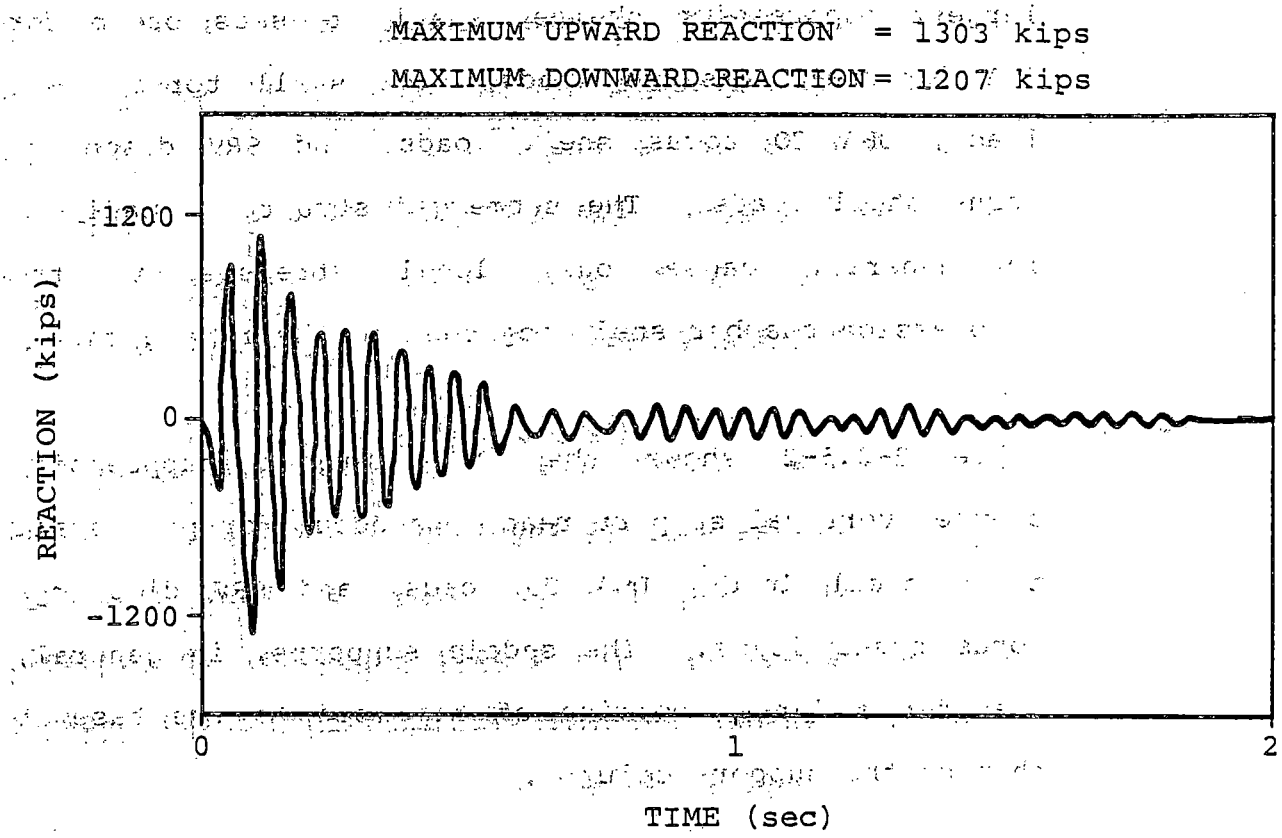

1. SEE FIGURE 2-2.2-17 FOR LOADING INFORMATION.
2. SEE TABLE 2-2.5-2 FOR MAXIMUM DOWNWARD REACTION.

Figure 2-2.5-4

SUPPRESSION CHAMBER RESPONSE DUE TO MULTIPLE VALVE SRV DISCHARGE TORUS SHELL LOADS - TOTAL VERTICAL LOAD PER MITERED CYLINDER

2-2.5.1 Discussion of Analysis Results

The results shown in Table 2-2.5-1 indicate that the largest suppression chamber shell stresses occur for IBA internal pressure loads, pool swell torus shell loads, DBA CO torus shell loads, and SRV discharge torus shell loads. The submerged structure loadings, in general, cause only local stresses in the suppression chamber shell adjacent to the ring girder.

Table 2-2.5-2 shows that the largest suppression chamber vertical support reactions occur for pool swell torus shell loads, DBA CO loads, and SRV discharge torus shell loads. The saddle supports, in general, transfer a larger portion of the load to the basemat than do the support columns.

The results shown in Table 2-2.5-3 indicate that the largest stresses in the suppression chamber shell are due to the IBA III and IBA IV load combinations. The largest stresses in the ring girder and associated welds are due to the IBA III and IBA IV for the SRV bays, and DBA III for the non-SRV bays. The largest stresses for the component supports and associated welds are due to the IBA III, IBA IV and DBA IV

combinations. The DBA IV load combination for these components is overly conservative due to the use of zero differential pressure pool swell loads rather than operating differential pool swell loads. The stresses in the suppression chamber components, component supports, and welds are all within allowable limits.

Table 2-2.5-4 shows that the largest downward vertical support reactions occur for the IBA III and DBA IV combinations. The largest upward vertical support reactions occur for the DBA I and DBA IV combinations. For the reason stated in reference to component stresses, the DBA IV combination is overly conservative. In general, the downward vertical support reactions are less than the upward vertical support reactions. The vertical support system reactions for all load combinations are less than allowable limits.

The results shown in Tables 2-2.5-5 and 2-2.5-6 indicate that the largest seismic restraint reactions and associated suppression chamber shell stresses occur for seismic loads and SRV discharge loads. Table 2-2.5-7 shows that the seismic restraint reactions and suppression chamber shell stresses adjacent to the seismic restraints for the IBA III load combination are less than allowable limits.

The results shown in Table 2-2.5-8 indicate that the largest contributor to suppression chamber fatigue effects are SRV discharge loads, which occur during normal operating conditions. The largest total fatigue usage occurs for the Normal Operating plus SBA events with usage factors for the suppression chamber shell and associated welds less than allowable limits. The usage factors for the Normal Operating plus IBA events are also less than allowable limits.

2-2.5.2 Closure

The suppression chamber loads described and presented in Section 2-2.2-1 are conservative estimates of the loads postulated to occur during an actual LOCA or SRV discharge event. Applying the methodology discussed in Section 2-2.4 to evaluate the effects of the governing loads on the suppression chamber results in bounding values of stresses and reactions in suppression chamber components and component supports.

The load combinations and event sequencing defined in Section 2-2.2.2 envelop the actual events postulated to occur during a LOCA or SRV discharge event. Combining the suppression chamber responses with the governing loads and evaluating fatigue effects using this methodology results in conservative values of the maximum suppression chamber stresses, support reactions, and fatigue usage factors for each event or sequence of events postulated to occur throughout the life of the plant.

The acceptance limits defined in Section 2-2.3 are at least as restrictive, and in many cases more restrictive, than those used in the original containment

design documented in the plant's SAR. Comparing the resulting maximum stresses and support reactions to these acceptance limits results in a conservative evaluation of the design margins present in the suppression chamber and suppression chamber supports. The results discussed and presented in the preceding sections show that all of the suppression chamber stresses and support reactions are within these acceptance limits.

As a result, the components of the suppression chamber described in Section 2-2.1, which are specifically designed for the loads and load combinations used in this evaluation, exhibit the margins of safety inherent in the original design of the primary containment documented in the plant's SAR. The intent of the NUREG-0661 requirements is therefore considered to be met.

2-3.0 LIST OF REFERENCES

1. "Mark I Containment Long-Term Program," Safety Evaluation Report, USNRC, NUREG-0661, July 1980; Supplement 1, August 1982.

2. "Mark I Containment Program Load Definition Report," General Electric Company, NEDO-21888, Revision 2, November 1981.

3. "Mark I Containment Program Plant Unique Load Definition," Dresden Station Units 2 and 3, General Electric Company, NEDO-24566, Revision 2, April 1982.

4. "Dresden 2 and 3 Nuclear Generating Plants Suppression Pool Temperature Response," General Electric Company, NEDC-22170, July 1982.

5. "Containment Data," Dresden 2, General Electric Company, 22A5743, Revision 1, April 1979.

6. "Containment Data," Dresden 3, General Electric Company, 22A5744, Revision 1, April 1979.

7. "Containment Vessels Design Specification," Dresden Units 2 and 3, Sargent & Lundy Incorporated, K-2152, March 4, 1966.

8. "Mark I Containment Program Structural Acceptance Criteria Plant Unique Analysis Applications Guide, Task Number 3.1.3," Mark I Owners Group, General Electric Company, NEDO-24583, Revision 1, October 1979.

9. ASME Boiler and Pressure Vessel Code, Section III, Division 1, 1977 Edition with Addenda up to and including Summer 1977.

10. "Safety Analysis Report (SAR)," Dresden Station Units 2 and 3, Commonwealth Edison Company, November 17, 1967.

11. "Field Column and Sway Rod Assembly, Dresden 2," Chicago Bridge and Iron Company, Drawing Number 204, Revision 0, January 19, 1966.

12. "Field Column and Sway Rod Assembly, Dresden 3," Chicago Bridge and Iron Company, Drawing Number 204, Revision 0, January 19, 1966.

13. "Torus Support Modification, Saddle Support," Dresden Units 2 and 3, NUTECH, B-1580, Revision A, July 1982.

14. "Torus Support Modification, Column Anchorage Reinforcement," Dresden Units 2 and 3, NUTECH, B-1581, Revision A, July 1982.

15. American Concrete Institute (ACI) Code, Code Requirements for Nuclear Safety-Related Concrete Structures, ACI-349-80, 1980.

16. "Stress Report for Nuclear Containment Vessel at Dresden Station Unit #2," United Engineers and Constructors, CB&I Contract 9-3600, November 1966.

17. "Stress Report for Nuclear Containment Vessel at Dresden Station Unit #3," United Engineers and Constructors, CB&I Contract 9-4646, November 1966.

18. "Damping Values for Seismic Design of Nuclear Power Plants," U.S. Atomic Energy Commission Regulatory Guide, Directorate of Regulatory Standards, Regulatory Guide 1.61, Revision 0, October 1973.

19. "Mark I Torus Seismic Slosh Evaluation," Mark I Containment Program, Task 5.4, General Electric Company, NEDE-24519-P, March 1978.